Table of contents

1. General experimental remarks

If not stated otherwise, all reactions and manipulations were carried out under dry nitrogen atmosphere using Schlenk techniques. THF was distilled from Na/benzophenone and degassed by purging with dry argon or nitrogen for at least 30 min (coupling reactions). Chlorobenzene, dimethylformamide (DMF) and Et_3N were distilled from CaH_2 and stored over molecular sieves (3 Å). C_6D_6 and $CDCl_3$ were stored over molecular sieves (3 Å). MesMgBr and *n*-BuLi were titrated according to the literature before use.[S1] Reaction mixtures in flasks were heated by using an oil bath.

If not stated otherwise, commercially available compounds were used as received.

In photochemical experiments, 385 and 405 nm LED lamps (*Sahlmann Photochemical Solutions*) were used.

Column chromatography was performed using silica gel 60 (*Macherey–Nagel*, *Sigma Aldrich*; 70–230 mesh).

Melting points were measured with Melting points were recorded with a Büchi Melting Point B-540 apparatus.

NMR spectra were recorded at 298 K using the following spectrometers: Bruker Avance-300, Avance-400, Avance Neo-400, Avance-500, or DRX-600. Chemical shift values are referenced to (residual) solvent signals ($^1H/^{13}C\{^1H\}$; C_6D_6: δ = 7.16/128.06; $CDCl_3$: δ = 7.26/77.16) or external $BF_3•Et_2O$ (^{11}B: δ = 0.00). Abbreviations: s = singlet, d = doublet, dd = doublet of doublets, br. = broad, n.o. = not observed, eq. = equivalent, Mp = melting point. Resonances of carbon atoms attached to boron atoms were typically broadened and sometimes not observed due to the quadrupolar relaxation of boron. Resonance assignments were aided by ^{13}C APT, ^{H,H}COSY, ^{H,C}HSQC, and ^{H,C}HMBC spectra.

High-resolution mass spectra were measured using an electron ionization (EI) spectrometer (FISONS-Vg Autospec-M246), *Thermo Fisher Scientific* MALDI LTQ Orbitrap XL spectrometer (2,5-dihydroxybenzoic acid or α-cyano-4-hydroxycinnamic acid as the matrix), MALDI-TOF/TOF Autoflex III-Bruker Daltonics.

UV–vis absorption spectra were obtained on a *Shimadzu* UV–vis–NIR 3600 spectrophotometer in a 1 cm path length quartz cell.

Photoluminescence quantum yields (Φ_{PL}) were measured with a C11347 *Quantaurus* - Absolute Photoluminescence Quantum Yield Spectrometer (Hamamatsu Photonics U.K), equipped with a 150 W Xenon lamp, an integrating sphere, and a multi-channel detector.

Steady state emission and excitation spectra and photoluminescence lifetimes were obtained with a FLS 980 spectrofluorimeter (Edinburg Instrument Ltd.). Continuous excitation for the steady state measurements was provided by a 450 W Xenon arc lamp. Emission spectra were corrected for the detector sensitivity. Photoluminescence lifetime measurements, determined by TCSPC (time-correlated single-photon counting) method, were performed using an Edinburgh Picosecond Pulsed Diode Laser EPL-375 (Edinburg Instrument Ltd.), in nitrogen degassed solutions (10^{-5}-10^{-7} mol L^{-1}).

Cyclic voltammetry (CV) measurements were performed using an AutoLab PGStat potentiostat and a classical three electrode glass minicell (working volume about 3 mL), including as working electrode a glassy carbon

GC disk (Metrohm, S=0.033 cm2) polished by diamond powder (1 µm Aldrich) on a wet cloth (Struers DP-NAP), as counter electrode a platinum disk, and as reference electrode a saturated aqueous calomel one (SCE) or Ag/AgCl. SCE was inserted in a compartment with the working medium ending in a porous frit (to avoid contamination of the working solution by water and KCl traces. Experiments were run at scan rates ranging from 0.1–2 V/s on 0.00075 M solutions in THF+0.1 M [nBu$_4$N][PF$_6$] (used as received; *Sigma Aldrich*) was employed as the supporting electrolyte, previously deaerated by nitrogen bubbling. Positive and negative half cycles have been separately recorded to avoid reciprocal contamination by electron transfer products. The reported potentials have been normalized *vs.* the formal potential of the intersolvental ferricinium/ferrocene (FcH+|FcH) reference redox couple, recorded in the same conditions. All potential values were referenced against the FcH/FcH$^+$ redox couple (FcH = ferrocene; $E_{1/2}$ = 0 V).

The chromatographic system employed for HPLC separation consisted of an *Ultimate 3000 UHPLC*$^+$ (*Dionex, Sunnyvale,* California, US*)* equipped with a pump, autosampler, column compartment, and UV detector. This same system was used for both analytical and semipreparative separations. For these methods, two columns with different geometries were utilized. The first column had dimensions of 100 × 4.6 mm (L × I.D.) with 1.8 µm particles, while the second column had dimensions of 250 × 10.0 mm (I.D.) with 5 µm particles ((*S, S*)-Whelk-O1 as chiral stationary phase for both). Optical rotation and ECD spectra were recorded using a *Jasco* P-1020 Polarimeter and a *Jasco* J-815 CD spectrometer, respectively.

2. Starting materials preparation

2.1 Thiophene starting materials

2.1.1 Synthesis of S4[S2]

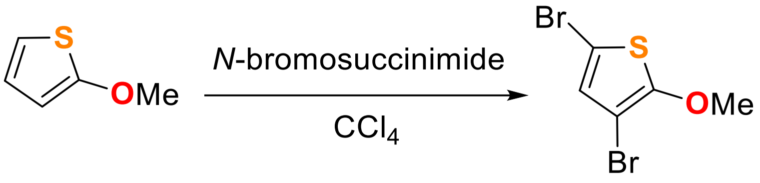

S4

A 250 ml two-necked flask equipped with a thermometer was charged with 2-methoxythiophene (5.00 g, 43.80 mmol) and CCl_4 (88 mL). The resulting yellowish solution was cooled to 5 °C and *N*-bromosuccinimide (15.65 g, 87.93 mmol, 2.00 equiv) was added in six portions during 1 h. The reaction mixture (yellow) was therefore allowed to warm up to room temperature and stirred for 24 hours (the reaction progress was checked by ^{1}H NMR). The reaction mixture was cooled with ice and then filtered to remove insoluble residues. The solution thus obtained was washed with water (150 mL). The organic phases were dried over Na_2SO_4, filtered and the solvent removed under reduced pressure. The crude product thus obtained was distilled under vacuo (bp. 94-95 °C, 2.5 mmHg) yielding 10.90 g of **S4** as a yellow oil (40.1 mmol, 92%).

The ^{1}H NMR chemical shifts correspond to the reference values.

^{1}H NMR (250 MHz, $CDCl_3$): δ = 6.75 (s, 1H), 3.93 (s, 3H).

2.1.2 Synthesis of S5[S2]

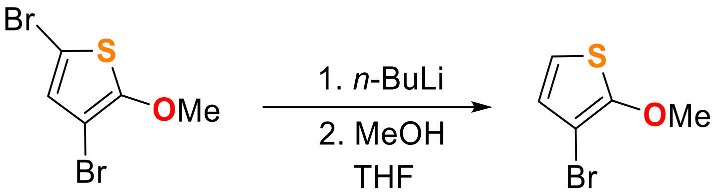

S4 **S5**

A 100 ml flame dried two-necked flask (equipped with a dropping funnel) was charged with **S4** (3.71 g, 14.32 mmol, 1 equiv) and THF (34 mL). The resulting dark red solution was cooled to –78 °C and *n*-BuLi (1.35 M in hexanes; 10.6 mL, 14.32 mmol, 1.05 eq) was diluted with dry THF (9 mL) and added dropwise (20 min). The resulting brown mixture was therefore stirred at the same temperature for 10 min, quenched with MeOH (5 mL, added slowly) and allowed to warm up to room temperature.

The solvent was removed and the residue was taken up with CH_2Cl_2 (50 ml). Water (70 mL) was added, the organic phase was separated and the aqueous phase was extracted with CH_2Cl_2 (4×30 mL). The combined organic layers were dried over Na_2SO_4 and filtered. The solvent was removed and the crude product was distilled under vacuo (56-58 °C, 1.5 mmHg) yielding 2.15 g of **S5** as a yellowish oil (11.15 mmol, 82%).

^{1}H NMR (600 MHz, $CDCl_3$): δ = 6.75 (d, ^3J(H,H) = 6.0 Hz, 1H), 6.65 (d, ^3J(H,H) = 6.0 Hz, 1H), 3.97 (s, 3H).

2.1.3 Synthesis of S6[S4]

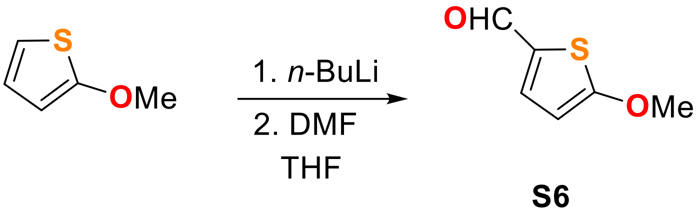

S6

A flame-dried two-necked flask equipped with a dropping funnel was charged with 2-methoxythiophene (2.5 g, 21.19 mmol) and THF (30 mL). The resulting yellowish mixture was cooled to –78 °C. *n*-BuLi (1.40 M in hexanes; 16.12 mL, 22.68 mol, 1.04 eq.) was added dropwise during 10 min and the resulting yellow clear solution was stirred at –78 °C for 1 hour.

DMF (4.72 g, 64.6 mmol, 2.95 eq.) was added dropwise yielding a deep yellow solution which was stirred at –78 °C for 45 min. NH_4Cl sat. aqueous solution (5 mL) was added, and the reaction mixture was allowed to warm up to room temperature. THF was removed and the residue was taken up with AcOEt (30 mL). Water (50 mL) was added, and the two layers were separated. The aqueous phase was extracted with AcOEt (3×20 mL) and the combined organic phases were dried over Na_2SO_4 and filtered. **S6** was obtained as a red-orange oil (3.10 g, 21.8 mmol, y = quantitative) and it was proved to be the desired product by ^{1}H NMR analysis.

^{1}H NMR (300 MHz, $CDCl_3$): δ = 9.66 (s, 1H), 7.50 (d, J(H,H) = 4.3 Hz, 1H), 6.34 (d, J(H,H) = 4.3 Hz, 1H), 3.98 (s, 3H).

2.1.4 Synthesis of S3[S5]

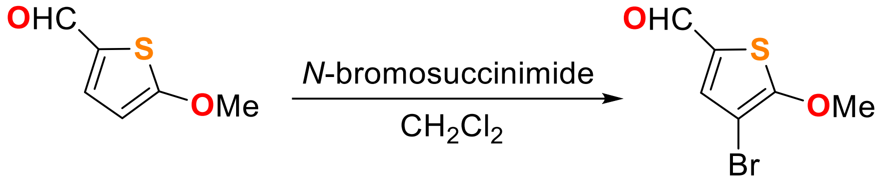

S6 **S3**

S6 (2.02 g, 14.18 mmol) was dissolved in CH_2Cl_2 (30 mL) and the resulting mixture was treated with *N*-bromo succinimide (2.63 g, 14.75 mmol, 1.04 eq.), added in portions during 30 min. The reaction progress was checked by TLC. After 5 h, TLC showed complete conversion of the starting material.

The reaction mixture was thus poured into water (50 mL) and, after separation of the two layers, the organic phase was washed with water (3×30 mL), while the aqueous phase was extracted with CH_2Cl_2 (30 mL). The combined organic phases were dried over Na_2SO_4, filtered and the solvent was removed. The crude product thus obtained was washed with Et_2O yielding **S3** as a pale-yellow solid (2.27 g, 10.30 mmol, 73%). Et_2O mother liquors were evaporated and the residue thus obtained was purified *via* column chromatography (*n*-hexane/CH_2Cl_2 (1:3)), yielding additional 630 mg of **S3** (2.85 mmol, 20%). Total yield: 93%.

^{1}H NMR (300 MHz, $CDCl_3$): δ = 9.66 (s, 1H), 7.55 (s, 1H), 4.09 (s, 3H).
Mp: 113-114 °C.

2.1.1 Synthesis of S2[S8]

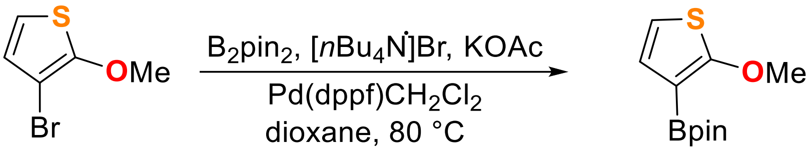

S5 **S2**

A flame-dried J-Young flask was charged with **S5** (1.50 g, 7.77 mmol, 1.00 eq.), bis-pinacolato diboron (2.24 g, 9.32 mmol, 1.20 eq.), KOAc (1.53 g, 15.5 mmol, 2.00 eq.), TBAB (56 mg, 170 µmol, 0.025 eq.), Pd(dppf)·CH_2Cl_2 (140 mg, 155 µmol, 0.02 eq.) and evacuated for 1 h. Dioxane (8 mL) was added and the resulting mixture was heated to 80 °C for 18 h. The solvent was evaporated, and the residue was purified via column chromatography (*c*-hex/CH_2Cl_2 (1:1)). **S2** was obtained as a yellow solid, in mixture with 7% B_2pin_2 (255 mg, 1.06 mmol, 14%).

^{1}H NMR (250 MHz, $CDCl_3$): $\delta = 7.01$ (d, $^3J(H,H) = 5.7$ Hz, 1H), 6.53 (d, $^3J(H,H) = 5.7$ Hz, 1H), 3.98 (s, 3H), 1.32 (s, 12H).

2.1.2 Synthesis of S1[S7]

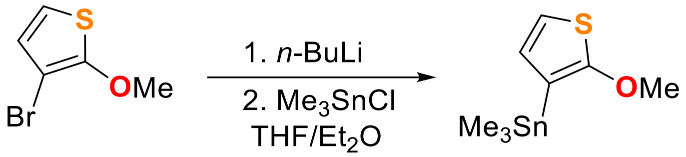

S5 **S1**

A flame-dried two-necked flask equipped with a dropping funnel was charged with **S5** (3.22 g, 16.68 mmol) and Et_2O (16 mL). The orange solution thus obtained was cooled to –78 °C and *n*-BuLi (1.40 M in hexanes; 13 mL, 18.20 mmol , 1.05 eq.) was added dropwise during 15 min. The dropping funnel was washed with THF (16 mL).

The orange suspension thus obtained was stirred at –78 °C for additional 45 min and then treated with a THF solution (16 mL) of Me_3SnCl (3.08 g, 19.05 mmol, 1.1 eq.), added during 3-5 min. The resulting orange solution was stirred at –78 °C for 2 h. The reaction mixture was therefore allowed to warm up to room temperature and water (30 mL) was added. The two layers were separated, and the aqueous phase was extracted with Et_2O. The combined organic phases were dried over Na_2SO_4, filtered and the solvent evaporated. The crude product was purified *via* distillation under vacuum (55-58 °C, 0.7 mmHg). **S1** was thereby obtained as yellowish oil (4.06 g, 14.65 mmol, 88%).

^{1}H NMR (300 MHz, $CDCl_3$): δ = 6.73 (d, J(H,H) = 5.5 Hz, 1H), 6.71 (d, J(H,H) = 5.5 Hz, H), 3.89 (s, 3H), 0.28 (s, 9H).

3. Synthesis of tetrathia[7]helicene 2

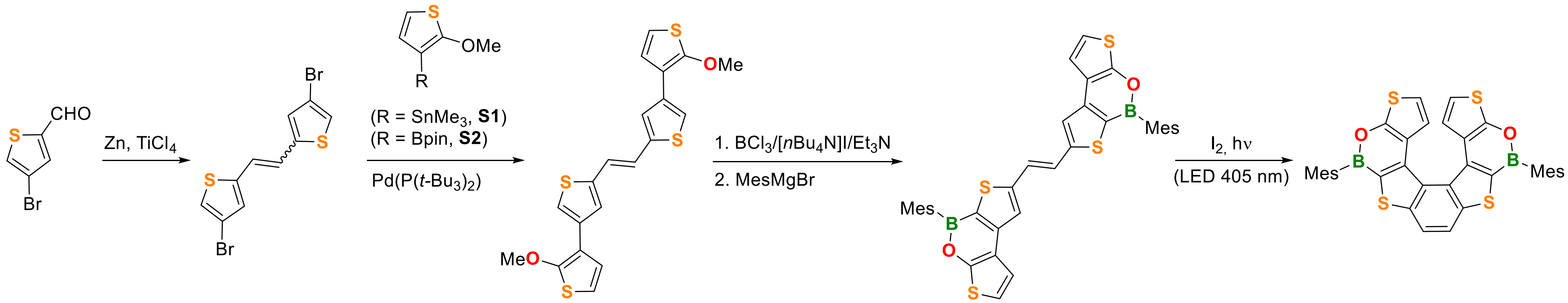

trans-**4** (89%)

trans-**5**

S1, R = $SnMe_3$ 41%
S2, R = Bpin 60%

***trans*-6** (31%)

2 (25%)

Scheme S1. Synthetic route to tetrathia[7]helicene **2**.

Synthesis of S1[S7] and S2[S8] starting materials

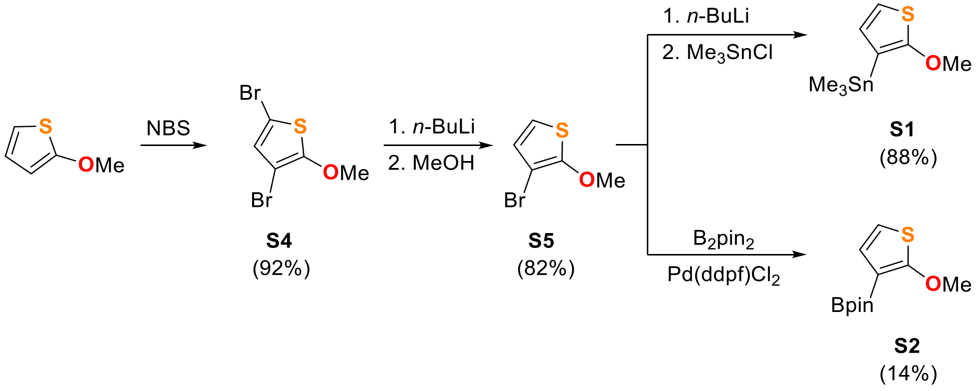

S4 (92%)

S5 (82%)

S1 (88%)

S2 (14%)

Scheme S2. Preparation of tetrathia[7]helicene **2** intermediates. Full details about the synthesis of **S4**, **S5**, **S1** and **S2** are provided in section *2.1 Thiophene starting materials*.

3.1 Synthesis of 4[S8a]

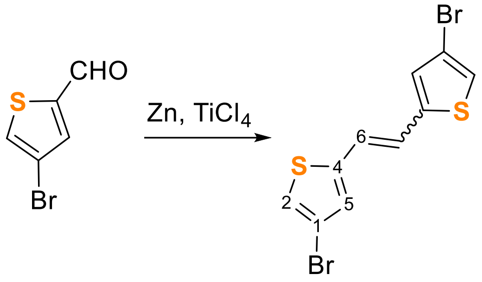

4

(89%)

A three-necked flame-dried 250 mL flask equipped with a thermometer and a reflux condenser was charged with THF (50 mL) and zinc powder (3.45 g, 52.67 mmol, 2.57 eq.). The resulting suspension was cooled to 0 °C and $TiCl_4$ (2.70 mL, 25.13 mmol, 1.2 eq.) was added dropwise during 10 min.

Note: the temperature increased due to the progressive addition of $TiCl_4$ (to ≈10-15 °C). The dark-green mixture thus obtained was heated to reflux for 1 h. In the meantime, a dropping funnel (equipped with a stirring bar) was flame-dried under vacuum and then charged with 4-bromo-2-thiophencarbaldehyde (3.91 g, 20.49 mmol) and THF (20 mL). The aldehyde solution was added dropwise during 10 min and the reaction mixture thus obtained was refluxed for 2 h. The reaction progress was checked by TLC.

After cooling to room temperature the THF was removed under reduced pressure, the residue was taken up with CH_2Cl_2 and filtered over a celite plug (washing with CH_2Cl_2). The CH_2Cl_2 black solution was treated with water (200 mL) and after separation of the two layers, the aqueous phase was extracted with CH_2Cl_2.

Note: for each extraction step, after separation of the two phases, the organic layer was filtered over a celite plug prior to combine with the collected organic phases.

The collected organic phases were dried over Na_2SO_4, filtered and the solvent was removed under reduced pressure. The crude product was washed with Et_2O yielding 2.93 g (8.37 mmol, 82%) of an orange solid which was proved to be *trans*-**4** *via* ^1H NMR analysis.

Et_2O mother liquors were evaporated to dryness yielding a dark brown wet solid which was purified *via* column chromatography (*n*-hexane/CH_2Cl_2 (2:1)) yielding 263 mg (0.75 mmol, 7%) of a yellow solid which was proved to be a *cis/trans* mixture (3:1) of **4** as inferred from ^1H NMR analysis. Total yield = 89%.

Trans-**4** single crystals suitable for X-ray crystallography were obtained by slow evaporation of a *trans*-**4** CH_2Cl_2 saturated hot solution.

Characterization data of *trans*-**4**:

^{1}H NMR (300 MHz, $CDCl_3$): $\delta = 7.10$ (d, ^4J(H,H) = 1.3 Hz, 2H; H-2), 6.97 (d, ^4J(H,H) = 1.3 Hz, 2H; H-5), 6.94 (s, 2H; H-6).

^{13}C{^{1}H} NMR (75 MHz, $CDCl_3$): $\delta = 142.6$ (C-4), 128.6 (C-5), 122.0 (C-2), 121.4 (C-6), 110.6 (C-1).

HRMS (EI+): Calculated m/z for $[C_{10}H_6Br_2S_2]^+$: 347.8278; found: 347.8288.

Characterization data of a **4** cis/trans (3:1) mixture:

^{1}H NMR (300 MHz, $CDCl_3$): δ = 7.17 (d, ^3J(H,H) = 1.4 Hz, 2H; *cis*-**4**-H2), 7.10 (d, ^3J(H,H) = 1.3 Hz; *trans*-**4**-H-2), 7.00 (d, ^3J(H,H) = 1.3 Hz, 2H; *cis*-**4**-H5), 6.97 (d, ^3J(H,H) = 1.3 Hz; *trans*-**4**-H-5), 6.94 (s; *trans*-**4**-H-6), 6.55 (s, 2H; *cis*-**4**-H6).

^{13}C{^{1}H} NMR (75 MHz, $CDCl_3$): δ = 142.6 (*trans*-**4**-C-4), 139.7 (*cis*-**4**-C-4), 130.9 (*cis*-**4**-C-5), 128.6 (*trans*-**4**-C-5), 124.0 (*cis*-**4**-C-2), 123.2 (*cis*-**4**-C-6), 122.0 (*trans*-**4**-C-2), 121.4 (*trans*-**4**-C-6), 110.6 (*trans*-**4**-C-1), 109.9 (*cis*-**4**-C-1).

3.2 Synthesis of 5 *via* Stille coupling

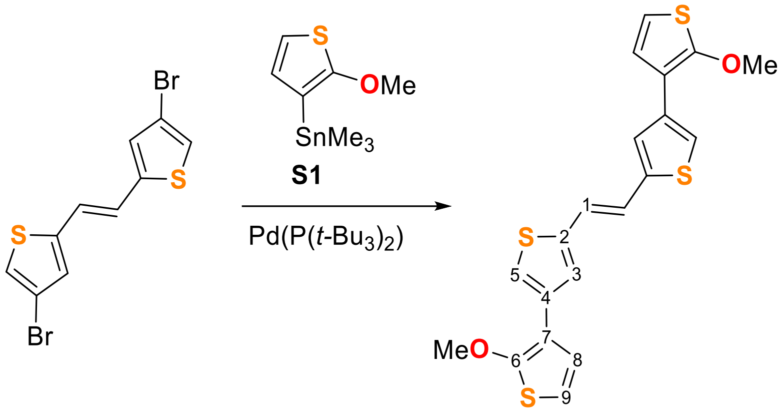

trans-**4**

trans-**5**

(42%)

A flame-dried 250 mL J-Young tube was charged with *trans*-**4** (430 mg, 1.23 mmol) and evacuated for 30 min. Toluene (60 mL) was added and the orange solution thus obtained was treated with **S1** (714 mg, 2.58 mmol, 2.10 eq.) and Pd(P(*t*-Bu$_3$)$_2$) (61 mg, 0.12 mmol, 0.10 eq.) and the resulting deep orange solution was heated to 80 °C and stirred for 17 h.

Note: after roughly 10 min heating the reaction mixture turns to dark brown.

After cooling to room temperature, toluene was removed under reduced pressure and the grey residue thus obtained was purified *via* column chromatography (*n*-hexane/CH$_2$Cl$_2$ (2:1)). The fractions containing *trans*-**5** were combined and evaporated to dryness. The yellow residue thus obtained was washed with *n*-pentane (to remove the stannane homocoupling byproduct and unknown minor impurities). *Trans*-**5** was thereby obtained as a pale-yellow solid (215 mg, 0.52 mmol, 42%).

^{1}H NMR (500 MHz, CDCl$_3$): δ = 7.39 (d, ^4J(H, H) = 1.4 Hz, 2H; H-3), 7.36 (d, ^4J(H, H) = 1.4 Hz, 2H; H-5), 7.08 (s, 2H; H-1), 7.04 (d, ^3J(H, H) = 5.9 Hz, 2H; H-9), 6.62 (d, ^3J(H, H) = 5.9 Hz, 2H; H-8), 4.01 (s, 6H; OMe).

^{13}C{^{1}H} NMR (126 MHz, CDCl$_3$): δ = 160.7 (C-6), 141.9 (C-2), 135.6 (C-4), 125.8 (C-3), 125.7 (C-9), 121.7 (C-1), 119.2 (C-5), 116.3 (C-7), 111.1 (C-8), 61.9 (OMe).

HRMS (MALDI): *Calc. m/z* for [C$_{20}$H$_{16}$O$_2$S$_4$]$^+$: 416.0028, found 416.0026.

3.3 Synthesis of 5 *via* Suzuki coupling

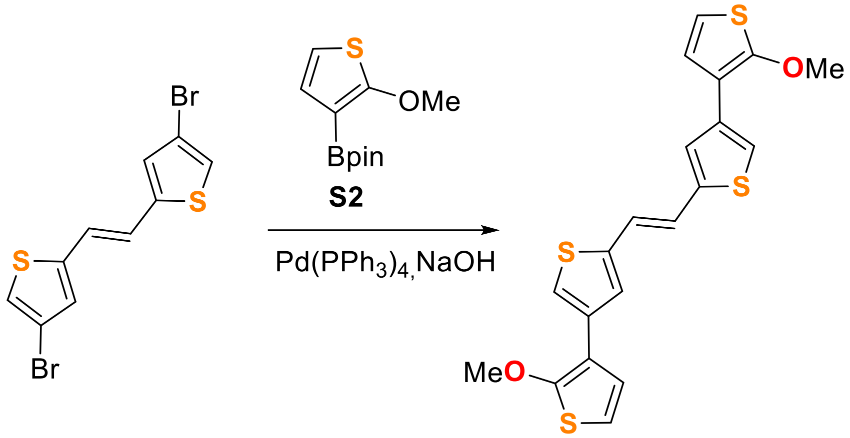

trans-**4**

trans-**5**

(60%)

A flame-dried J-young flask was charged with *trans*-**5** (153 mg, 0.44 mmol) and **S2** (252 mg, 1.05 mmol, 2.40 eq.) and then evacuated for 30 min. THF (9 mL), $NaOH_{(aq)}$ (3M; 0.58 mL, 1.75 mmol, 4.0 eq.) and $Pd(PPh_3)_4$ (51 mg, 0.044 mmol, 0.10 eq.) were added. The dark brown mixture thus obtained was heated to 80 °C for 15 h. After cooling to room temperature, the solvent was removed under reduced pressure and the crude product was purified *via* column chromatography (*n*-hexane/CH_2Cl_2 (1:1), $R_f = 0.60$). The fractions containing *trans*-**5** were evaporated to dryness and the yellow residue thus obtained was washed with *n*-pentane (to remove unknown minor impurities). *Trans*-**5** was obtained as a pale-yellow solid (110 mg, 0.26 mmol, 60%). Single crystals of *trans*-**5** were obtained by slow evaporation of a saturated solution of *trans*-**5** in CH_2Cl_2/*n*-hexane (2:1).

3.4 Synthesis of 6

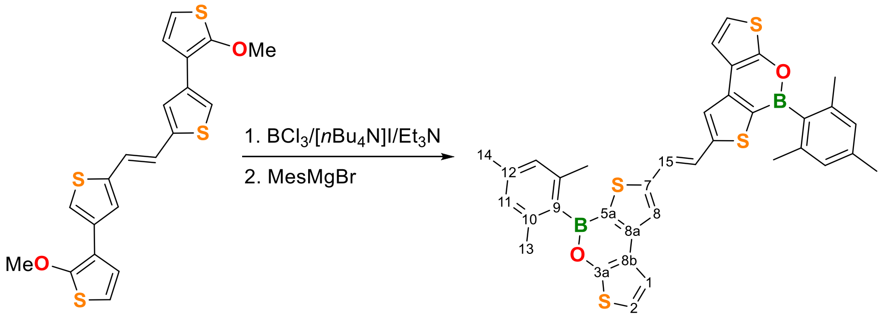

***trans*-19**

***trans*-6**

(31%)

A flame-dried 100 mL J-Young tube was charged with *trans*-**5** (150 mg, 0.36 mmol), [nBu$_4$N]I (319 mg, 0.86 mmol, 2.40 eq.) and then evacuated for 30 min. Chlorobenzene (15 mL) was added and the mixture was cooled to –10 °C. BCl_3 (1.0 M in hexanes; 0.79 mL, 0.79 mmol, 2.20 eq.) and Et_3N (1.0 M in chlorobenzene; 0.72 mL, 0.72 mmol, 2.00 eq.) were added, the Young-tap was closed, and the reaction mixture was allowed to warm to room temperature. The mixture thus obtained was stirred for 24 h at 135 °C. After cooling to room temperature, the yellow-brown mixture was evaporated to dryness and THF (15 mL) was added. MesMgBr (0.95 M in THF; 2.27 mL, 2.16 mmol, 6.00 eq.) was added dropwise at room temperature to give a red mixture, which was stirred for 1 h. The solvent was removed under reduced pressure and the residue was purified by column chromatography ($d = 2.0$ cm, n-hexane/CH_2Cl_2 (2:1)). The fractions containing *trans*-**6** were combined and evaporated to dryness. The yellow residue thus obtained was treated with n-pentane (to remove unknown minor impurities). *Trans*-**6** was thereby obtained as a yellow solid (72 mg, 0.11 mmol, 31%).

Single crystals of *trans*-**6** suitable for X-ray analysis were obtained by slow evaporation of a saturated solution of *trans*-**6** in n-hexane/CH_2Cl_2 (2:1).

^{1}H NMR (400 MHz, $CDCl_3$): δ = 7.56 (s, 2H; H-8), 7.37 (s, 2H; H-15), 7.32 (d, ^3J(H,H) = 6.0 Hz, 2H; H-2), 6.96 (d, ^3J(H,H) = 6.0 Hz, 2H; H-1), 6.93 (s, 4H; H-11), 2.36 (s, 6H; H-14), 2.27 (s, 12H; H-13).

^{13}C{^{1}H} NMR (101 MHz, $CDCl_3$): δ = 158.9 (C-3a), 153.2 (C-8a), 147.9 (C-7), 140.6 (C-10), 139.0 (C-12), 133.6 (C-9), 131.6 (C-5a), 127.6 (C-11), 124.8 (C-15), 122.5 (C-8), 120.3 (C-2), 120.0 (C-8b), 114.9 (C-1), 22.8 (C-13), 21.5 (C-14).

^{11}B NMR (128 MHz, $CDCl_3$): not detected.

Note: the presence of boron is evidenced by the typical broadened resonances of B(sp^2)-bound quaternary carbons (C-9, C-5a) and by the ^3J(C,H) coupling between C-9 (133.6 ppm) and H-11 (6.93 ppm) observed in the ^{H,C}HMBC spectrum.

HRMS (MALDI): Calculated *m/z* for [$C_{36}H_{30}B_2O_2S_4$]$^+$: 644.1315; found: 644.1326.

UV/Vis (*c*-hexane): λ_{max} (ε / mol^{-1}dm^{3}cm^{-1}) = 270 (26500), 355 (30700), 370 (30000), 393 (21500), 414 (sh).

Fluorescence (*c*-hexane, λ_{ex} = 375 nm): λ_{max} = 429, 452 nm (resolved vibrational fine structure), 489 nm (sh); Φ_{PL} = 6%.

Cyclic voltammetry (THF, 0.1 M [nBu$_4$N][PF$_6$], 200 mV s^{-1}, vs. FcH/FcH$^+$): Cathodic scan: $E^{I}_{1/2} = -1.97$ V, $E^{II}_{pc} = -2.26$ V, $E^{II}_{pa} = -2.14$ V.

3.5 Synthesis of 2

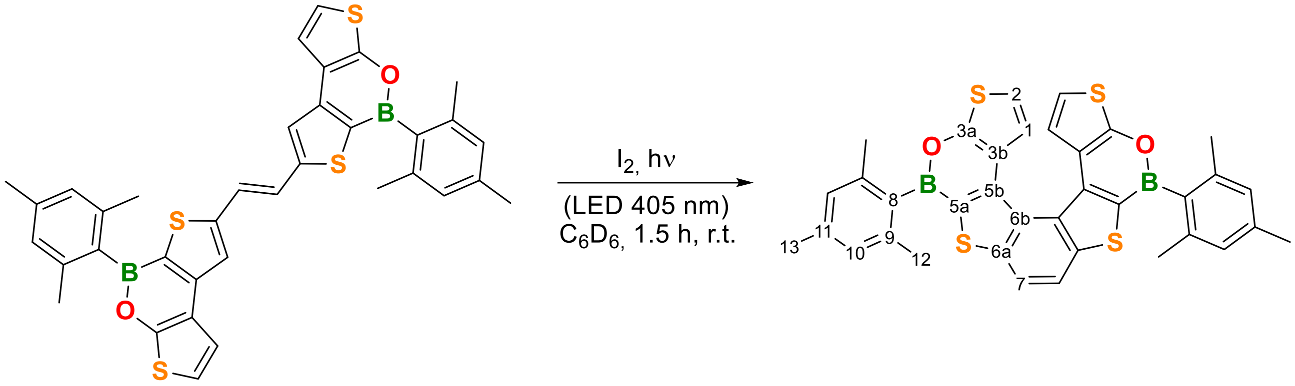

***trans*-6**

2

(25%)

Four NMR tubes charged with *trans*-**6** and C_6D_6 (10 mg/1mL), for total amount of: *trans*-**6** (40 mg, 0.015mmol) and C_6D_6 (40 mL). The resulting yellow solutions were irradiated with the 405 nm LED lamp (placed close to the tubes, approx. 5 cm; NMR tubes glass is transparent to 405 nm light[S13]) until almost complete disappearance of the alkene precursors (1.5 h; reaction progress monitored by ^{1}H NMR). Reaction mixtures of the four NMR tubes were combined, the solvent evaporated, giving a brown residue which was purified by preparative TLC (*n*-hexane/CH_2Cl_2 (3:1)). The yellow solid thus obtained was washed with CH_2Cl_2 to give **2** as an off-white solid (10 mg, 0.06 mmol, 25%).

^{1}H NMR (400 MHz, $CDCl_3$): δ = 8.03 (s, 2H; H-7), 6.99 (s, 4H; H-10), 6.93 (d, ^3J(H,H) = 6.0 Hz, 2H; H-2), 6.52 (d, ^3J(H,H) = 6.1 Hz, 2H; H-1), 2.39 (s, 6H; H-13), 2.36 (s, 12H; H-12).

^{13}C{^{1}H} NMR (100.6 MHz, $CDCl_3$): δ = 158.8* (C-3a), 145.5 (C-6a), 140.8 (C-11), 139.3 (C-9), 133.3* (C-8), 131.0 (C-6b), 127.8 (C-10), 123.0 (C-2), 122.6 (C-7) 121.3 (C-3b), 112.4 (C-1), 22.9 (C-12), 21.5 (C-13). *) unequivocally detected only in the ^{H,C}HMBC spectrum. C-5a, C-6a n.o..

^{11}B NMR (128.4 MHz, $CDCl_3$): not detected.

Note: the presence of boron is evidenced by the ^3J(C,H) coupling between C-8 (133.3* ppm) and H-10 (6.99 ppm) observed in the ^{H,C}HMBC spectrum.

HRMS (EI+): Calculated *m/z* for $[C_{36}H_{28}B_2O_2S_4]^+$: 642.1158; found: 642.1128.

UV/Vis (*c*-hexane): λ_{max} (ε / mol^{-1}dm^{3}cm^{-1}) = 258 (21900), 271 (sh), 319 (4600) 334 (4200), 368 (10600), 385 (12400), 413 (5000).

Fluorescence (*c*-hexane, λ_{ex} = 385 nm): λ_{max} = 424, 446, 472 nm (resolved vibrational fine structure); 506 nm (sh); Φ_{PL} = 7%.

Cyclic voltammetry (THF, 0.1 M [*n*Bu_4N][PF_6], 500 mV s^{-1}, vs. FcH/FcH$^+$): Cathodic scan: E^{I}_{pc} = −1.66 V, E^{II}_{pc} = − 2.36 V E_{pa} = 0.82 V.

4. Synthesis of tetrathia[7]helicene 3

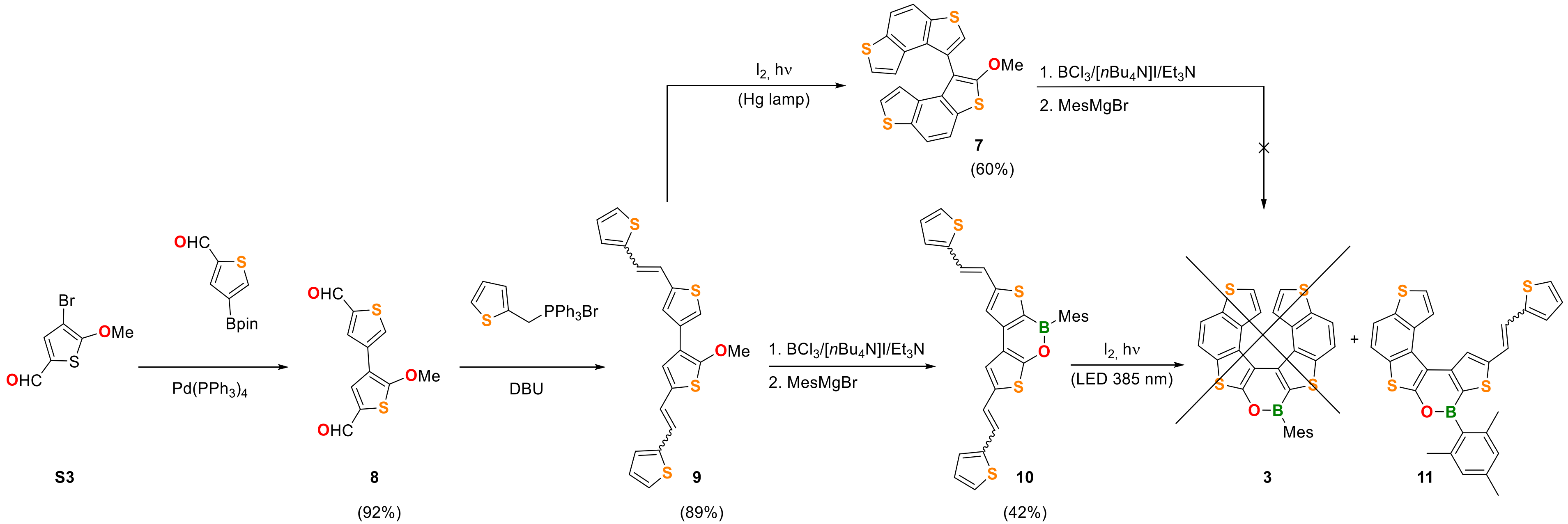

Scheme S3. Synthetic route to tetrathia[7]helicene **3**.

Synthesis of S3[S6]

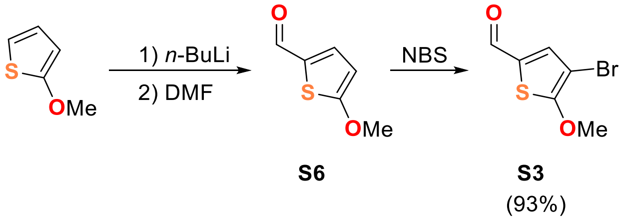

Scheme S4. Preparation of tetrathia[7]helicene **3** intermediates. Full details about the synthesis of **S6** and **S3** are provided in section *2.1 Thiophene starting materials*.

4.1 Synthesis of 8

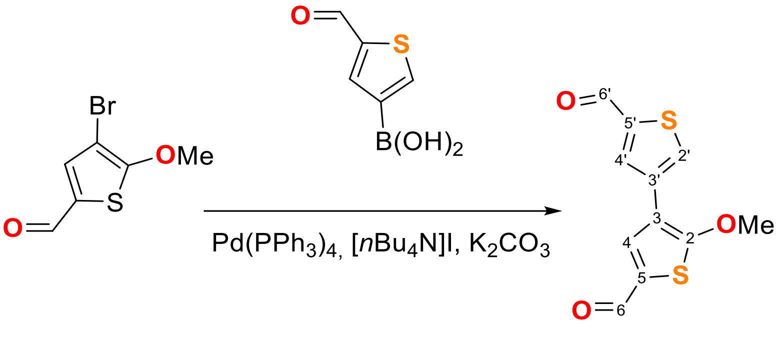

S3

8

(92%)

A flame-dried 100 mL J-Young tube was charged with 2-thiophenecarbaldehyde-3-boronic acid (332 mg, 1.50 mmol), **S3** (357 mg, 1.50 mmol, 1.0 eq.), [*n*Bu_4N]I (48 mg, 0.15 mmol, 0.1 eq) and then evacuated for 20 min. THF/H_2O (5:1; 11 mL) was added and the resulting suspension was treated with $Pd(PPh_3)_4$ (87 mg, 0.075 mmol, 0.05 eq) and K_2CO_3 (415 mg, 3.0 mmol, 2 eq). The Young-tap was closed, and the black mixture thus obtained was heated with stirring to 80 °C for 14 h. After cooling to room temperature, the solvent was removed under reduced pressure, and the residue was purified by column chromatography (CH_2Cl_2, then CH_2Cl_2/AcOEt (20:1), $R_f = 0.30$). **8** was obrained as a yellow solid (350 mg, 1.39 mmol, 92%). Single crystals of **8** suitable for X-ray crystallography were grown by slow evaporation of a saturated solution of **8** in *n*-pentane/CH_2Cl_2 (1:1).

^{1}H NMR (500 MHz, $CDCl_3$): δ = 9.97 (d, ^4J(H,H) = 1.3 Hz, 1H; H-6'), 9.74 (s, 1H; H-6), 8.07 (d, ^3J(H,H) = 1.3 Hz, 1H; H-2'), 7.97 (t, ^3J(H,H) = 1.3 Hz, 1H; H-4'), 7.83 (s, 1H; H-4), 4.18 (s, 3H; CH_3).
Note: H-4' couples with H-6' and H-2' (as evidenced by the ^{HH}COSY spectrum) with almost identical coupling constant (1.2, 1.4, 1.3 Hz respectively, which have been all rounded to 1.3 Hz) giving rise to a triplet (originated by a collapsed doublet of doublets).

^{13}C{^{1}H} NMR (126 MHz, $CDCl_3$): δ = 183.0 (C-6'), 182.1 (C-6), 170.6 (C-2), 143.9 (C-3'), 136.1 (C-4), 134.9 (C-2'), 130.4 (C-4'), 128.7 (C-5), 117.1 (C-3), 62.1 (CH_3), n.o. (C-5).
HRMS (MALDI): Calculated *m/z* for $[C_{11}H_9O_3S_2]^+$: 252.9988; found: 252.9988.

4.2 Synthesis of 9

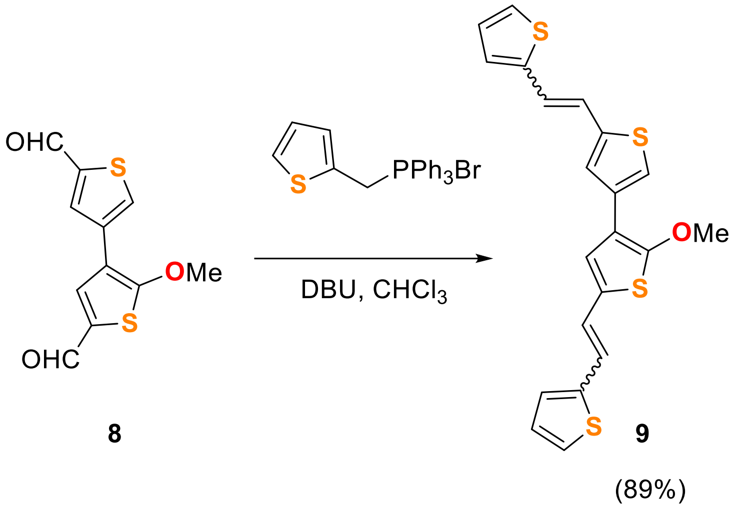

A three-necked flask (equipped with a reflux condenser and a thermometer) was charged with triphenyl(2-thienylmethyl)phosphonium bromide (1.20 g, 2.73 mmol, 2.2 eq) and $CHCl_3$ (30 mL). DBU (416 mg, 2.73 mmol, 2.2 eq) was added and the rsulting orange solution was heated to 40 °C. **8** (313 mg, 1.24 mmol) was added in portions (during 5 min) as $CHCl_3$ suspension (12 mL). The reaction mixture was heated to 60 °C and stirred for 4 h. TLC after 4 h showed complete conversion of the starting aldehyde **8** and the presence of the desired compound **9** ($R_f = 0.95$) besides the mono-olefinated compound ($R_f = 0.50$). Additional 0.2 eq of DBU were added and the reaction mixture was stirred at 60 °C for additional 3 h. After cooling to room temperature the reaction mixture was poured into water (20 mL) and HCl 0.5 M (10 mL) was added. After separation of the two layers, the aqueous phase was extracted with CH_2Cl_2 (3 × 25 mL). The combined organic phases were dried over Na_2SO_4, filtered and the solvent removed. The brown residue thus obtained was purified by column chromatography (30 cm silica gel, $d = 2.5$ cm, CH_2Cl_2, $R_f = 0.95$). **9** was obtained as a yellow-brown solid (456 mg, 1.10 mmol, 89%). ^{1}H NMR (Figure S13) revealed the presence of the four isomers (*trans,trans; trans,cis; cis,trans; cis,cis*): those are easily detectable since the -OMe group shows four well-distinguished resonances in the ^{1}H NMR spectrum. Single crystals of *E,E*-**9** suitable for X-ray crystallography were grown by slow evaporation of a saturated solution of **9** in *n*-pentane/CH_2Cl_2 (1:1).

To reduce the complexity of the isomers mixture and facilitate NMR characterization, **9** was treated with Et_2O and *n*-pentane and decanted and the solid thus obtained was used for NMR characterization (^{1}H and ^{13}C spectra in Figure S14 and S15). Assignment of **9** proton and carbon resonances was attempted but, due to the high complexity of both 1D and 2D spectra, it was only possible to identify few resonances (aromatic CH, double bonds and OMe protons). For simplicity, ^{1}H NMR integrals have not been listed and are shown in Figure S14. Quaternary carbons (Cq), CH (CH) and CH_3 (OMe) resonances were identified *via* ^{13}C APT.

Note: following photocyclization and borylation experiments were carried out using **9** as obtained after column chromatography purification (mixture of the four isomers, ^{1}H in Figure S13).

^{1}H NMR (600 MHz, $CDCl_3$): δ 7.46 (s), 7.42 (d, $J = 1.3$ Hz), 7.35 (d, $J = 1.3$ Hz), 7.34 (s), 7.33 – 7.32 (m), 7.29 (dd, $J = 5.1, 1.1$ Hz), 7.27 (s), 7.19 (t, $J = 4.4$ Hz), 7.17 – 7.13 (m), 7.11 (s), 7.06 (s), 7.06 – 6.97 (m), 6.96 (s), 6.92 (dd, J = 15.8, 6.7 Hz), 6.84 (dd, J (H,H) = 15.8; two overlapped isomers double bond resonances), 6.64 (d, J(H,H) = 12.0 Hz; double bond), 6.60 (d, J(H,H) = 12.0 Hz; double bond), 6.49 (d, J(H,H) = 12.0 Hz; double bond), 6.48 (d; double bond), 4.04 (s; OMe), 4.01 (s; OMe), 3.96 (s; OMe), 3.93 (s; OMe).

^{13}C NMR (150 MHz, $CDCl_3$): δ = 160.9 (Cq), 159.3 (Cq), 159.2 (Cq), 142.6 (Cq), 142.6 (Cq), 142.4 (Cq), 141.8 (Cq), 141.8 (Cq), 139.1 (Cq), 138.6 (Cq), 135.1 (Cq), 135.0 (Cq), 134.3 (Cq), 128.4 (Cq), 128.2 (Cq), 127.9 (Cq), 127.9 (Cq), 127.8 (CH), 127.7 (CH), 127.6 (CH), 127.5 (CH), 127.0 (CH), 126.8 (CH), 126.3 (CH), 126.1 (CH), 125.7 (CH), 125.6 (CH), 125.4 (CH), 125.3 (CH), 125.01 (CH), 124.9 (CH), 124.3 (CH), 124.3 (CH), 123.8 (CH), 123.8 (CH), 123.0 (CH), 122.7 (CH), 122.1 (CH), 122.0 (CH), 121.6 (CH), 121.6 (CH), 121.5 (CH), 121.4 (CH), 121.2 (CH), 120.2 (CH), 119.3 (CH), 118.9 (CH), 118.8 (CH), 116.9 (Cq), 116.7 (Cq), 115.7 (Cq), 61.7 (OMe), 61.7 (OMe), 61.5 (OMe).

HRMS (MALDI): Calculated m/z for $[C_{21}H_{16}OS_4]^+$: 412.0078; found: 412.0077.

4.3 Synthesis of 7

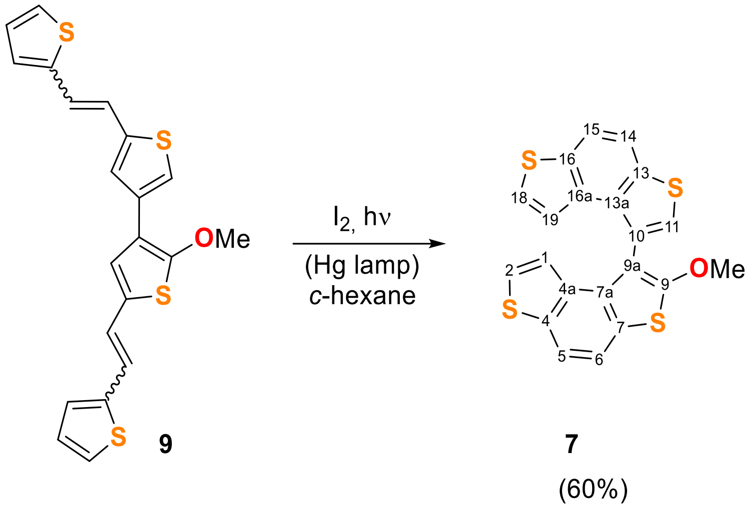

A solution of **9** (0.48 mmol) and iodine (18 mg, 0.14 mmol, 0.3 eq) in *c*-hexane (750 mL) was stirred at room temperature and irradiated with a 125 W medium-pressure Hg lamp for 2 h and 45 min. The reaction progress was checked by TLC. After the complete conversion of the starting material, the reaction mixture was filtered to remove insolubles. The purple clear solution thus obtained was washed with a saturated aqueous solution of $Na_2S_2O_3$ yielding a yellow solution. The collected organic phases were dried over Na_2SO_4, filtered and the solvent was removed under reduced pressure. The brown oily residue thus obtained was purified by column chromatography (15 cm silica gel, d = 2.0 cm, n-hexane/CH_2Cl_2 (3:1), R_f = 0.32). **7** was obtained as an off white solid (119 mg, 0.29 mmol, 60%).

^{1}H NMR (300 MHz, $CDCl_3$): δ = 7.92 (d, ^3J(H,H) = 8.6 Hz, 1H; H-15), 7.88 (d, ^3J(H,H) = 8.7 Hz, 1H; H-14), 7.78 (d, ^3J(H,H) = 8.6 Hz, 1H; H-6), 7.72 (d, ^3J(H,H) = 8.6 Hz, 1H; H-5), 7.56 (s, 1H; H-11), 7.17 (d, ^3J(H,H) = 5.5 Hz, 1H; H-19), 7.04 (d, ^3J(H,H) = 5.5 Hz, 1H; H-1), 6.82 (d, ^3J(H,H) = 5.5 Hz, 1H; H-18), 6.41 (d, J = 5.5 Hz, 1H; H-2), 3.91 (s, 3H).

^{13}C NMR (75 MHz, $CDCl_3$): δ = 162.4 (C-9), 138.2 (C-4), 137.7 (C-16), 137.1 (C-10), 134.8 (C-16a), 134.1 (C-9a), 133.8 (C-4a), 133.3 (C-7), 130.1 (C-13), 126.6 (C-11), 126.3 (C-7a), 126.2 (C-19), 125.6 (C-1), 121.7 (C-18), 121.5 (C-2), 119.5 (C-14), 119.2 (C-15), 118.7 (C-5), 117.7 (C-6), 112.2 (C-13a), 62.0 (CH_3).

HRMS (EI+): Calculated m/z for $[C_{21}H_{12}OS_4]^+$: 407.9737; found: 407.9771.

4.4 7 borylation attempts and synthesis of 7-OH

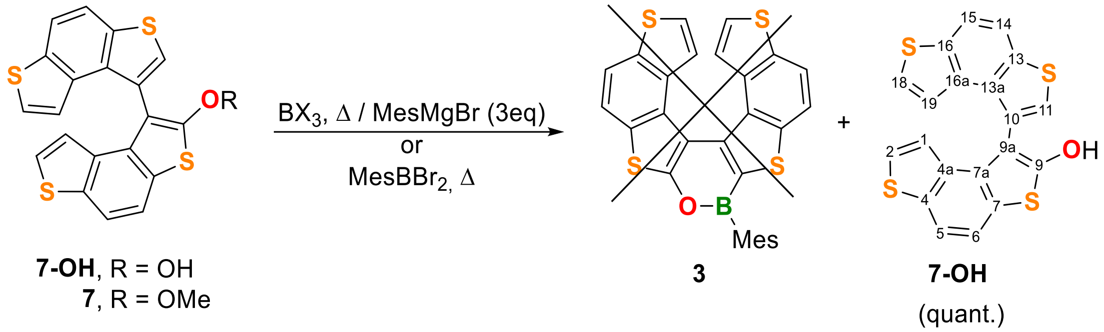

Table S1. 7 borylation attempts. Entries 1, 2,3 preparative experiments; entry 4, 5 NMR experiments performed using a flame-sealed NMR tube in a thermostated oven at temperatures ranging from 135 to 180 °C.

Entry	R	Borane	Base	additive	solvent	temperature	time
1	OMe	BCl_3 (1.5 equiv)	Et_3N (1.0 eq.)	*n*[Bu_4N]I (1.2 eq.)	chlorobenzene	135 °C	24h
2	OMe	BBr_3 (1.5 equiv)	Et_3N (1.0 eq.)	//	chlorobenzene	135 °C	18h
3	OH	BCl_3 (1.5 equiv)	Et_3N (1.0 eq.)	//	chlorobenzene	135 °C	24h
4	OMe	$MesBBr_2$ (1.5 equiv)	Et_3N (1.0 eq.)	//	C_6D_6	135 to 180 °C	18h + 30h
5	OMe	$MesBBr_2$ (1.5 equiv)	//	//	C_6D_6	135 to 180 °C	24h + 84h

Note: **7-OH** was purified *via* column chromatography or preparative TLC (*n*-hexane/CH_2Cl_2 (7:3).

Synthesis of 7-OH

A flame-dried Schlenk flask was charged with **7** (40 mg, 0.1 mmol) and CH_2Cl_2 (1 mL); the resulting colorless solution was cooled to 0 °C. BBr_3 (*d* = 2.64; 100 µl, 1.05 mmol, 10.5 equiv) was added *via* Hamilton syringe yielding a blue mixture which was stirred at 0 °C for 10 min and then allowed to warm up to r.t.. Ice-cold water (5 mL) was added and the resulting mixture was extracted with CH_2Cl_2 (4x10 mL). The combined organic phases were dried over Na_2SO_4, filtered and the solvent removed under reduced pressure. A yellowish solid was obtained and it was proved to be the desired compound by NMR and HRMS analysis (39 mg, 0.099 mmol; y = quantitative).

^{1}H NMR (400 MHz, $CDCl_3$): δ = 8.16 (d, ^3J(H,H) = 5.5 Hz, 1H; H-19), 7.97 – 7.91 (m, 2H; H-6, H-15), 7.83 (d, ^3J(H,H) = 8.6 Hz, 1H; H-14), 7.67 (d, ^3J(H,H)= 5.6 Hz, 1H; H-18), 7.46 (d, ^3J(H,H) = 8.4 Hz, 1H; H-5), 7.34 (d, ^3J(H,H) = 5.5 Hz, 1H; H-1), 6.85 (s, 1H; H-11), 6.62 (d, ^3J(H,H) = 5.5 Hz, 1H; H-2), 6.31 (s, 1H; OH). Note: the assignment of the -OH resonance (6.31 ppm) was confirmed by deuteration test, see Figure S19.
^{13}C{^{1}H} NMR (101 MHz, $CDCl_3$) δ = 139.0 (C-4), 138.5 (C-16), 138.2 (C-13), 136.4 (C-4a), 134.2 (C-16a), 132.8 (C-13/13a), 131.9 (C-13/13a), 131.0 (C-9a), 130.00 (C-7/C-7a) , 129.9 (C-7/C-7a), 129.3 (C-1), 126.7 (C-18), 125.3 (C-11), 123.7 (C-5), 122.0 (C-19), 121.8 (C-2), 119.7 (C-15), 119.4 (C-14), 118.9 (C-5). C-9 n.o.

HRMS (MALDI): Calculated *m/z* for $[C_{20}H_{10}OS_4]^+$: 392.9536; found: 392.9536.

4.5 Synthesis of 10

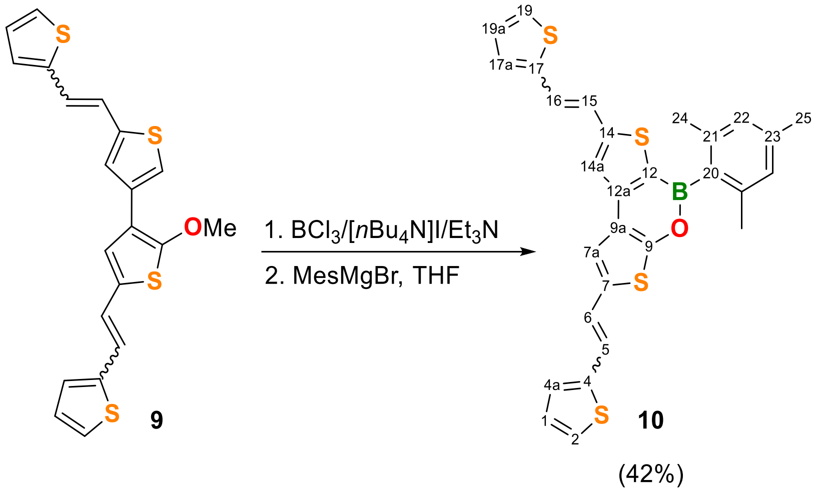

A flame-dried 100 mL J-Young tube was charged with **9** (150 mg, 0.36 mmol), [nBu$_4$N]I (161 mg, 0.44 mmol, 1.20 eq.), and evacuated for 30 min. Chlorobenzene (10 mL) was added and the resulting solution was cooled to –10 °C. BCl_3 (1.0 M in hexanes; 400 µL, 0.40 mmol, 1.1 eq.) and Et_3N (0.5 M in chlorobenzene; 730 µL, 0.36 mmol, 1.00 eq.) were added, the Young-tap was closed and the yellow-green reaction mixture was allowed to warm up to room temperature. The reaction mixture thus obtained was heated to 135 °C and stirred for 24 h. After cooling to room temperature a brown mixture was obtained. The solvent was evaporated to dryness and THF (10 mL) was added. MesMgBr (1.0 M in THF; 1.08 mL, 1.08 mmol, 3.00 eq.) was added dropwise at room temperature to give a red mixture, which was stirred for 1 h. The solvent was removed under reduced pressure and the residue was purified by column chromatography (17 cm silica gel, d = 2.0 cm, n-hexane/CH_2Cl_2 (5:1), R_f = 0.30). The fractions containing **10** were evaporated giving a yellow solid (80 mg, 0.15 mmol, 42%) containing the *trans,trans*-isomer as major component. **10** was washed with n-pentane and *E,E*-**10** (70 mg, 0.13 mmol, 37%) was thereby obtained as a bright-yellow solid. Single crystals of *E,E*-**10** suitable for X-ray crystallography were obtained by slow evaporation of a *E,E*-**10** saturated solution in n-heptane/CH_2Cl_2 (1:1).

^{1}H NMR (500 MHz, $CDCl_3$): δ = 7.46 (s, 1H; H-14a), 7.28/7.25 (d, ^3J(H,H) = 15.8 Hz, 1H; H-15), 7.27/7.26 (d, ^3J(H,H) = 5.2 Hz, 1H; H-19), 7.22 (s, 1H; H-7a), 7.21/7.20 (d, ^3J(H,H) = 5.2 Hz, 1H; H-19a), 7.18/7.15 (d, ^3J(H,H) = 15.8 Hz, 1H; H-16), 7.11(d, ^3J(H,H) = 3.4 Hz, 1H; H-17a), 7.08+7.05 (d, ^3J(H,H) = 15.8 Hz, 1H; H-6), 7.07 (d, ^3J(H,H) = 3.5 Hz, 1H; H-4a), 7.03-7.01 (dd, ^3J(H,H) = 4.8 Hz, ^4J(H,H) = 3.5 Hz, 2H; H-2, H-1), 7.01/6.98 (d, ^3J(H,H) = 15.8 Hz, 1H; H-5), 6.92 (s, 2H; H-22), 2.35 (s, 3H; H-25), 2.28 (s, 6H; H-24). Note: most of the proton resonances are overlapped and, ^{1}H assignment was aided by the analyisis of coupling constants and correlations found in ^{HH}COSY and HMBC spectra.

$^{13}C\{^1H\}$ NMR (126 MHz, $CDCl_3$): δ = 157.6 (C-9), 154.5 (C-14), 147.4 (C-12a), 142.3 (C-4), 141.8 (C-17), 140.6 (C-21), 139.0 (C-23), 133.5 (br.; C-20), 132.0 (C-7), 130.7 (br.; C-12), 128.0 (C-1/C-2), 128.0 (C-1/C-2), 127.8 (C-17a), 127.6 (C-22) , 126.3 (C-4a), 125.9 (C-19), 125.6 (C-15), 124.6 (C-19a), 122.0 (C-5), 121.2 (C-14a), 121.1 (C-6), 120.9 (C-16), 120.7 (C-9a), 119.1 (C-7a), 22.8 (C-25), 21.5 (C-24).

^{11}B NMR (96 MHz, $CDCl_3$): δ = 41.70 ($h_{1/2} \approx$ 375 Hz).

HRMS (MALDI): Calculated *m/z* for $[C_{29}H_{23}BOS_4]^+$: 526.0719; found: 526.0717.

UV/Vis (*c*-hexane): λ_{max} (ε / $mol^{-1}dm^3cm^{-1}$) = 283 (15400), 365 (41000), 382 (36500).

Fluorescence (*c*-hexane, λ_{ex} = 365 nm): λ_{max} = 445, 472, 500 nm (resolved vibrational fine structure), 535 (sh); Φ_{PL} = 12%.

Cyclic voltammetry (THF, 0.1 M [*n*Bu_4N][PF_6], 200 mV s^{-1}, vs. FcH/FcH^+): Cathodic scan: $E_{pc} = -2.21$ V, E^{I}_{pa} = 0.61V, E^{II}_{pa} = 0.99 V.

4.6 Attempt of 10 photocyclization

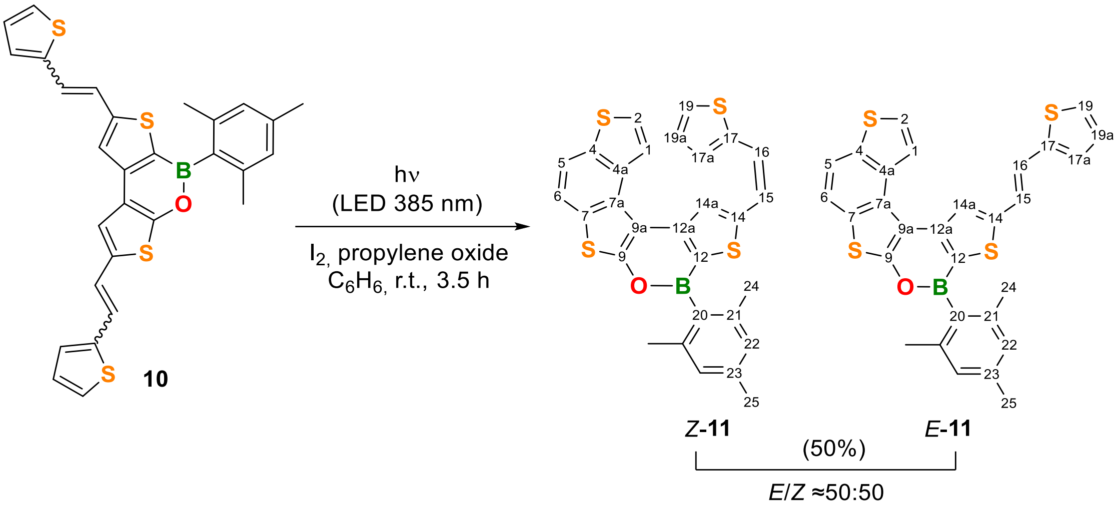

A flame-dried 250 mL J-Young tube was charged with **10** (70 mg, 0.13 mmol) and evacuated for 30 min. C_6H_6 (150 mL) was added and the resulting green solution was treated with I_2 (70 mg, 0.27 mmol, 2.1 eq.) and propylene oxide (1.86 mL, 26.5 mmol, 200 eq.). The red solution thus obtained was irradiated with an LED lamp (385 nm - placed close to the reaction vessel, approx. 5 cm; the Duran® glass used is transparent to 385 nm light).[S6] The reaction progress was monitored by TLC (*c*-hexane/CH_2Cl_2 (5:1)).

Note: Even though *Rf* of **10** and **11** is almost identical, it is possibile to differentiate the two products on TLC: **10** shows a yellow spot under 254, 366 nm light (the spot turns to green after exposure to air); **11** shows blue spot at 254 nm and light-blue spot at 366 nm.

The solvent was evaporated, and the residue was purified by column chromatography (15 cm silica gel, *d* = 2.0 cm, *n*-hexane/CH_2Cl_2 (5:1)). A green-yellow solid was obtained and it was proved to be a mixture of *E*-**11**/*Z*-**11** by ^{1}H, ^{HH}COSY NMR analysis (35 mg, 0.065 mmol; y = 50 %). The average *E*/*Z* ratio obtained in the above described conditions is ≈ 50:50. A mixture slightly enriched in the *E* or *Z* isomer can be also obtained.

Single crystals of *E*-**11** suitable for X-ray crystallography were grown by slow evaporation of a saturated solution of the *E*-**11**/*Z*-**11** (≈60:40) mixture in *n*-pentane/CH_2Cl_2 (2:1) in a glovebox.

Characterization data of *Z*-**11** (see Figure S24):

^{1}H NMR (400MHz, CD_2Cl_2): δ = 8.24 (s, 1H; H-14a, 8.08 (d, ^3J(H,H) = 5.6 Hz, 1H; H-1), 7.98-7.93 (m, 1H; H-5, overlapped with *E*-**11** resonances), 7.80-7.75 (m, 2H; H-5/H-6, overlapped with *E*-**11** resonances), 7.57 (d, ^3J(H,H) = 5.6 Hz, 1H; H-2), 7.33 (d, J(H,H) = 3.7 Hz, 1H; H-17a/H-19/H-19a, overlapped with *E*-**11** resonances), 7.22 (d, ^3J = 3.7 Hz, 1H; H-17a/H-19/H-19a), 7.01 (t (originated by two collapsed doublets), ^3J = 3.7 Hz, 1H; H-17a/H-19/H-19a), 6.93 (s, 2H; H-22), 6.89 (d, ^3J = 11.9 Hz, 1H; H-15), 6.77 (d, ^3J = 11.9 Hz, 1H; H-16), 2.34 (s, 3H; H-25), 2.28 (s, 6H; H-24). Assignment was aided by ^{HH}COSY spectrum.

Note: of high diagnostic value are the resonances of protons H-15 (6.89 ppm) and H-16 (6.77 ppm) showing a typical *cis*-coupling constant $^3J(H,H)_{cis}$ = 11.9 Hz.

Characterization data of *E*-**11** (see Figure S25):

^{1}H NMR (400MHz, CD_2Cl_2): δ = 8.28 (d, ^{3}J(H,H) = 5.6 Hz, 1H; H-1/H-2), 8.16 (s, 1H; H-14a), 7.98-7.96 (m, 1H; H-15/16, overlapped with H-5/H-6 and ***Z*-11** resonances), 7.97 (dd, ^{3}J(H,H) = 8.5 Hz, 1H; H-5/H-6, partly overlapped with ***Z*-11** resonances), 7.80-7.75 (m, 1H; H-15/16, overlapped with H-5/H-6 and ***Z*-11** resonances) 7.79(7.80/7.78) (d, ^{3}J(H,H) = 8.5 Hz, 1H; H-5/H-6, overlapped with ***Z*-11**resonances), 7.76 (d, ^{3}J(H,H) = 5.6 Hz, 1H; H-1/H-2, overlapped with H-5/H-6 and ***Z*-11**resonances), 7.34 (d, 1H; ^{3}J(H,H) = 4.1 Hz, 1H; H-17a/H-19/H-19a overlapped with ***Z*-11** resonances), 7.16 (d, ^{3}J(H,H) = 3.5 Hz, 1H; H-17a/H-19/H-19a), 7.05 (dd, J = ^{3}J(H,H) = 5.1, ^{3}J(H,H) = 3.5 Hz, 1H; H-17a/H-19/H-19a), 6.95 (s, 2H), 2.36 (s, 3H), 2.30 (s, 6H).

^{11}B NMR (128 MHz, CD_2Cl_2): δ **=** 40.9 ($h_{1/2} \approx$ 220 Hz).

HRMS (MALDI): Calculated *m/z* for $[C_{29}H_{21}BOS_4]^+$: 524.0563; found: 524.0567.

5. Plots of ^{1}H, ^{11}B and ^{13}C{^{1}H} NMR spectra of all new compounds

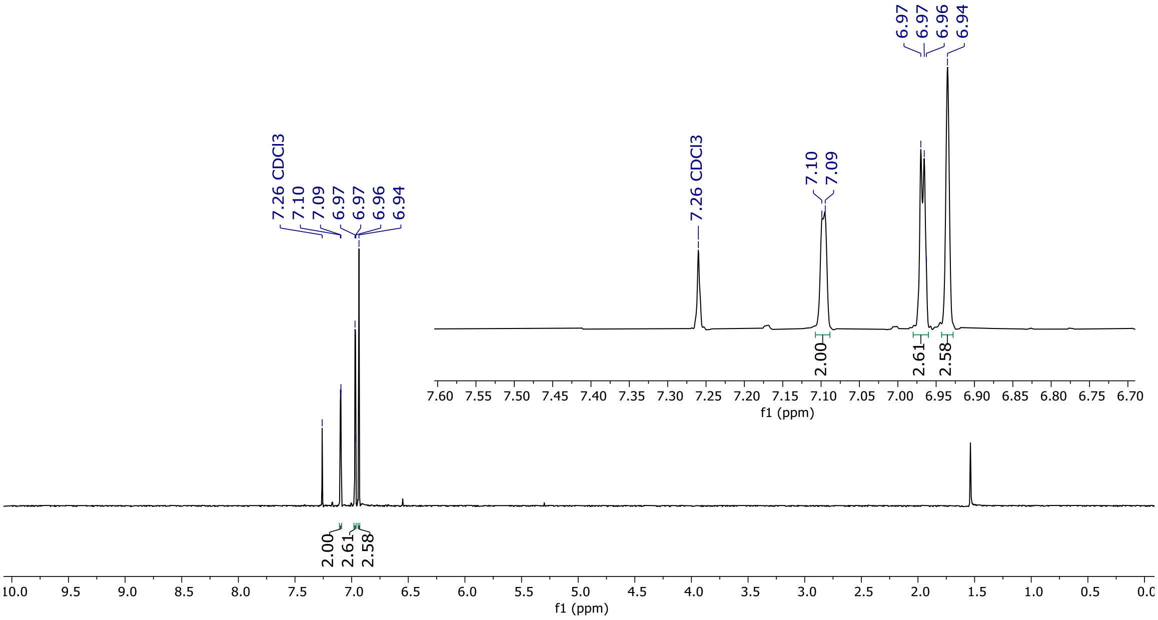

Figure S1. ^{1}H NMR spectrum of *trans*-**4** ($CDCl_3$, 300 MHz).

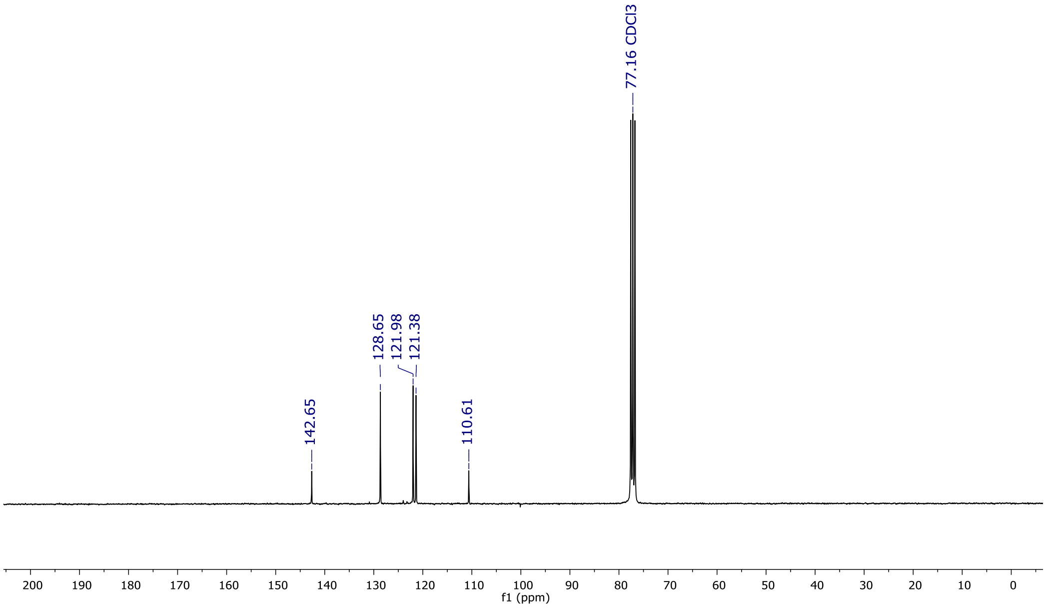

Figure S2. ^{13}C{^{1}H} NMR spectrum of *trans*-**4** ($CDCl_3$, 75 MHz).

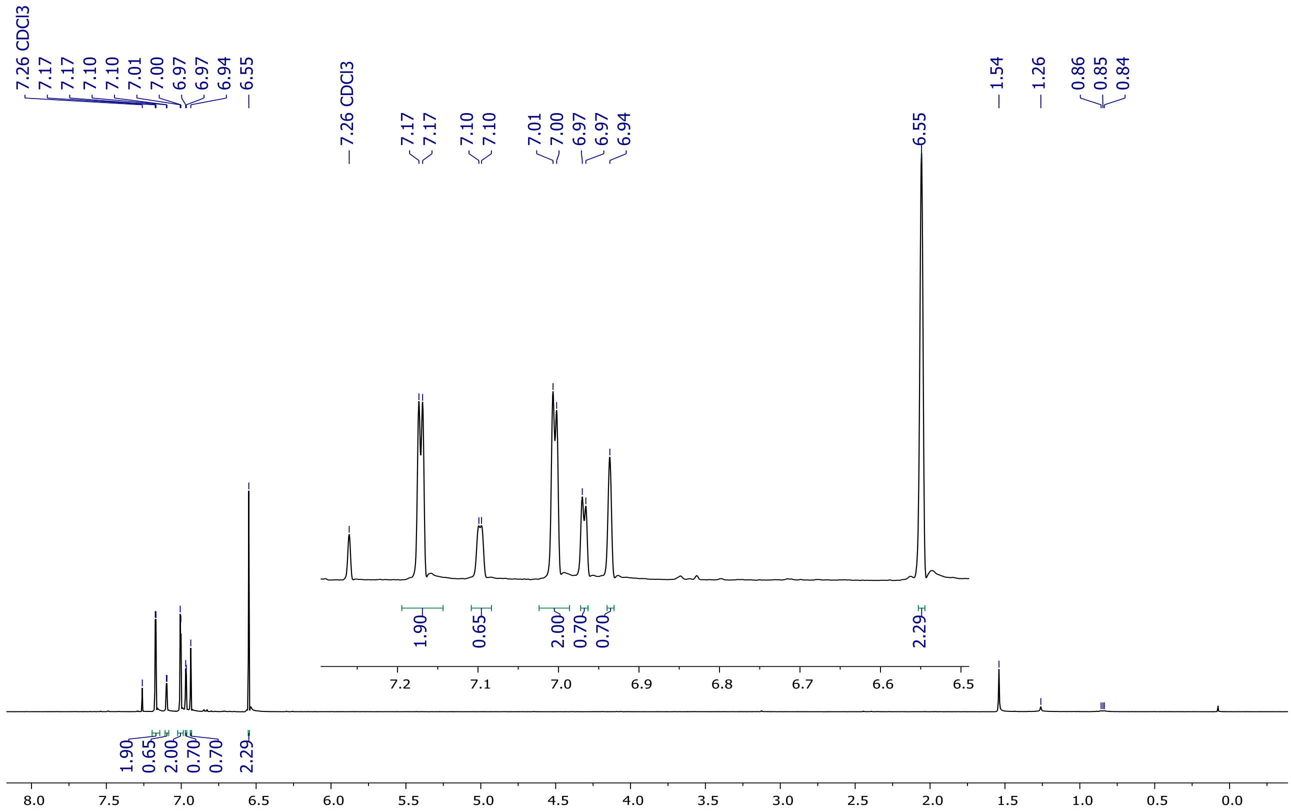

Figure S3. ^{1}H NMR spectrum of a cis/*trans*-**4** (≈3:1) mixture (CDCl$_3$, 300 MHz).

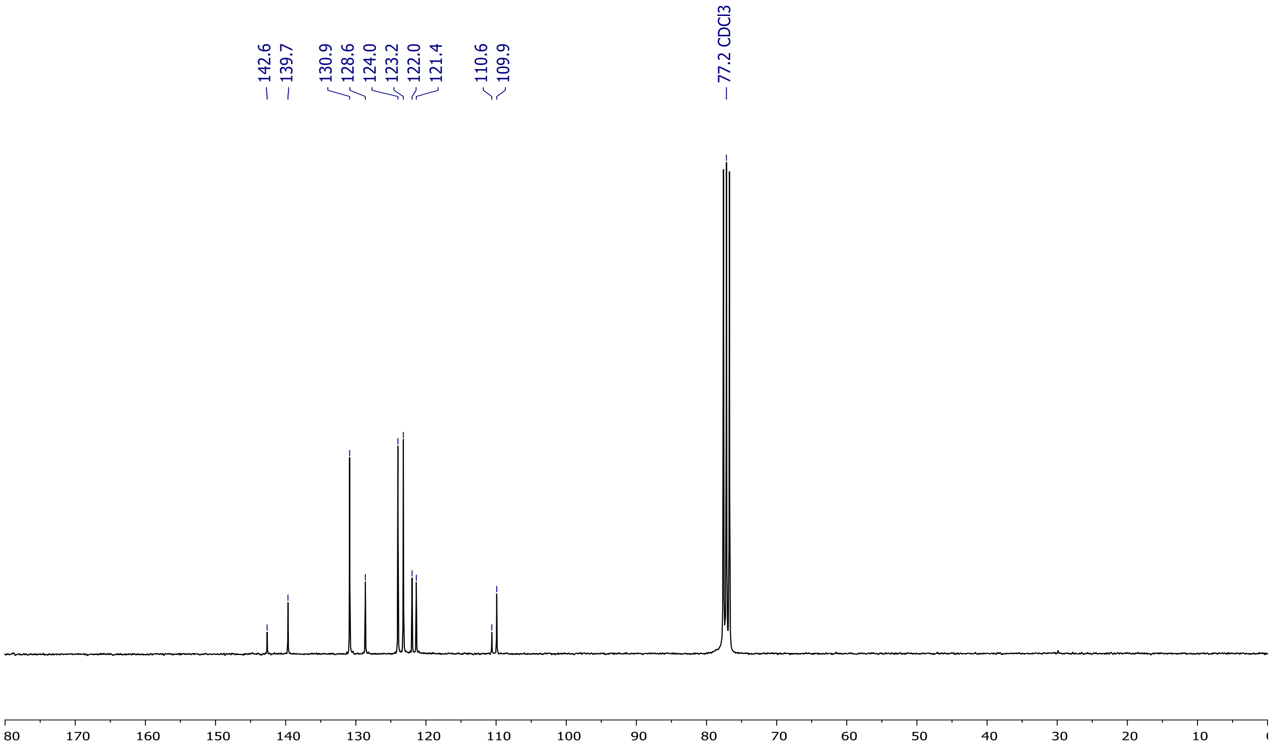

Figure S4. ^{13}C{^{1}H} NMR spectrum of a cis/*trans*-**4** (≈3:1) mixture (CDCl$_3$, 75 MHz).

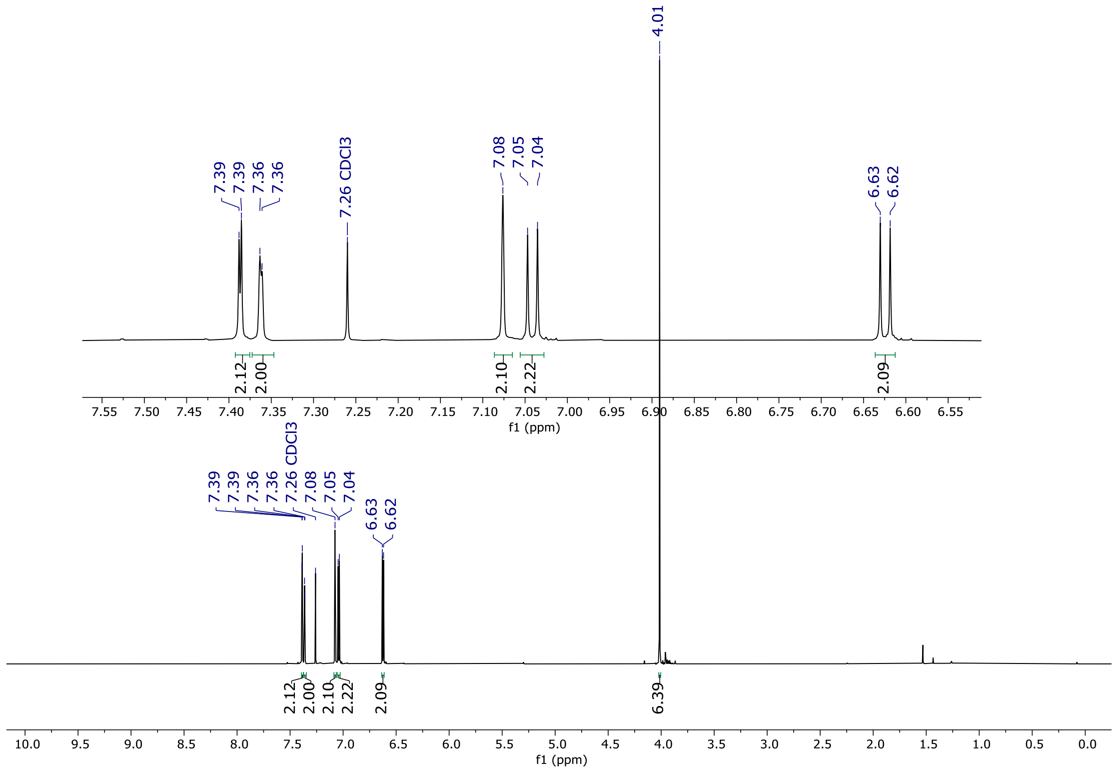

Figure S5. ^{1}H NMR spectrum of *trans*-**5** ($CDCl_3$, 500 MHz). The spectrum refers to the product obtained by Stille coupling.

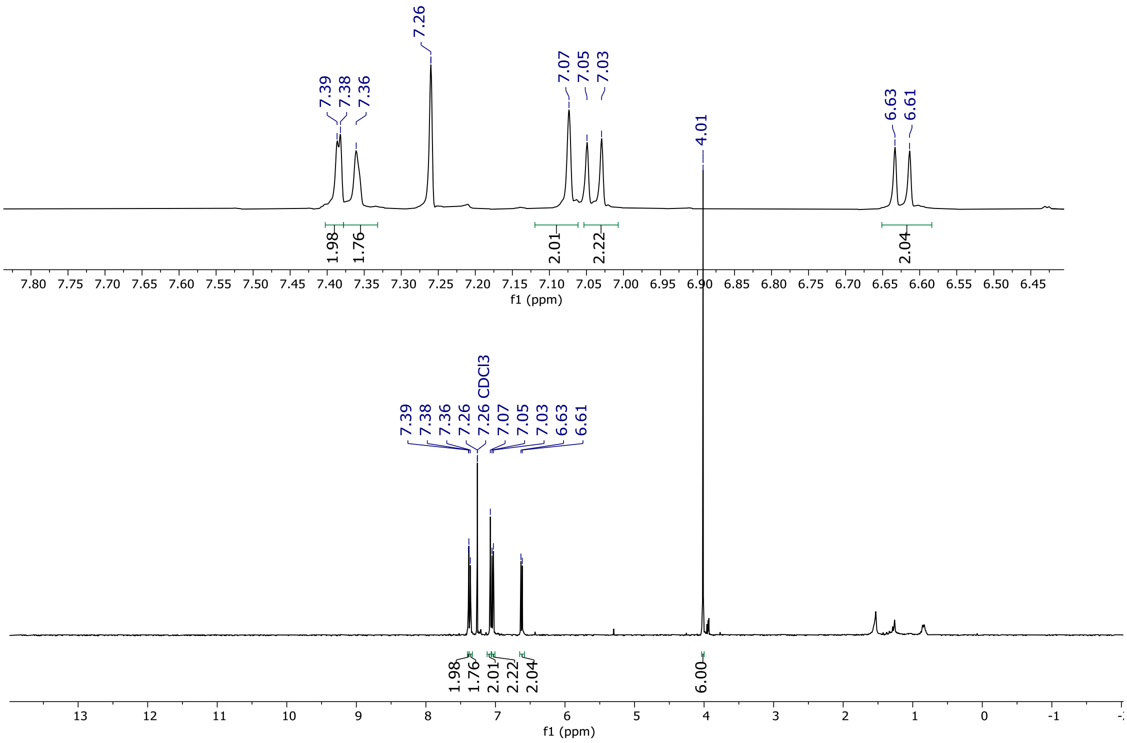

Figure S5A. ^{1}H NMR spectrum of *trans*-**5** ($CDCl_3$, 300 MHz). The spectrum refers to the product obtained by Suzuki Coupling.

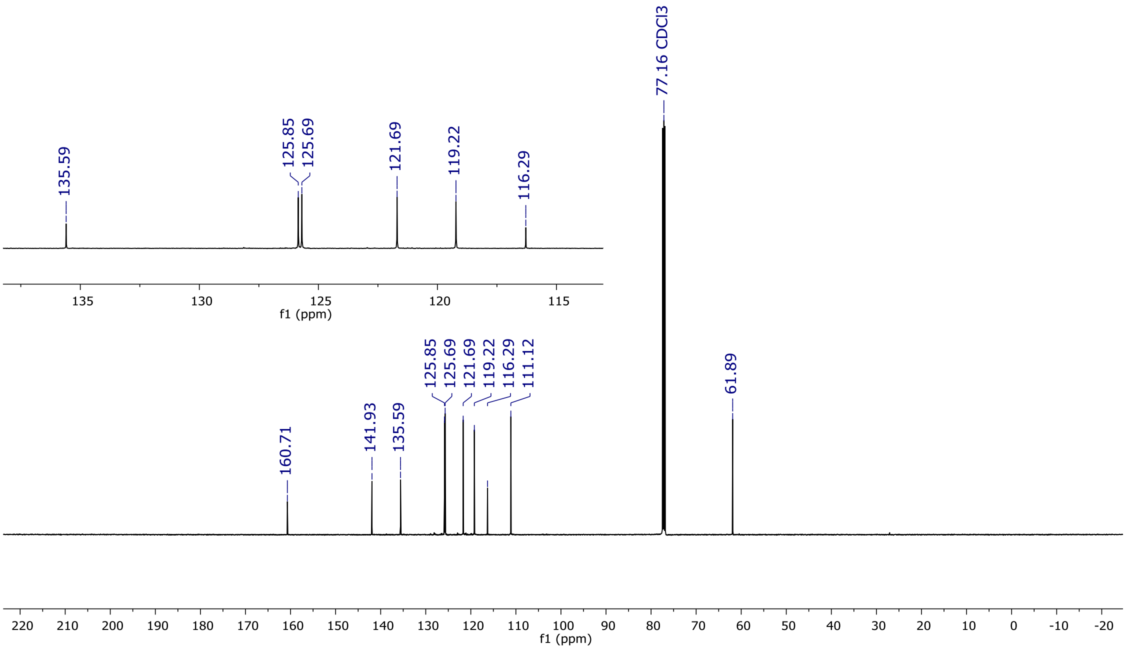

Figure S6. $^{13}C\{^1H\}$ NMR spectrum of *trans*-**5** ($CDCl_3$, 126 MHz). The spectrum refers to the product obtained by Stille coupling.

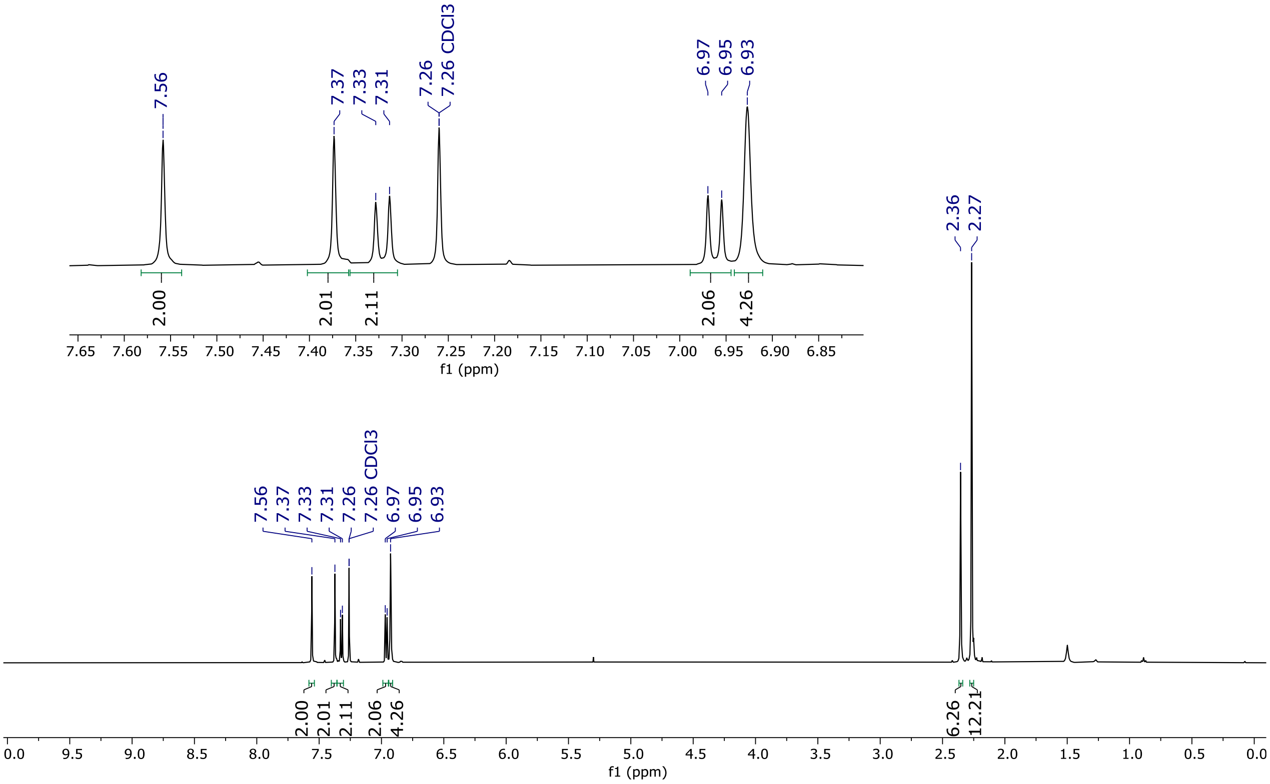

Figure S7. ^1H NMR spectrum of *trans*-**6** ($CDCl_3$, 400 MHz).

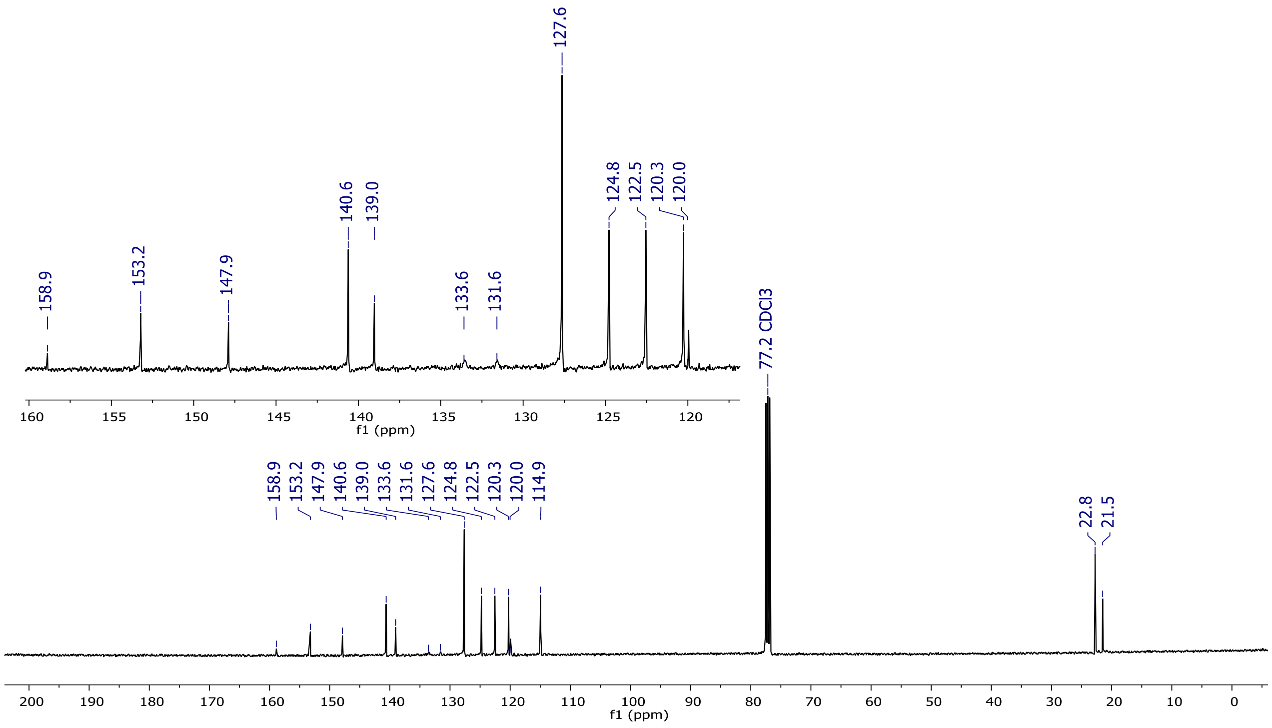

Figure S8. $^{13}C\{^{1}H\}$ NMR spectrum of *trans*-**6** ($CDCl_3$, 101 MHz).

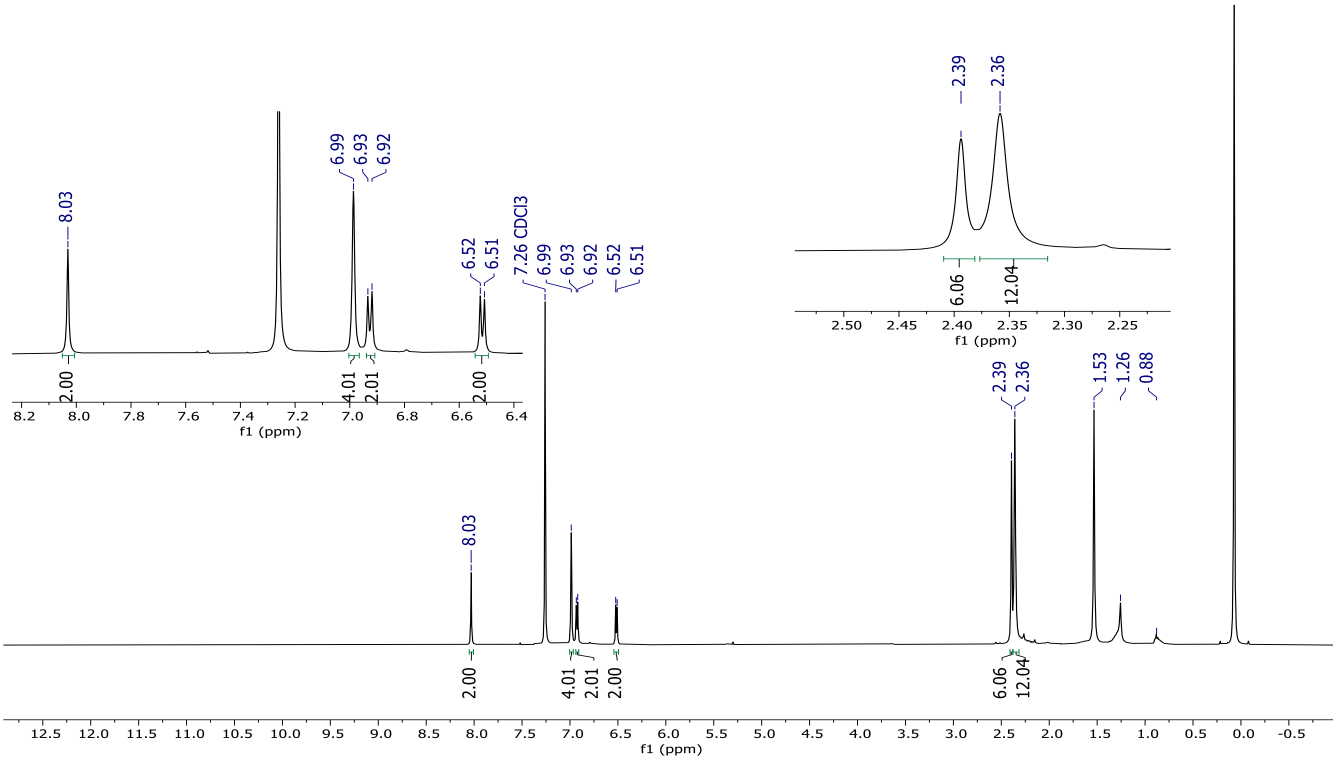

Figure S9. ^{1}H NMR spectrum of **2** ($CDCl_3$, 400 MHz).

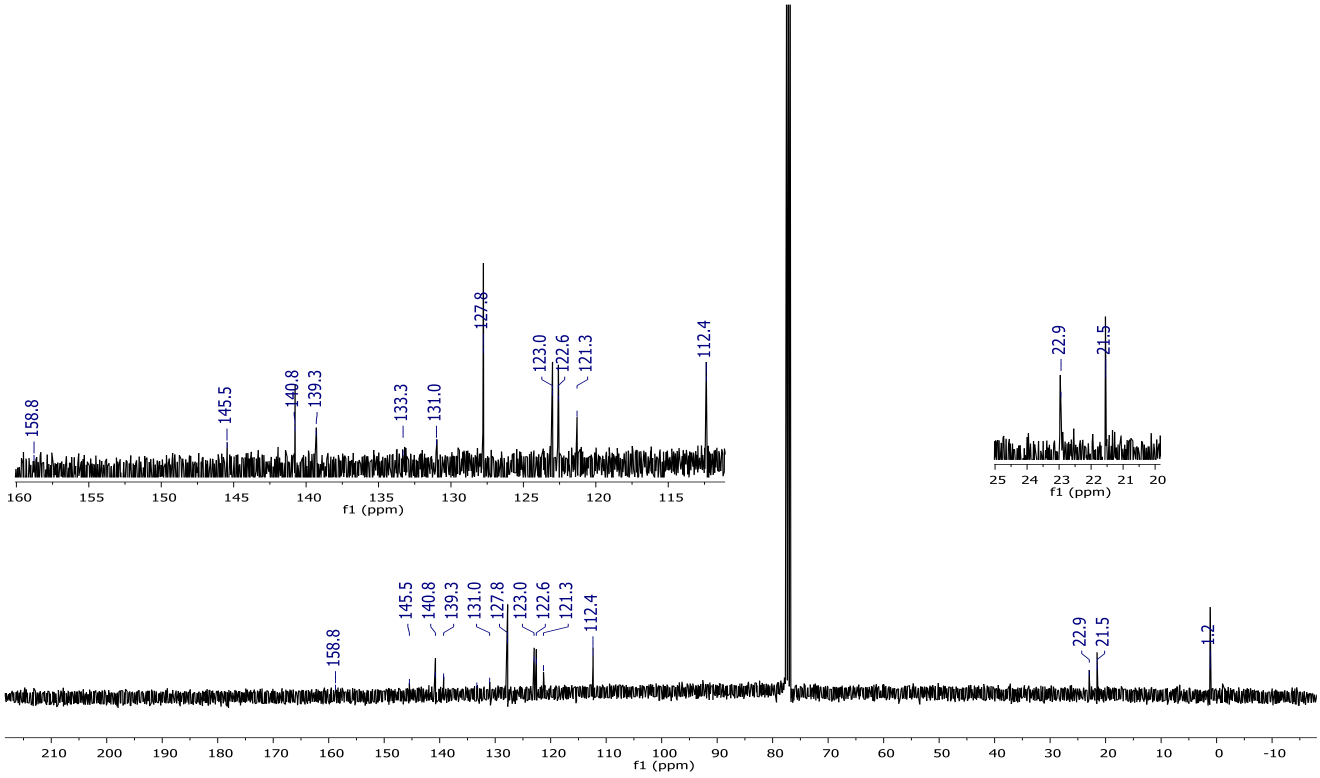

Figure S10. $^{13}C\{^1H\}$ NMR spectrum of **2** ($CDCl_3$, 101 MHz).

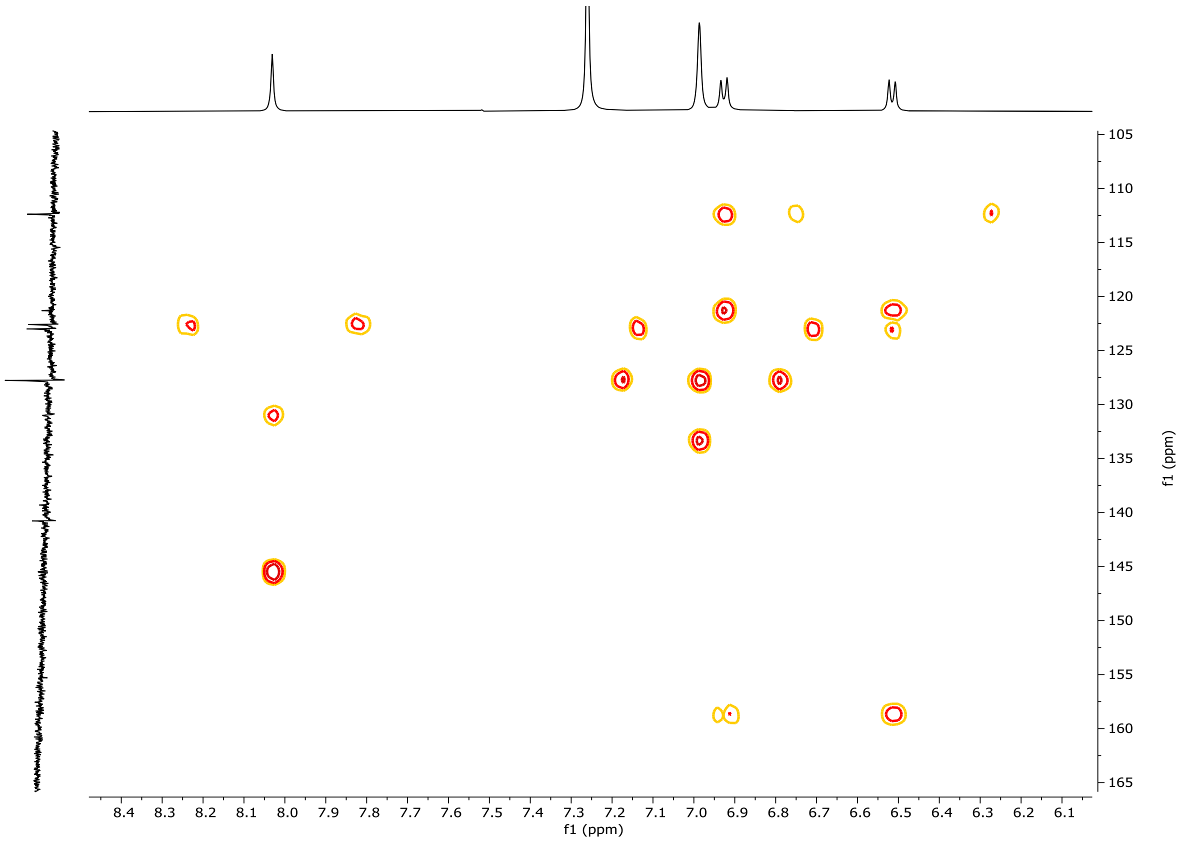

Figure S10A. ^{H,C}HMBC spectrum of **2** ($CDCl_3$, 101 MHz).

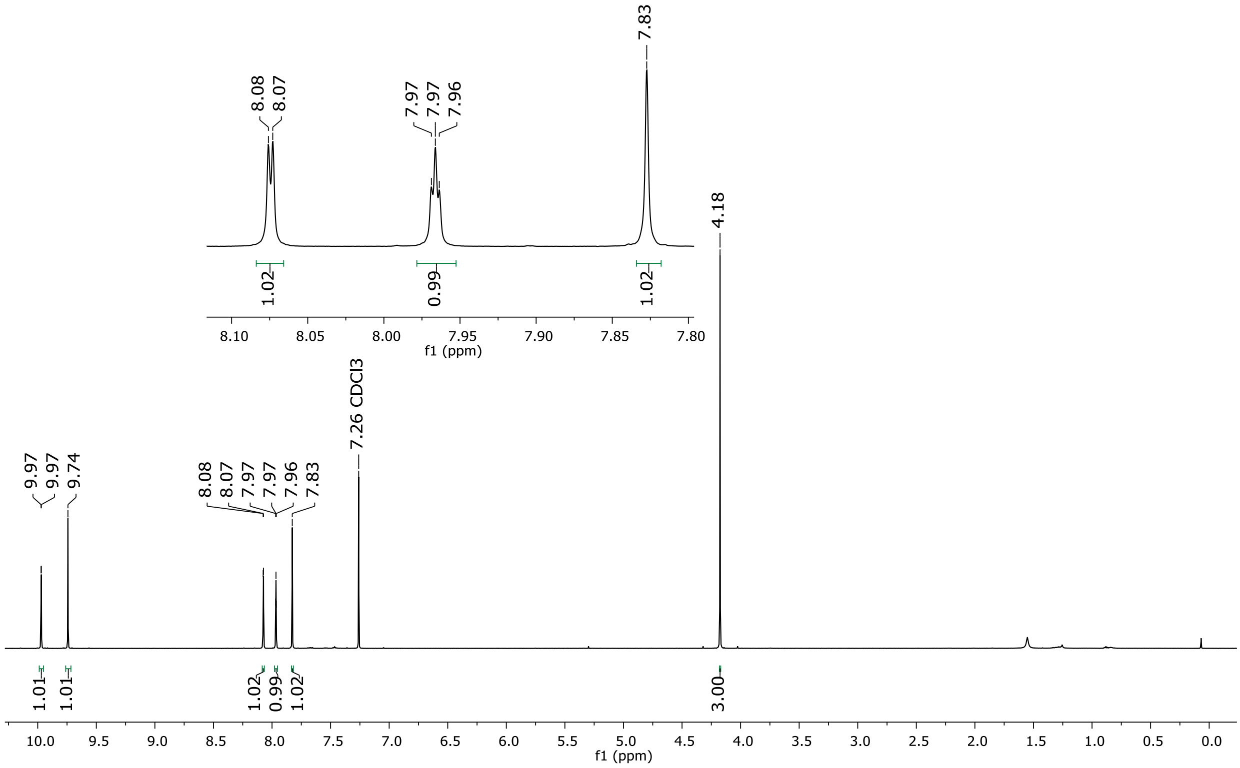

Figure S11. ^{1}H NMR spectrum of **8** ($CDCl_3$, 500 MHz).

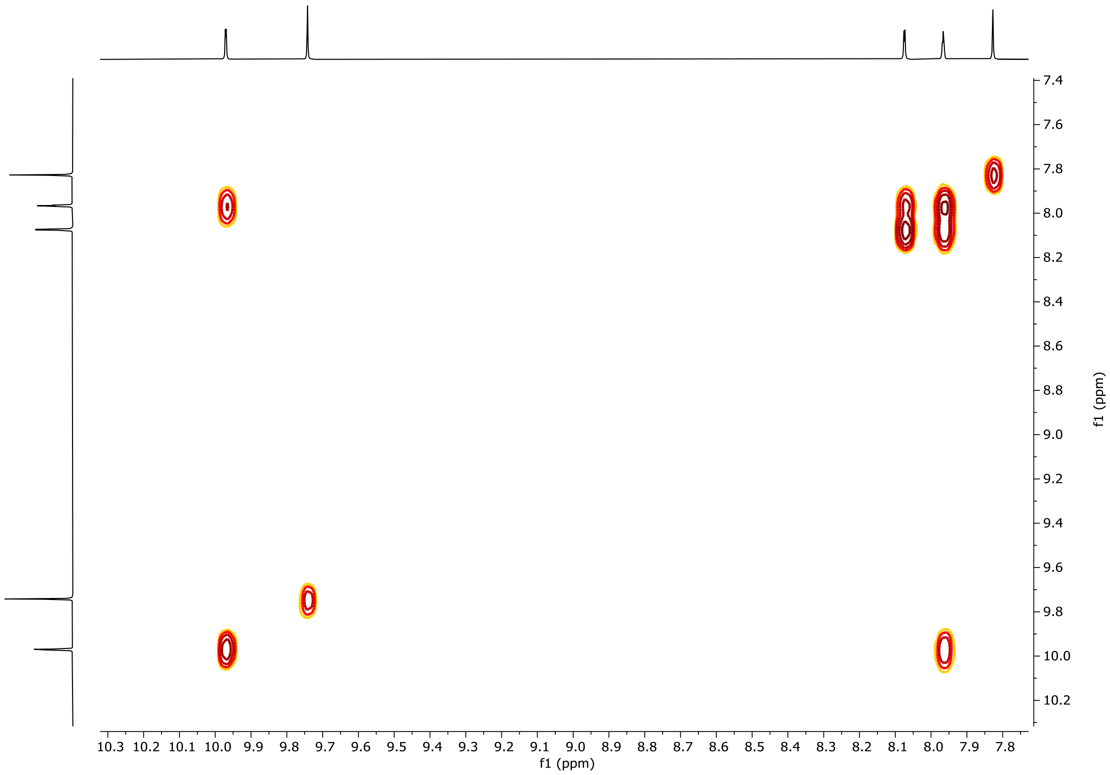

Figure S11A. ^{H,H}COSY spectrum of **8** ($CDCl_3$, 500 MHz).

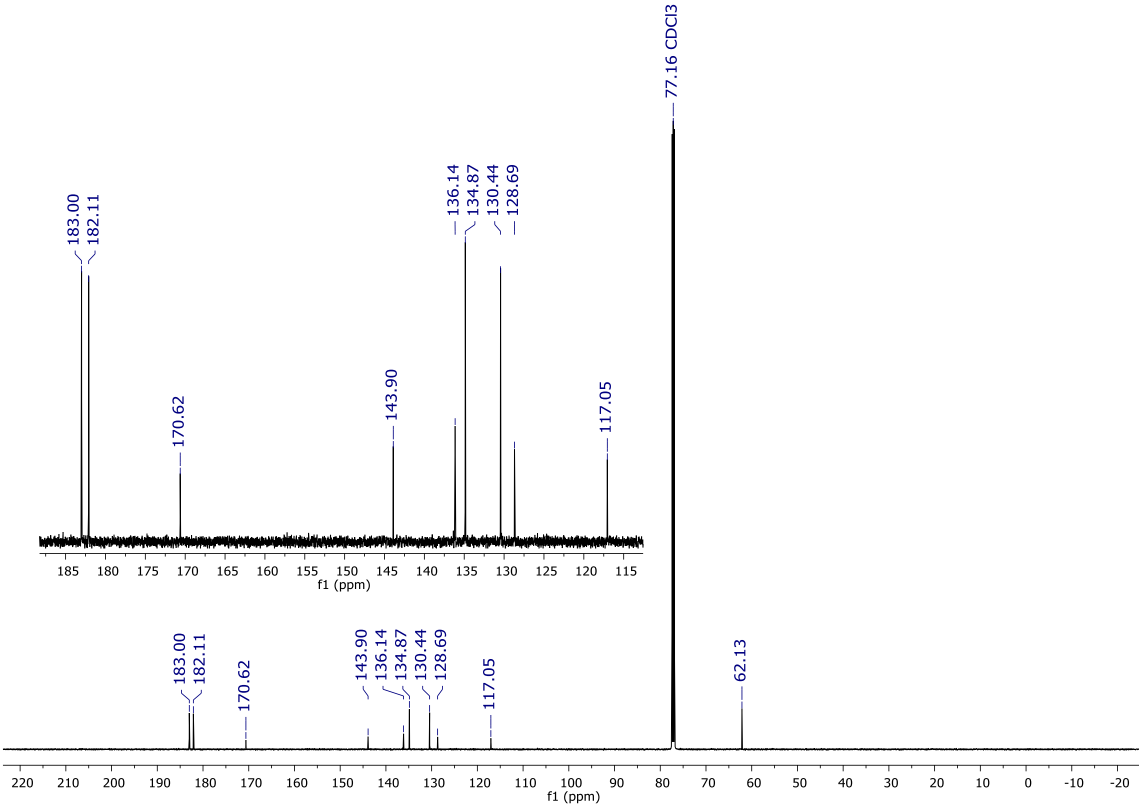

Figure S12. $^{13}C\{^{1}H\}$ NMR spectrum of **8** ($CDCl_3$, 126 MHz).

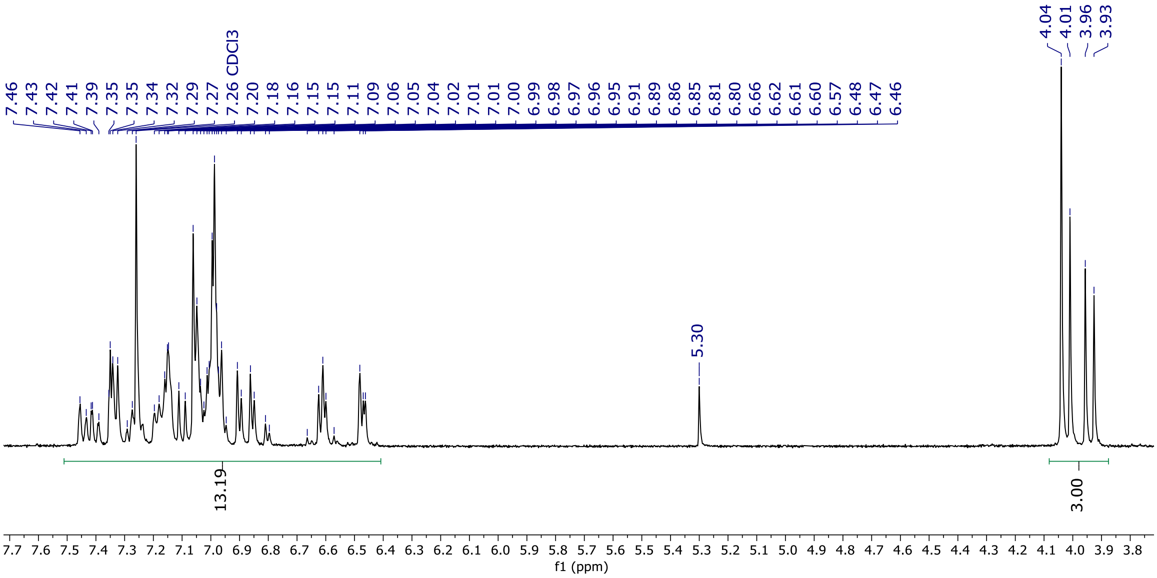

Figure S13. ^{1}H NMR spectrum of **9** mixture of isomers afer column chromatography ($CDCl_3$, 300 MHz).

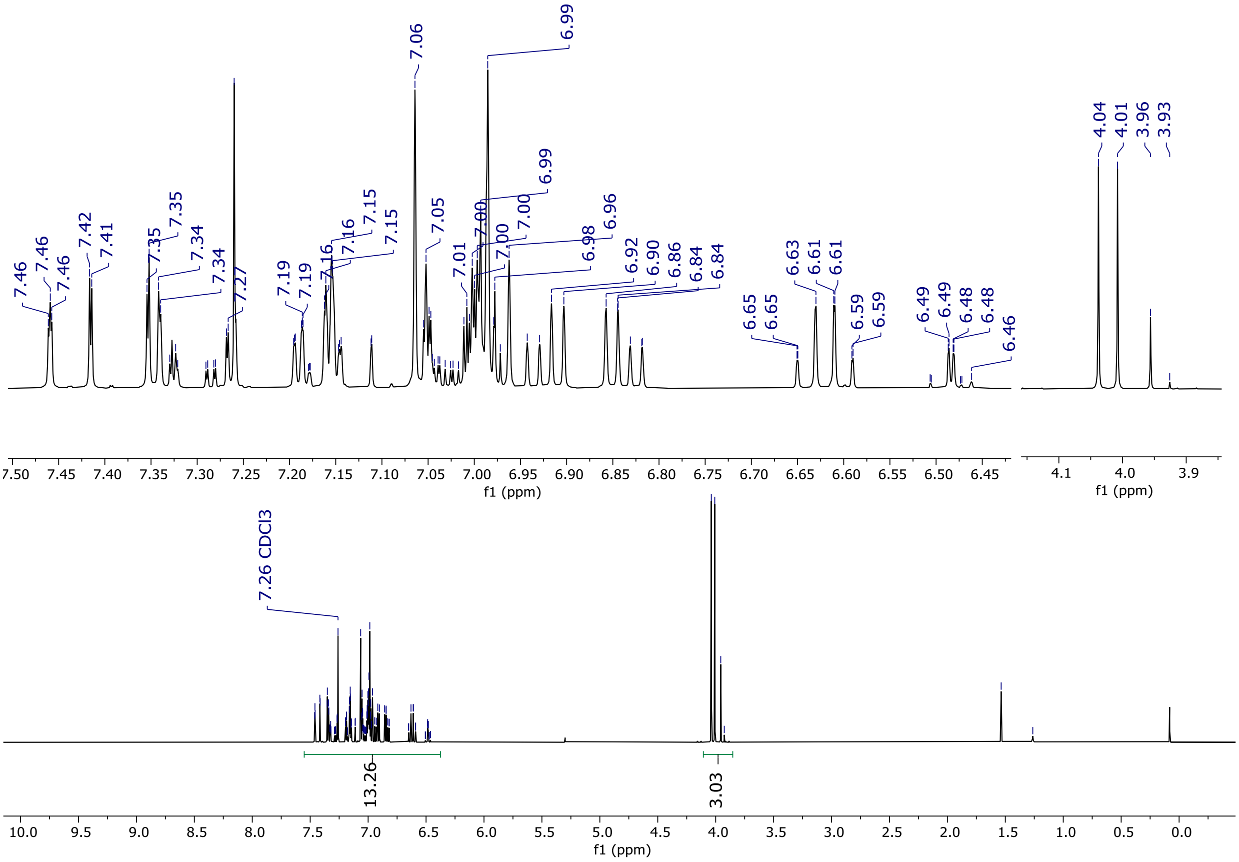

Figure S14. ^{1}H NMR spectrum of **9** after Et_2O and *n*-pentane washings ($CDCl_3$, 600 MHz).

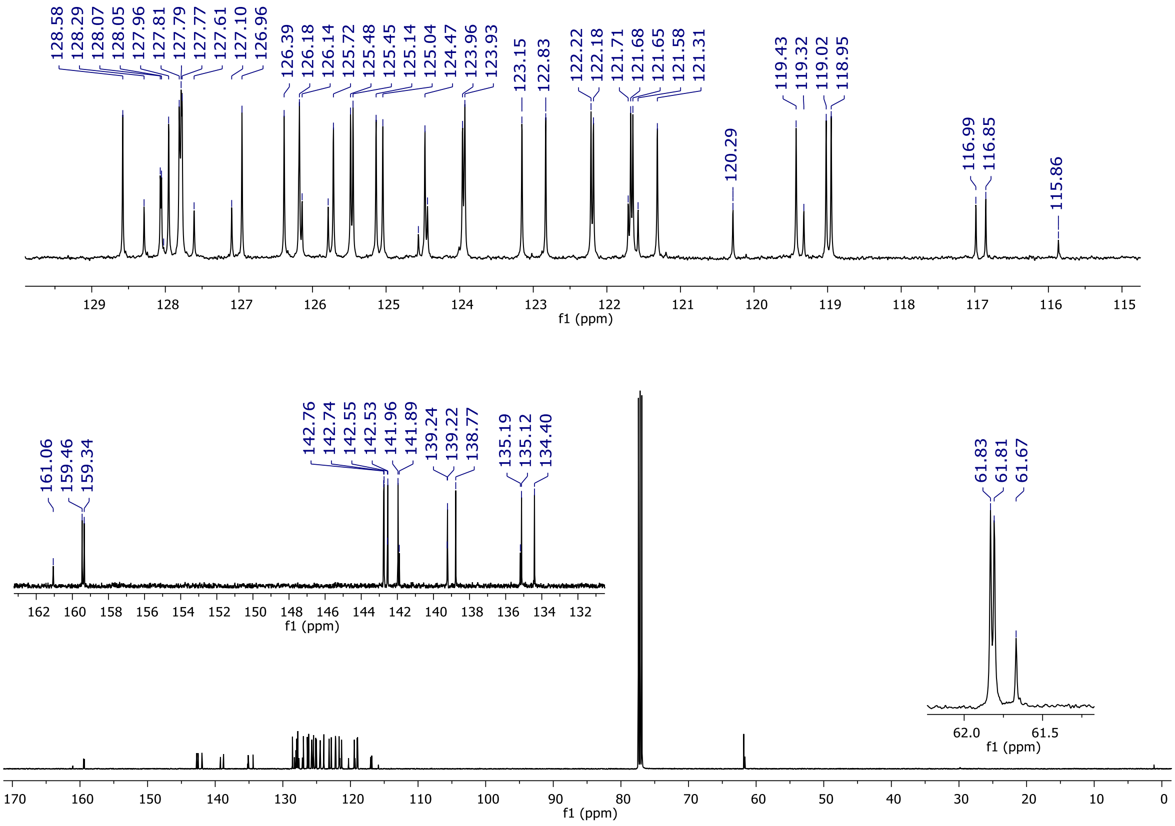

Figure S15. $^{13}C\{^1H\}$ NMR spectrum of **9** after Et_2O and *n*-pentane washings ($CDCl_3$, 151 MHz).

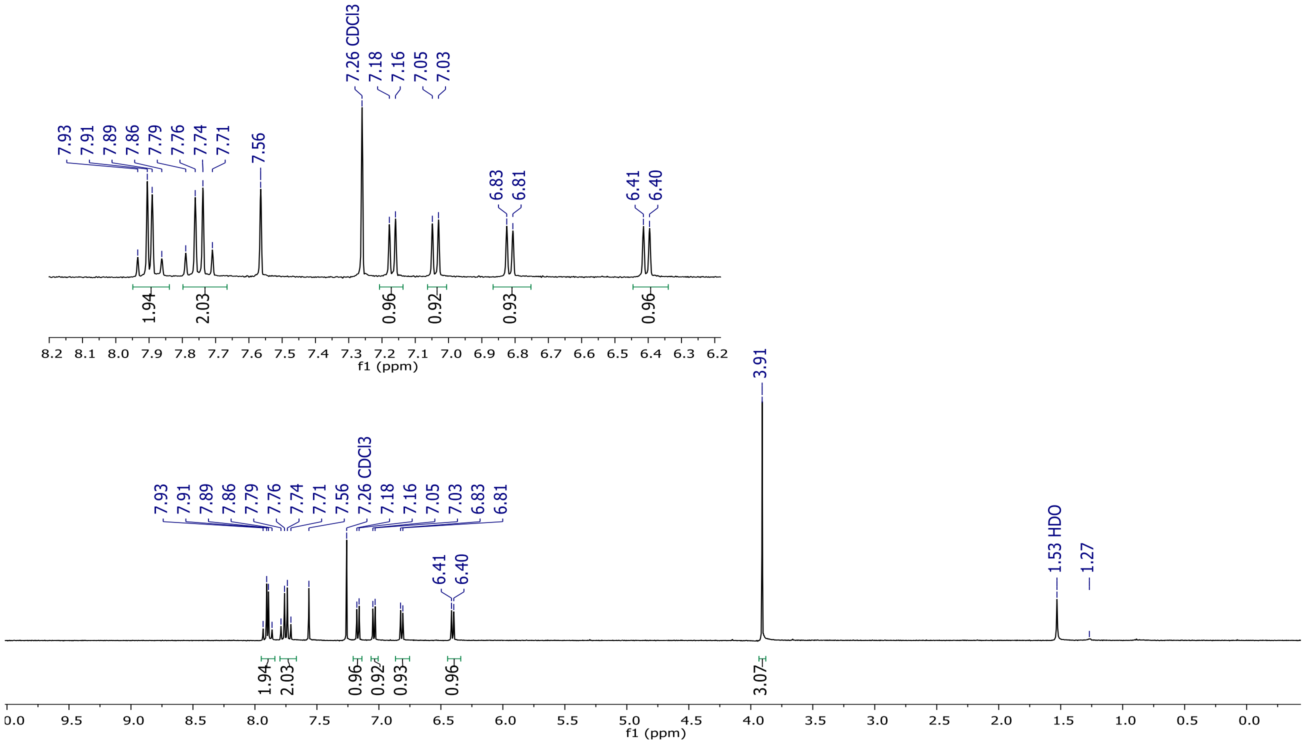

Figure S16. ^{1}H NMR spectrum of **7** ($CDCl_3$, 300 MHz).

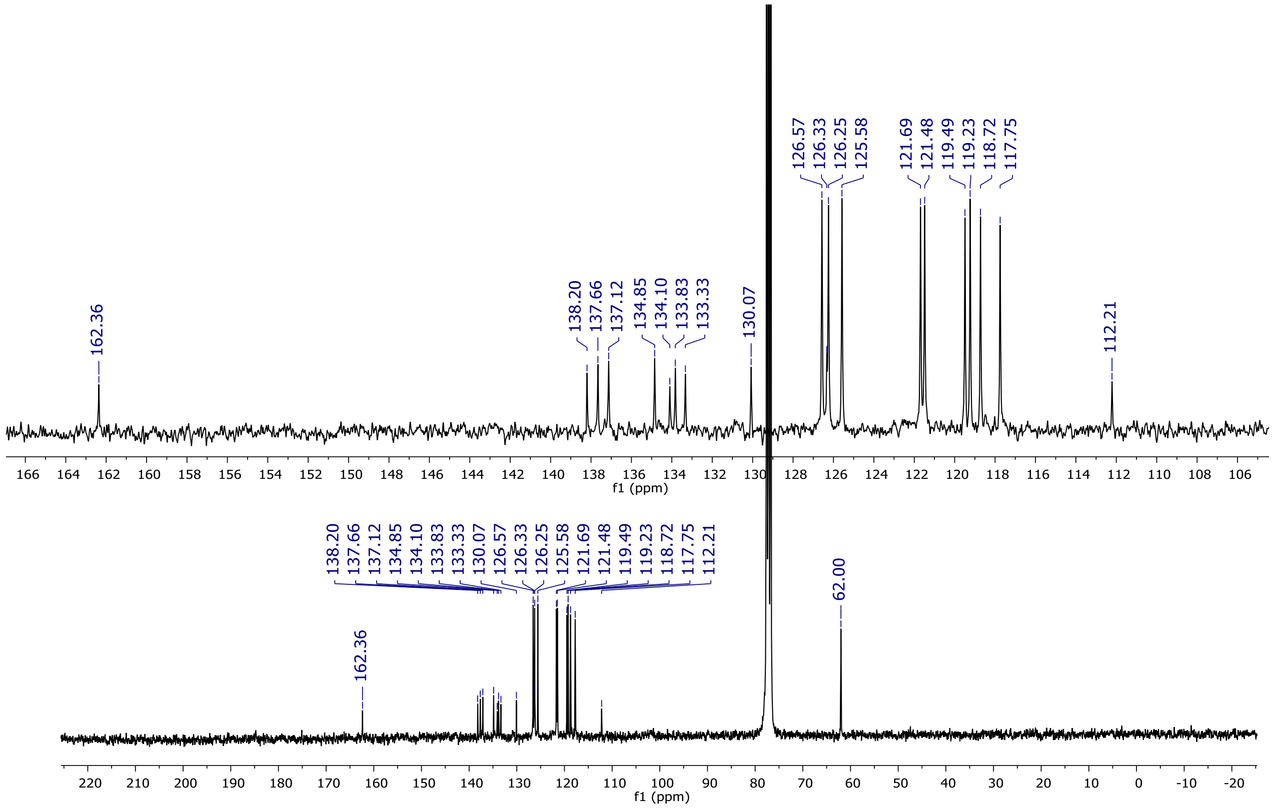

Figure S17. $^{13}C\{^{1}H\}$ NMR spectrum of **7** ($CDCl_3$, 75 MHz).

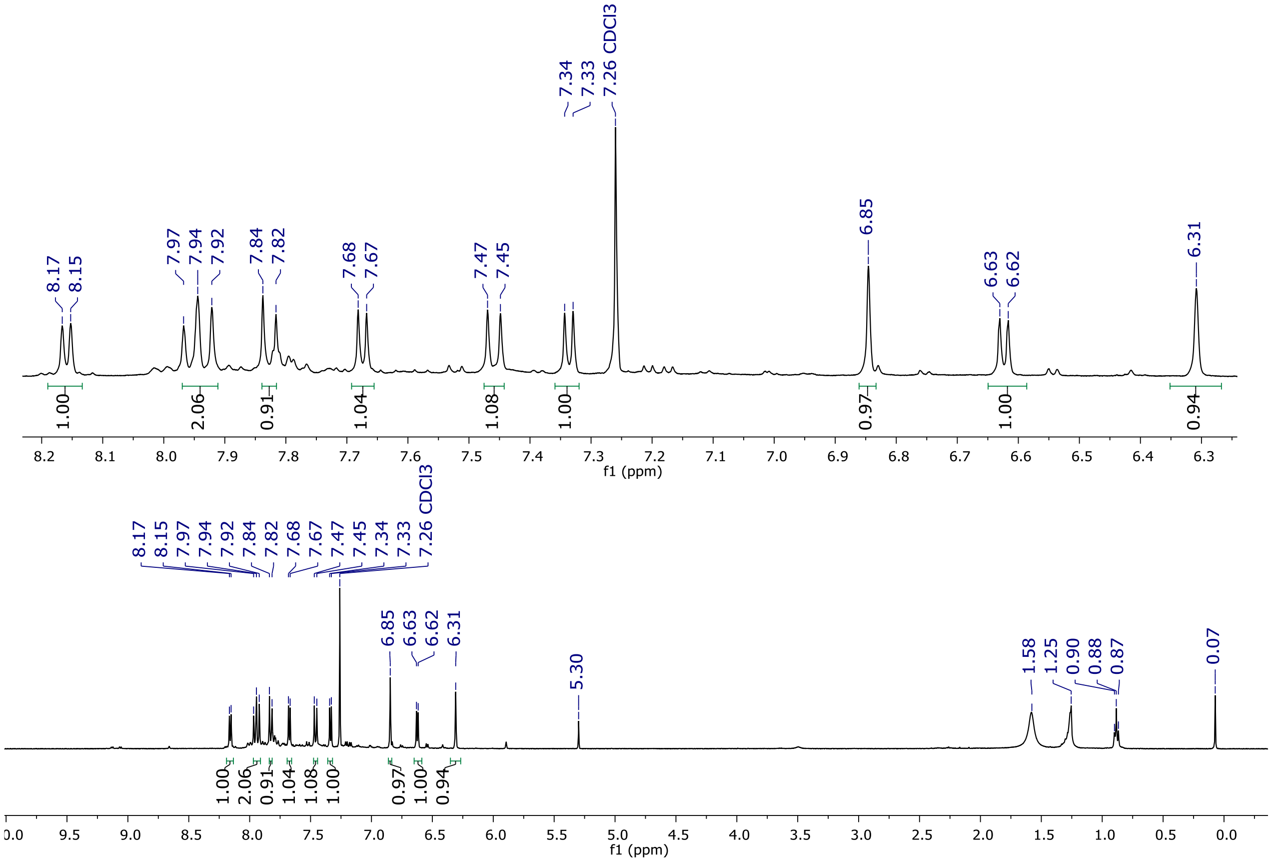

Figure S18. ^{1}H NMR spectrum of **7-OH** ($CDCl_3$, 400 MHz).

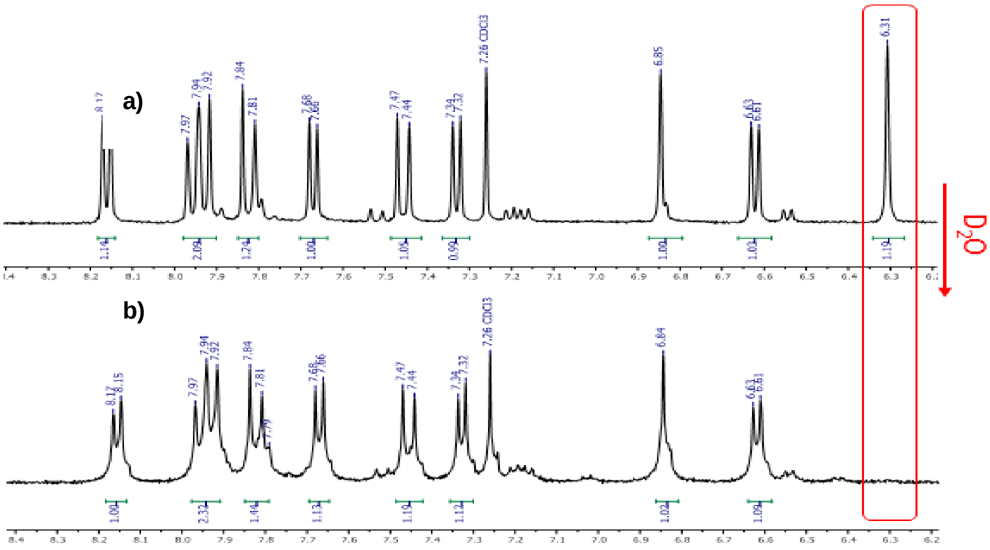

Figure S19. Deuteration test of **7-OH**, ^{1}H NMR spectrum ($CDCl_3$, 400 MHz). a) ^{1}H NMR of the **7-OH** sample; b) ^{1}H NMR of **7-OH** after the addition of D_2O.

The proton at 6.31 ppm (assigned to the -OH group) disappeared after the addition of D_2O, red box.

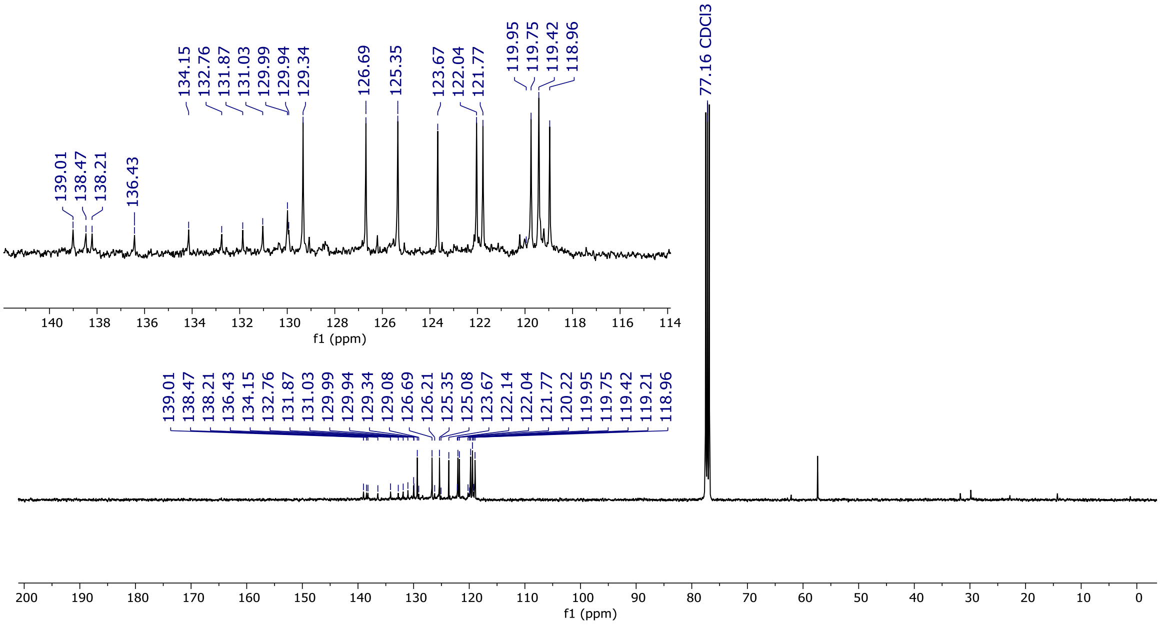

Figure S20. ^{13}C{^{1}H} NMR spectrum of **7-OH** ($CDCl_3$, 101 MHz).

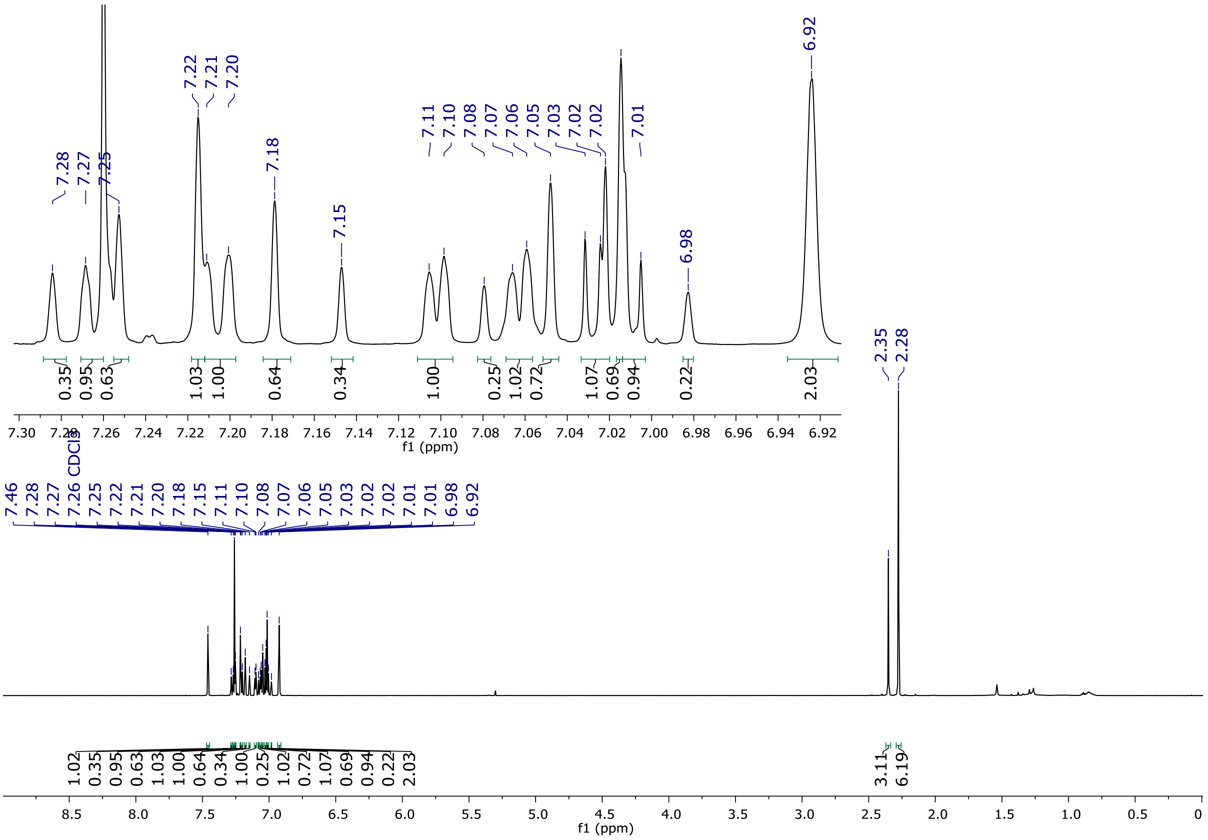

Figure S21. ^{1}H NMR spectrum of *E,E*-**10** ($CDCl_3$, 500 MHz).

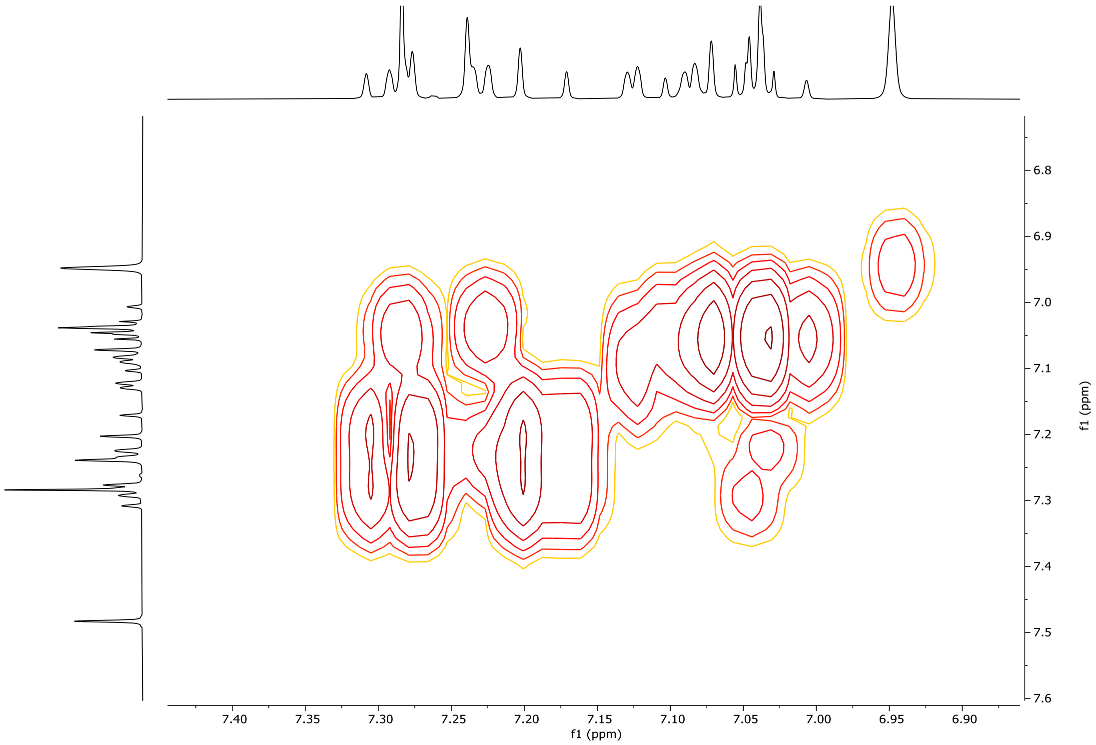

Figure S21A. ^{H,H}COSY spectrum of *E*,*E*-**10** ($CDCl_3$, 500 MHz).

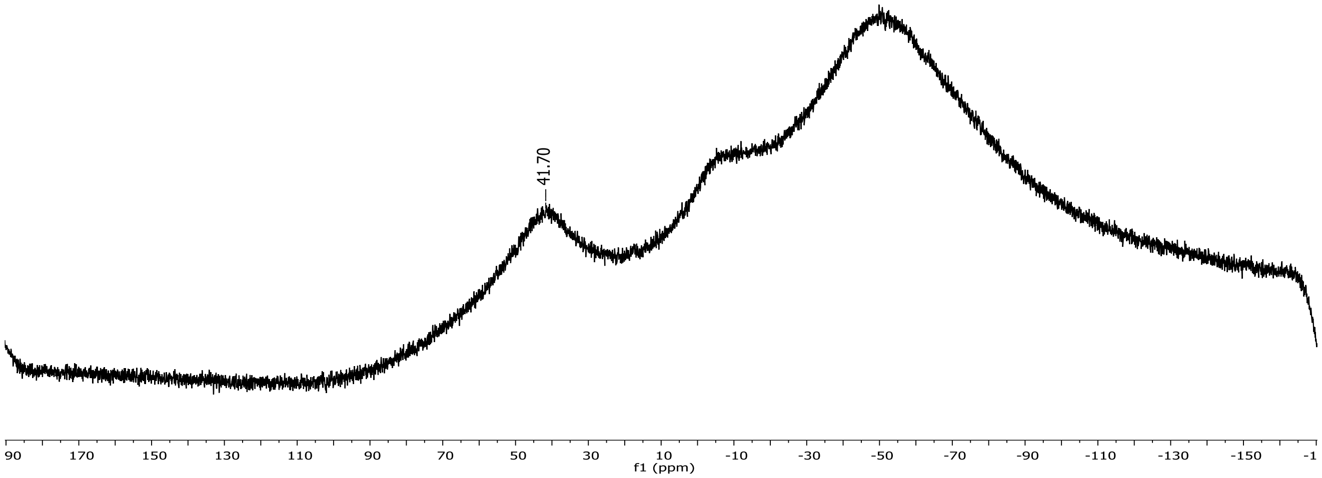

Figure S22. ^{11}B NMR spectrum of *E*,*E*-**10** ($CDCl_3$, 96 MHz).

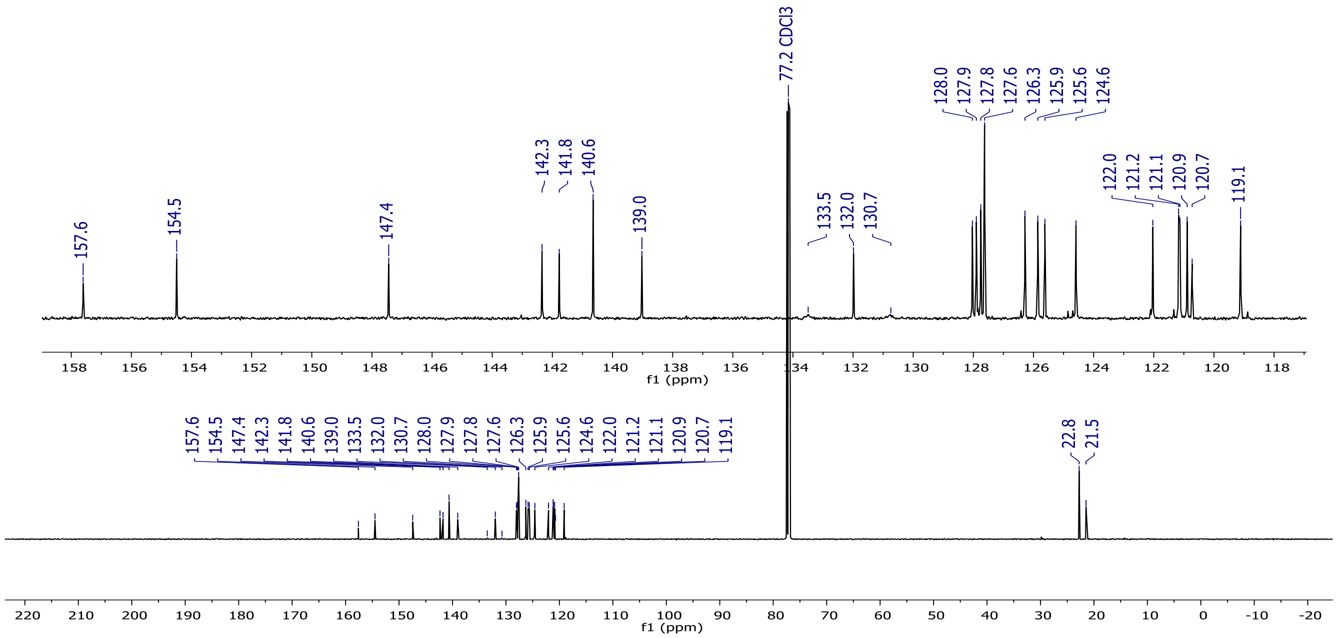

Figure S23. $^{13}C\{^{1}H\}$ NMR spectrum of *E*,*E*-**10** ($CDCl_3$, 125 MHz).

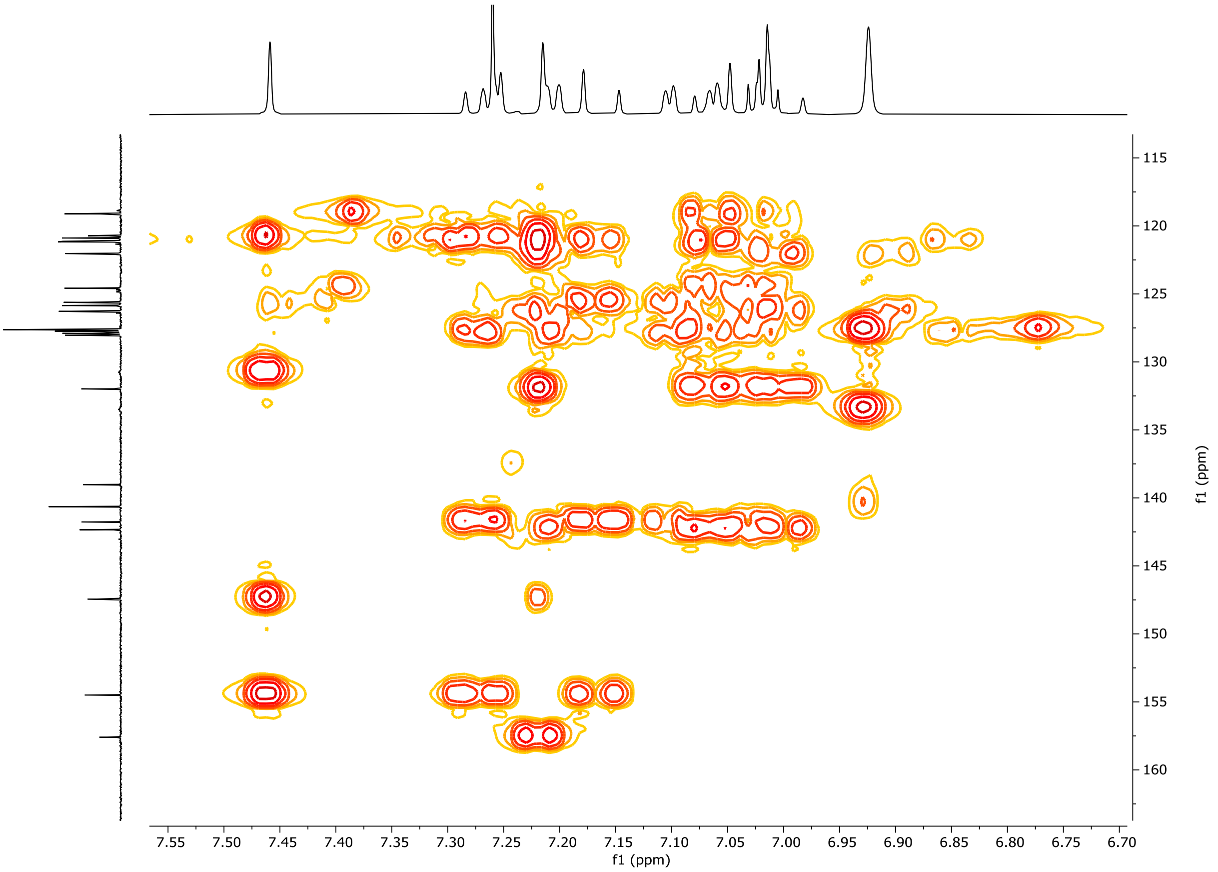

Figure S23A. ^{H,C}HMBC spectrum of *E*,*E*-**10** ($CDCl_3$, 126 MHz).

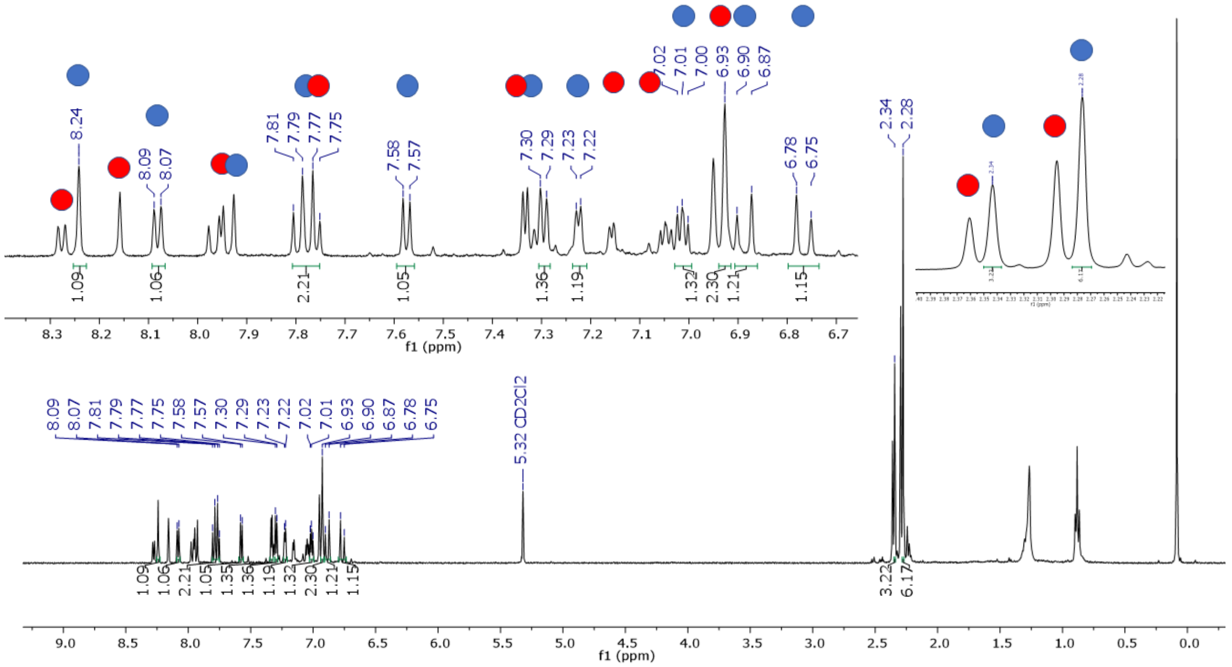

Figure S24. ^{1}H NMR spectrum of a *E*/Z-**11** (≈40:60) mixture (CD$_2$Cl$_2$, 400 MHz). Blue circles indicates *cis*-isomer proton resonances; red circles indicates *trans*-isomer resonances.

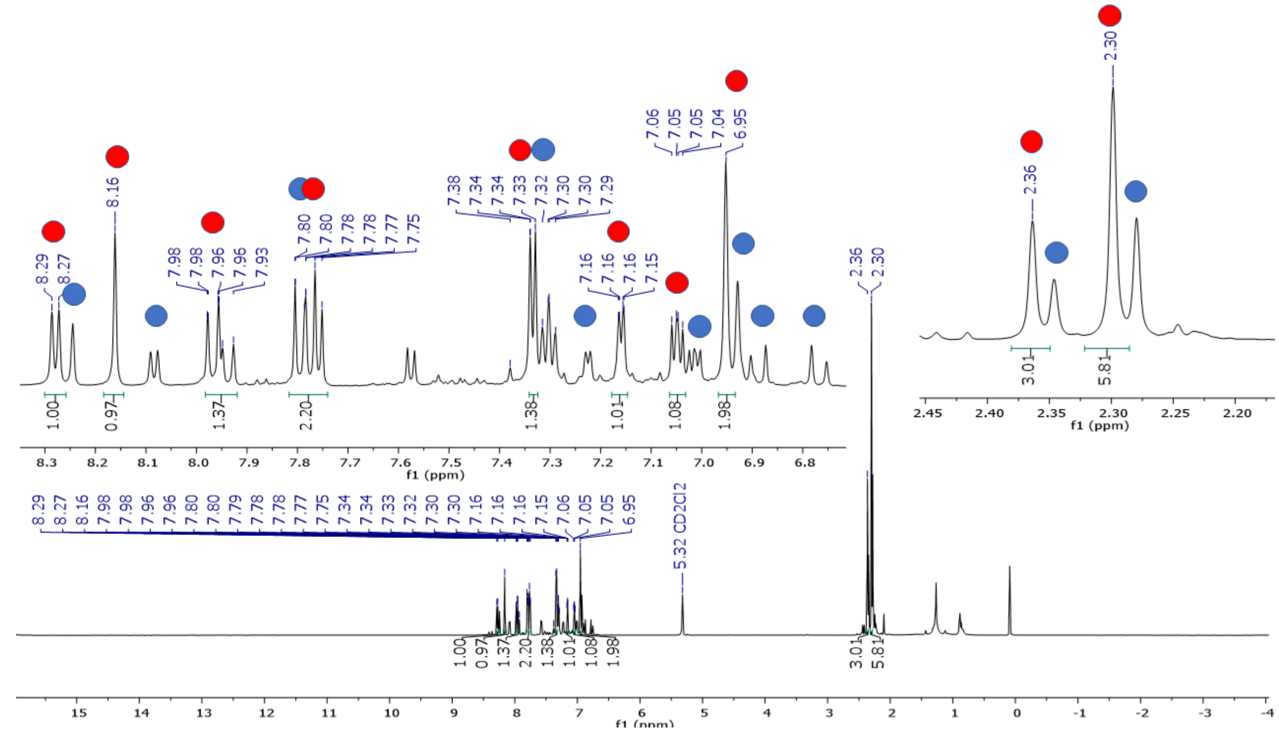

Figure S25. ^{1}H NMR spectrum of a *E*/Z-**11** (≈60:40) mixture (CD$_2$Cl$_2$, 400 MHz). Blue circles indicates *cis*-isomer proton resonances; red circles indicates *trans*-isomer resonances.

6. Electrochemical and photophysical properties of the BO-doped compounds

6.1 Cyclic voltammograms

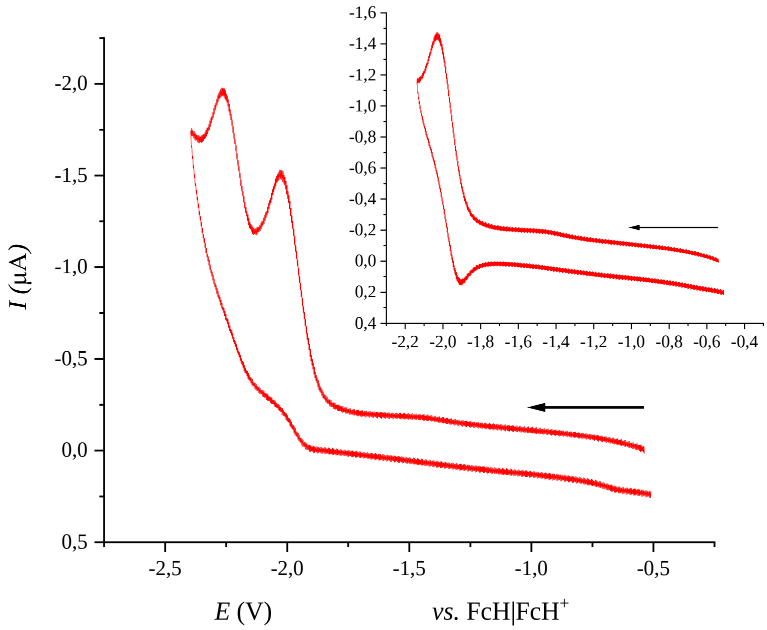

Figure S26. Cyclic voltammogram of *trans*-**6** in THF (cathodic scan; room temperature, supporting electrolyte:[nBu$_4$N][PF$_6$] (0.1 M), scan rate 200 mV s^{-1}). The inset refers to the cyclic voltammogram of *trans*-**6** first reduction process.

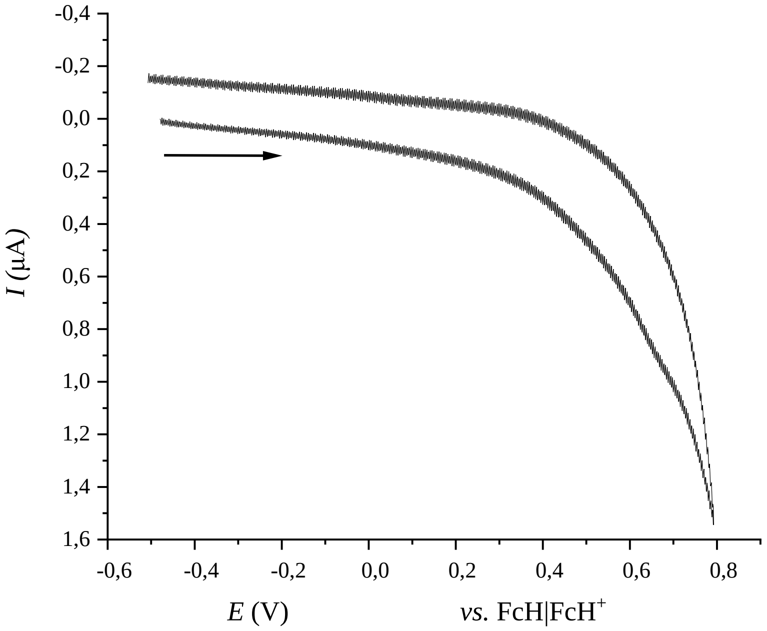

Figure S27. Cyclic voltammogram of *trans*-**6** in THF (anodic scan; room temperature, supporting electrolyte: [nBu$_4$N][PF$_6$] (0.1 M), scan rate 200 mV s^{-1}).

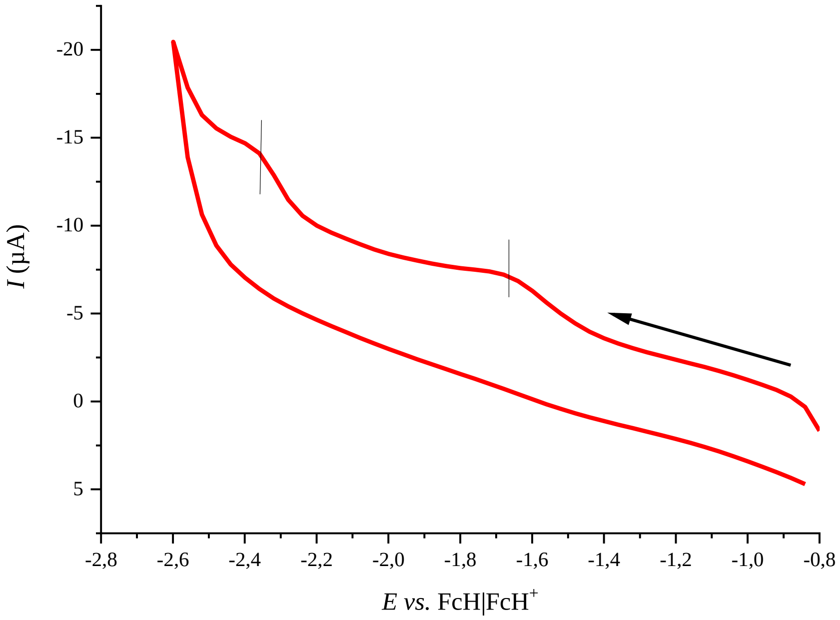

Figure S28. Cyclic voltammogram of **2** in THF (cathodic scan; room temperature, supporting electrolyte: [nBu$_4$N][PF$_6$] (0.1 M), scan rate 500 mV s^{-1}).

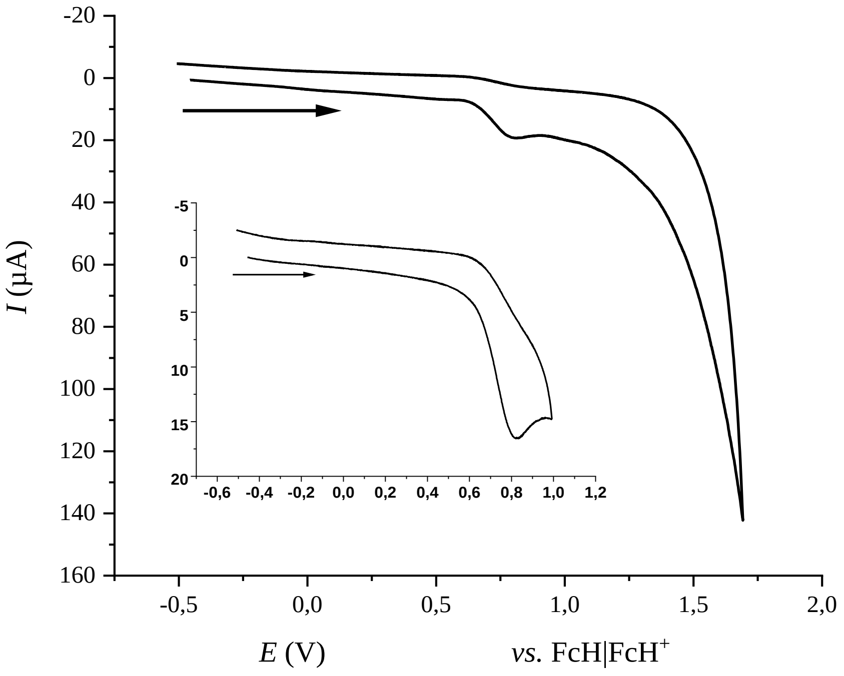

Figure S29. Cyclic voltammogram of **2** in THF (anodic scan; room temperature, supporting electrolyte: [nBu$_4$N][PF$_6$] (0.1 M), scan rate 200 mV s^{-1}). The inset refers to the cyclic voltammogram of **2** first oxidation process.

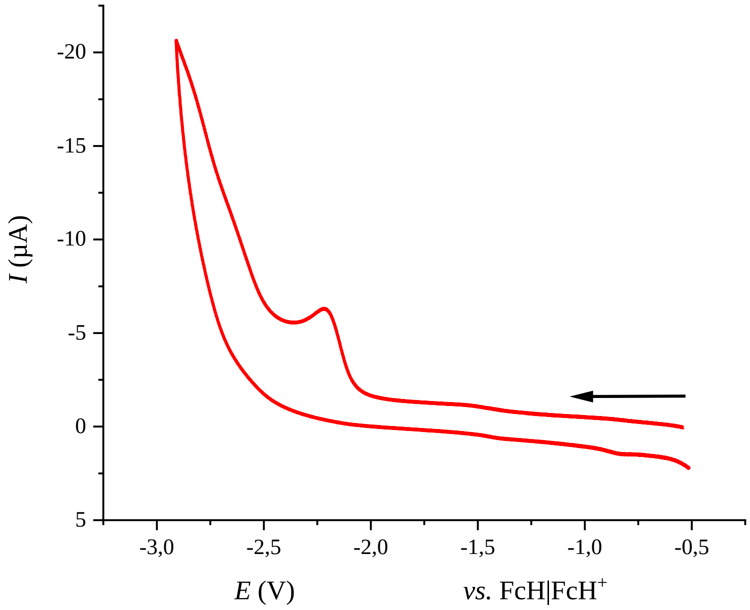

Figure S30. Cyclic voltammogram of *E,E*-**10** in THF (cathodic scan; room temperature, supporting electrolyte: [nBu$_4$N][PF$_6$] (0.1 M), scan rate 200 mV s^{-1}).

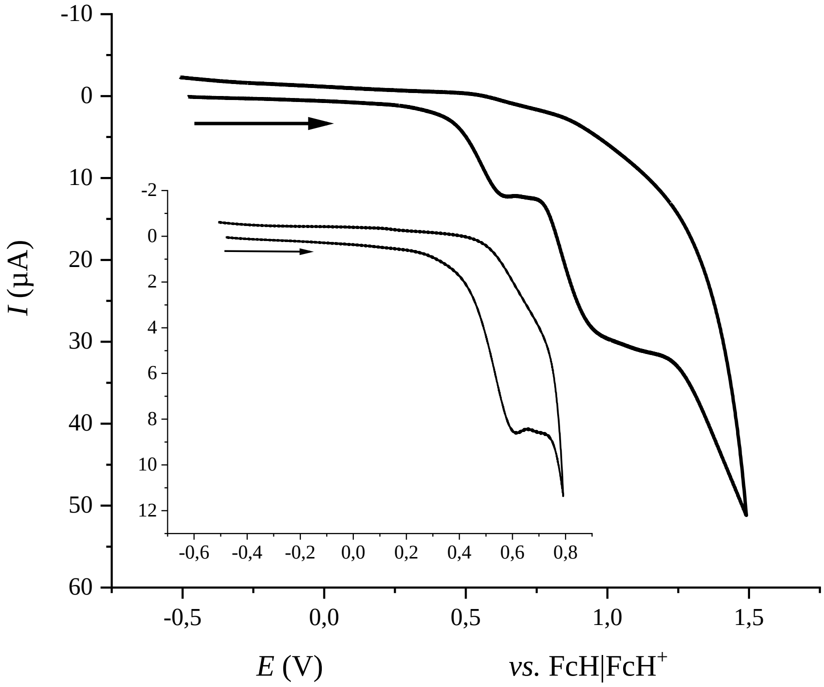

Figure S31: Cyclic voltammogram of *E,E*-**10** in THF (anodic scan; room temperature, supporting electrolyte:[nBu$_4$N][PF$_6$] (0.1 M), scan rate 200 mV s^{-1}). The inset refers to the cyclic voltammogram of *E,E*-**10** first oxidation process (100 mV s^{-1}).

6.2 UV/Vis absorption and emission spectra

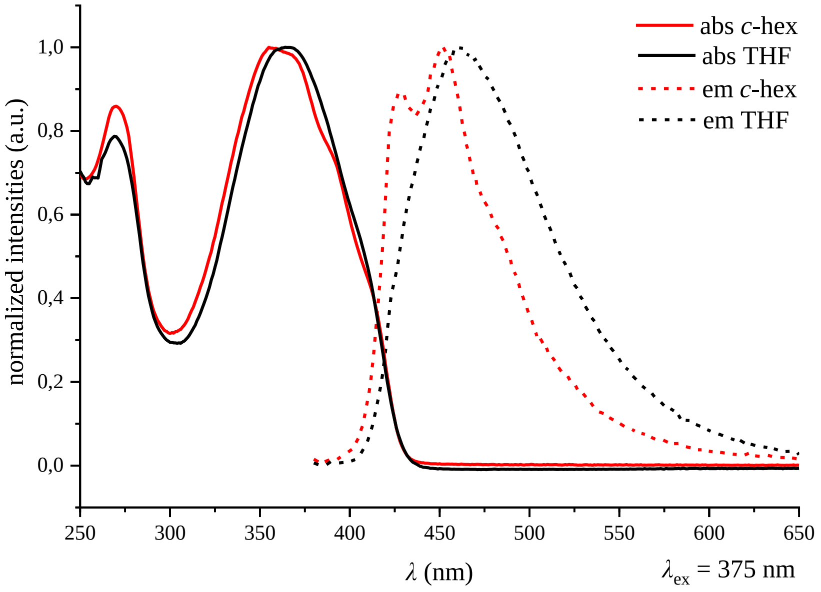

Figure S32. Normalized UV/Vis absorption and emission spectra of *trans*-**6** in *c*-hexane and THF.

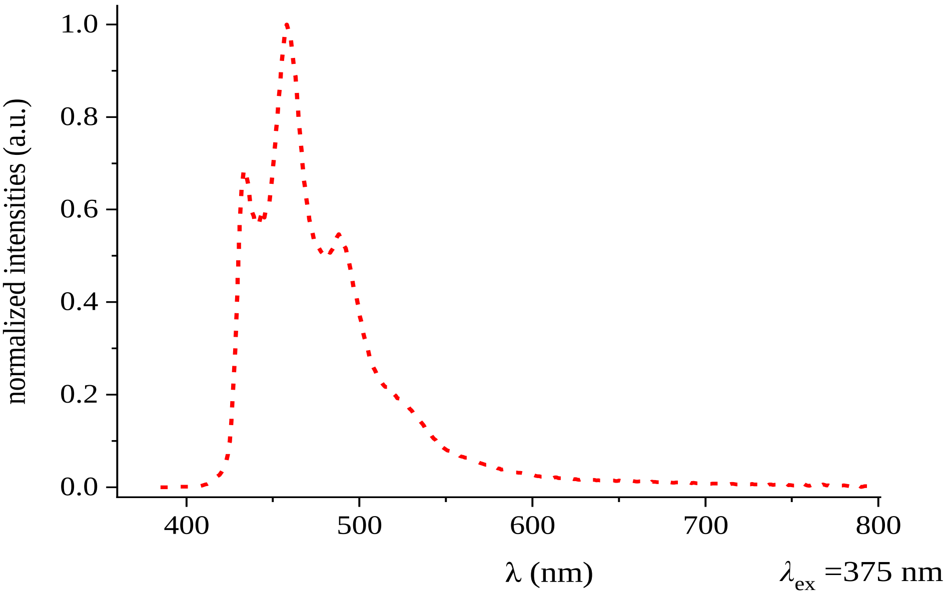

Figure S32A. Normalized low temperature emission spectrum of *trans*-**6** in a toluene frozen matrix (77K).

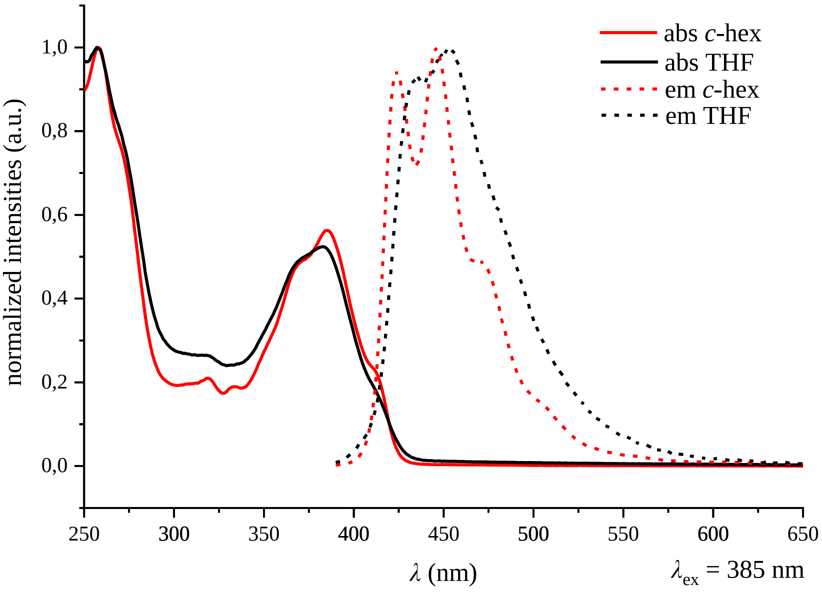

Figure S33. Normalized UV/Vis absorption and emission spectra of **2** in *c*-hexane and THF.

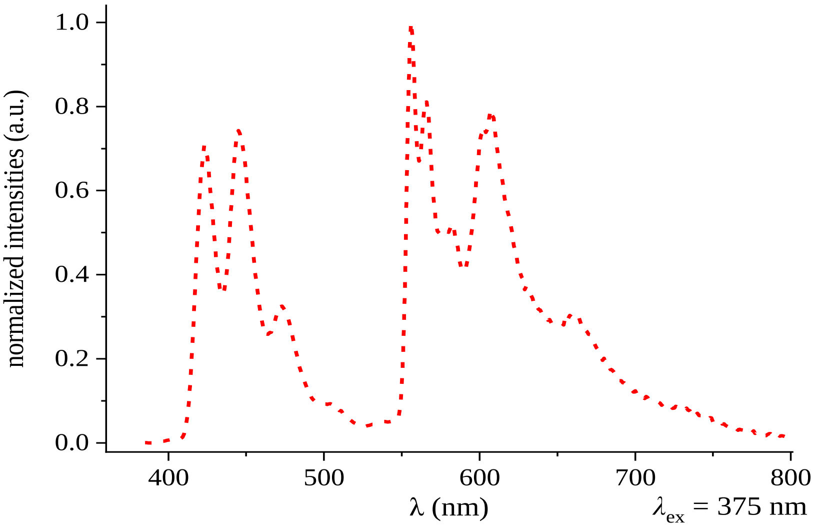

Figure S33A. Normalized low temperature emission spectrum of **2** in a toluene frozen matrix (77K).

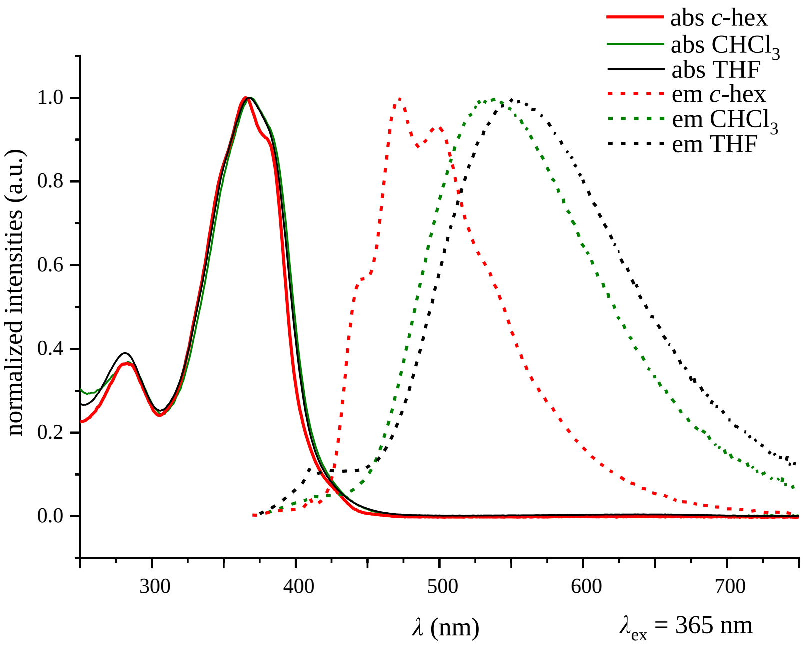

Figure S34. Normalized UV/Vis absorption and emission spectra of *E*,*E*-**10** in *c*-hexane, THF and $CHCl_3$.

6.3 Photophysical and electrochemical data

Table S2. Photophysical properties of all the new the boron-doped compounds and comparison with **1**, **7TH** and **MesDTOB**.

	c-hexane, r.t.						*toluene, 77 K*				
	λ_{abs} [nm] (ε [M^{-1} cm^{-1}])	**λ_{em} [nm]**	**τ [ns]**	**Φ_{PL} [%]**	**k_r [10^7]**	**k_{nr} [10^9]**	**$\lambda_{em,FL}$ [nm]**	**τ_{FL} [ns]**	**$\lambda_{em,PH}$ [nm]**	**τ_{PH} [ms]**	**E_T [eV]**
7TH[a]	244 (33758), 268 (sh), 277 (sh), 295 (14592), 303 (14436), 310 (14053), 329 (sh), 350 (sh) 370 (15392), 387 (16212)	403	0.74	6	8.1	1.27	397, 418, 441	1.11	531, 570, 614	124	2.33
1	269 (32400), 330 (29100), 340 (28700), 359 (29300), 374^{sh} (19900)	392, 411	--[b]	6	--[b]	--[b]	--[b]	--[b]	--[b]	--[b]	--[b]
2	258 (21900), 271 (sh), 319 (4600), 334 (4200), 368 (10600), 385 (12400), 413 (5000)	424, 446, 472, 506 (sh)	0.82	7	8.5	1.13	423, 445, 473, 505 (sh)	1.09	556, 566, 582 603, 607, 660 (sh), 735 (sh)	63.3	2.23
***trans*-6**	270 (26500), 355 (30700), 370 (30000), 393 (sh, 21500), 414 (sh, 12000)	429, 452, 489 (sh)	0.31	6	19.3	3.03	433, 457, 489, 530 (sh)	0.48	-[c]	-[c]	-[c]
E,E-10	283 (15400), 365 (41000), 382 (36500)	445 (sh), 472, 500, 535	2.0	12	6.0	0.44	--[b]	--[b]	--[b]	--[b]	--[b]
Mes DTOB	269 (32400), 330 (29100), 341 (28600), 359 (25300), 374 (sh)	366, 380	0.30	6	20.0	3.13	375, 395	0.70	436, 452, 464, 480	104	2.84

[a] measured in CH_2Cl_2 at r.t. and in 2-MeTHF at 77 K; [b] not measured. [c] not detected. [FL] = fluorescence. [PH] = phosphorescence. sh = shoulder. Rate constants k_r and k_{nr} are calculated using the equations $k_r = \Phi_{PL}/\tau$ and $k_{nr} = (1-\Phi_{PL})/\tau$.

Table S3. Optical and electrochemical data of all the new synthesized boron-doped compounds and comparison with **1**. Optical measurements were performed in *c*-hexane, and electrochemical measurements were performed in THF (room temperature, supporting electrolyte: [nBu$_4$N][PF$_6$] (0.1 M), scan rate 100-500 mV s^{-1}).

	$E_{1/2}$ [V]	**E^{I}_{pc} [V]**	**E^{II}_{pc} [V]**	**E^{I}_{pa} [V]**	**E^{II}_{pa} [V]**	**E_{HOMO}/E_{LUMO} [eV]**	**λ_{onset} [nm][c]**	**E_g^{opt} [eV][d]**
1	-[e]	–2.83	–3.01	–0.09	-[e]	–4.89 / –1.97[a]	393	3.16
trans-**6**	–1.97	–1.97	–2.26	-	-[e]	–5.68 / –2.83[a] –5.63/ –2.78[b]	435	2.85
2	-[e]	–1.66	–2.36	0.82	-[e]	–5.62 / –3.14[a]	428	2.90
E,E-**10**	-[e]	–2.21	-[e]	0.61	0.95	–5.41/–2.59[a]	460	2.69

[a] E_{HOMO}/E_{LUMO} calculated with the *maxima criterion*: $E_{HOMO} = -1e\times((E^{I}_{pa}/V([FcH]^{+} | FcH)+4.8\ V([FcH]^{+} | FcH\ vs.\ zero))$; $E_{LUMO} = -1e\times((E^{I}_{pc}/V([FcH]^{+} | FcH)+4.8\ V([FcH]^{+} | FcH\ vs.\ zero))$. sh = shoulder. [b] $E_{HOMO} = E_{LUMO} - E_g^{opt}$, $E_{LUMO} = -\ 4.8\ eV - E_{1/2}^{Red1}$ ($FcH/FcH^{+} = -\ 4.8$ eV vs vacuum level). [c] Each onset wavelength (λ_{onset}) was determined by constructing a tangent on the point of inflection of the bathochromic slope of the most red-shifted absorption maximum. [d] Optical band gap $E_g^{opt} = 1240/\lambda_{onset}$. [e] not detected.

7. X-ray crystal structure analyses

Single-crystal diffraction data for all structures except for compound **2** were collected at –100°C on a STOE IPDS II two-circle diffractometer equipped with a Genix Microfocus MoK_α X-ray source (λ = 0.71073 Å). The finalization of the data, including empirical absorption corrections, was done using X-Area program set v.1.50 (Stoe & Cie, 2006)[S15] or *CrysAlisPro* software v.1.171.42.43a (Rigaku Oxford Diffraction, 2022).

The diffraction data for compound **2** collected at T = 170(2) K in the *P24* beamline of the *DESY PETRA III* synchrotron (Hamburg, Germany) equipped with a four-circle *HUBER* diffractometer with Eulerian geometry and a X-*Spectrum Lambda 7.5M CdTe* photon-counting detector. The radiation with a wavelength of λ = 0.56 Å (E = 22.140 keV) was used. The data were acquired by two runs at two different detector 2Θ positions, 0° and -10°, to compensate the data loss from the gaps between the detector chips. Each run was done by 360° ϕ rotation with a 0.5° scan width and an exposure time of 8 s per frame. The finalization of the data, including empirical absorption corrections, was done using *CrysAlisPro* software 1.171.43.126a (Rigaku Oxford Diffraction, 2024).

The structures were solved by direct methods using the programs *SHELXS* (G. M. Sheldrick, 2008) or *SHELXT* [S15a] and refined against F^2 with full-matrix least-squares techniques using the program *SHELXL* (Sheldrick, 2008).[S16a]

In the structure of compound **6** the Mes groups suffer from slight disorder that was approximated by the elongated atomic displacement ellipsoids of the corresponding carbon atoms.

The crystal of compound **7** was twinned with the second twin domain rotated by ~180° around [0 0 1] in the reciprocal space. At that, the relative weight of the minor domain was refined as 28.5%. The refinement was based on both domains using SHELXL 'HKLF 5' instruction.

The crystal of compound **8** was also twinned, in addition to very weak scattering ability, resulting in very low diffraction intensities from the second, minor (26.2%) domain. For the final refinement, the non-overlapping reflections from this domain were excluded using the *HKLF5tools* routine (https://www.uni-marburg.de/en/fb15/researchgroups/ag-kraus/research/hklf5tools).

The crystal of compound **9** scattered so weakly that we had to discard all reflections above d_{min} = 1 Å.

The molecules in the compounds **2**, **4-11** in the crystals are depicted on the Figs. S35-S43 with selected geometrical characteristics in the figures' captions. The CIF files containing the crystallographic information are deposited in the Cambridge Crystallographic Data Centre under the deposition codes 2384683-2384691 and can be obtained free of charge via www.ccdc.cam.ac.uk/data_request/cif. Crystallographic data and parameters of the diffraction experiments are given in Tables S4-S8.

Table S4. Experimental details for compounds 2 and 4

	2, **CCDC: 2384683**	*trans*-**4**, **CCDC: 2384684**
Chemical formula	$C_{36}H_{28}B_2O_2S_4$	$C_{10}H_6Br_2S_2$
M_r	642.44	350.09
Crystal system, space group	Monoclinic, *C*2/*c*	Orthorhombic, *Pbca*
Temperature (K)	170	173
a, *b*, *c* (Å)	20.9778(6), 20.7457(5), 7.3237(2)	10.3682(4), 7.5629(3), 14.4299(6)
α, β, γ (°)	90, 98.674(3), 90	90, 90, 90
V (Å^3)	3150.80(15)	1131.49 (7)
Z	4	4
F(000)	1336	672
D_x (Mg m^{-3})	1.354	2.055
Radiation source	Synchrotron, λ = 0.560 Å	Mo Kα, λ = 0.71073 Å
μ (mm^{-1})	0.18	7.49
Crystal shape	Needle	Plate
Colour	Pale brown	Brown
Crystal size (mm^3)	0.15 × 0.02 × 0.02	0.26 × 0.25 × 0.06
Absorption correction	Multi-scan	Multi-scan
T_{min}, T_{max}	0.081, 1.000	0.171, 1.000
No. of measured, independent and observed [$I > 2s(I)$] reflections	19919, 3224, 2501	21643, 1516, 1344
R_{int}	0.069	0.061
Θ_{max} (°)	20.5	29.1
Range of *h*, *k*, *l*	$h = -26 \rightarrow 26$, $k = -25 \rightarrow 25$, $l = -9 \rightarrow 9$	$h = -14 \rightarrow 14$, $k = -10 \rightarrow 10$, $l = -19 \rightarrow 18$
$R[F^2 > 2s(F^2)]$, $wR(F^2)$, S	0.041, 0.110, 1.10	0.026, 0.061, 1.11
No. of reflections	3224	1516
No. of parameters	202	65
$\Delta\rho_{\text{max}}$, $\Delta\rho_{\text{min}}$ (e Å^{-3})	0.27, -0.33	0.33, -0.50

Table S5. Experimental details for compounds 5 and 6

	trans-**5**, **CCDC: 2384685**	*trans*-**6**, **CCDC: 2384686**
Chemical formula	$C_{20}H_{16}O_2S_4$	$C_{36}H_{30}B_2O_2S_4$
M_r	416.57	644.46
Crystal system, space group	Orthorhombic, $Fdd2$	Monoclinic, $P2_1/c$
Temperature (K)	173	173
a, b, c (Å)	35.371(2), 38.7786(17), 5.5772(3)	12.7041(5), 6.2990(3), 20.8628(11)
α, β, γ (°)	90, 90, 90	90, 99.828(4), 90
V (Å^3)	7650.0(7)	1645.01(13)
Z	16	2
F(000)	3456	672
D_x (Mg m^{-3})	1.447	1.301
Radiation source	Mo Kα, λ = 0.71073 Å	Mo Kα, λ = 0.71073 Å
μ (mm^{-1})	0.51	0.32
Crystal shape	Needle	Plank
Colour	Colourless	Brown
Crystal size (mm^3)	0.22 × 0.04 × 0.04	0.55 × 0.30 × 0.03
Absorption correction	Multi-scan	Multi-scan
T_{min}, T_{max}	0.335, 1.000	0.081, 1.000
No. of measured, independent and observed [$I > 2s(I)$] reflections	13908, 3586, 3016	11399, 3352, 2506
R_{int}	0.055	0.059
Θ_{max} (°)	25.7	26.4
Range of h, k, l	$h = -42 \rightarrow 42$, $k = -45 \rightarrow 46$, $l = -6 \rightarrow 6$	$h = -14 \rightarrow 15$, $k = -7 \rightarrow 7$, $l = -26 \rightarrow 25$
$R[F^2 > 2s(F^2)]$, $wR(F^2)$, S	0.058, 0.138, 1.16	0.043, 0.115, 1.04
No. of reflections	3586	3352
No. of parameters	235	202
$\Delta\rho_{max}$, $\Delta\rho_{min}$ (e Å^{-3})	0.24, -0.27	0.44, -0.22
Absolute structure parameter	0.01(18)	–

Table S6. Experimental details for compounds 7 and 8

	7, CCDC: 2384687	**8, CCDC: 2384688**
Chemical formula	$C_{21}H_{12}OS_4$	$C_{11}H_8O_3S_2$
M_r	408.55	252.29
Crystal system, space group	Triclinic, $P\bar{1}$	Monoclinic, $P2_1/n$
Temperature (K)	173	173
a, b, c (Å)	15.1300(11), 15.3597(9), 17.5595(16)	3.8781(3), 8.6909(6), 32.175(2)
α, β, γ (°)	102.360(7), 108.006(8), 102.859(6)	90, 91.658(7), 90
V (Å^3)	3603.2(5)	1083.99(14)
Z	8	4
$F(000)$	1680	520
D_x (Mg m^{-3})	1.506	1.546
Radiation source	Mo Kα, λ = 0.71073 Å	Mo Kα, λ = 0.71073 Å
μ (mm^{-1})	0.54	0.48
Crystal shape	Plate	Needle
Colour	Light yellowish-brown	Orange
Crystal size (mm^3)	0.42 × 0.41 × 0.05	0.09 × 0.02 × 0.01
Absorption correction	Multi-scan	Multi-scan
T_{min}, T_{max}	0.791, 1.000	0.016, 1.000
No. of measured, independent and observed [$I > 2s(I)$] reflections	16557, 16557, 6590	2393, 2393, 1158
R_{int}	0.141	0.220
Θ_{max} (°)	26.4	25.4
Range of h, k, l	$h = -18 \rightarrow 18$, $k = -19 \rightarrow 19$, $l = -21 \rightarrow 21$	$h = -4 \rightarrow 4$, $k = -10 \rightarrow 10$, $l = -38 \rightarrow 38$
$R[F^2 > 2s(F^2)]$, $wR(F^2)$, S	0.053, 0.093, 0.74	0.076, 0.182, 0.91
No. of reflections	16557	2393
No. of parameters	942	147
$\Delta\rho_{max}$, $\Delta\rho_{min}$ (e Å^{-3})	0.31, -0.36	0.42, -0.44

Table S7. Experimental details for compounds 9 and 10

	E,*E*-**9**, **CCDC: 2384689**	*E*,*E*-**10**, **CCDC: 2384690**
Chemical formula	$C_{21}H_{16}OS_4$[+solvent]	$C_{29}H_{23}BOS_4$
M_r	412.58	526.52
Crystal system, space group	Monoclinic, $P2_1/n$	Orthorhombic, $P2_12_12_1$
Temperature (K)	173	173
a, b, c (Å)	28.003(7), 5.6280(12), 28.991(6)	6.3515 (5),18.4915(11), 22.5750(11)
α, β, γ (°)	90, 93.94(2), 90	90, 90, 90
V (Å^3)	4558.2 (18)	2651.4(3)
Z	8	4
F(000)	1712	1096
D_x (Mg m^{-3})	1.202	1.319
Radiation source	Mo Kα, λ = 0.71073 Å	Mo Kα, λ = 0.71073 Å
μ (mm^{-1})	0.42	0.38
Crystal shape	Needle	Needle
Colour	Colourless	Green
Crystal size (mm^3)	0.12 × 0.03 × 0.02	0.18 × 0.04 × 0.01
Absorption correction	Multi-scan	Multi-scan
T_{min}, T_{max}	0.032, 1.000	0.293, 1.000
No. of measured, independent and observed [$I > 2s(I)$] reflections	15410, 4758, 2016	14919, 4991, 3786
R_{int}	0.195	0.090
Θ_{max} (°)	20.8	25.8
Range of h, k, l	$h = -28 \rightarrow 27$, $k = -5 \rightarrow 5$, $l = -28 \rightarrow 28$	$h = -7 \rightarrow 7$, $k = -22 \rightarrow 22$, $l = -27 \rightarrow 25$
$R[F^2 > 2s(F^2)]$, $wR(F^2)$, S	0.064, 0.161, 0.69	0.083, 0.198, 1.15
No. of reflections	4758	4991
No. of parameters	471	319
$\Delta\rho_{max}$, $\Delta\rho_{min}$ (e Å^{-3})	0.32, -0.31	0.39, -0.42
Absolute structure parameter	–	-0.19(17)

Table S8. Experimental details for compound 11

	***E*-11, CCDC: 2384691**
Chemical formula	$C_{29}H_{21}BOS_4$
M_r	524.51
Crystal system, space group	Monoclinic, $P2_1/c$
Temperature (K)	173
a, b, c (Å)	6.3634(6), 15.1793(12), 26.884(3)
α, β, γ (°)	90, 94.709(10), 90
V (Å^3)	2588.0 (4)
Z	4
F(000)	1088
D_x (Mg m^{-3})	1.346
Radiation source	Mo Kα, λ = 0.71073 Å
μ (mm^{-1})	0.39
Crystal shape	Needle
Colour	Yellow
Crystal size (mm^3)	0.48 × 0.15 × 0.08
Absorption correction	Multi-scan
T_{min}, T_{max}	0.658, 1.000
No. of measured, independent and observed [$I > 2s(I)$] reflections	8910, 8910, 4064
R_{int}	0.285
Θ_{max} (°)	25.7
Range of h, k, l	h = -7→7, k = -18→18, l = -32→32
$R[F^2 > 2s(F^2)]$, $wR(F^2)$, S	0.079, 0.187, 0.90
No. of reflections	8910
No. of parameters	320
$\Delta\rho_{max}$, $\Delta\rho_{min}$ (e Å^{-3})	0.53, -0.43

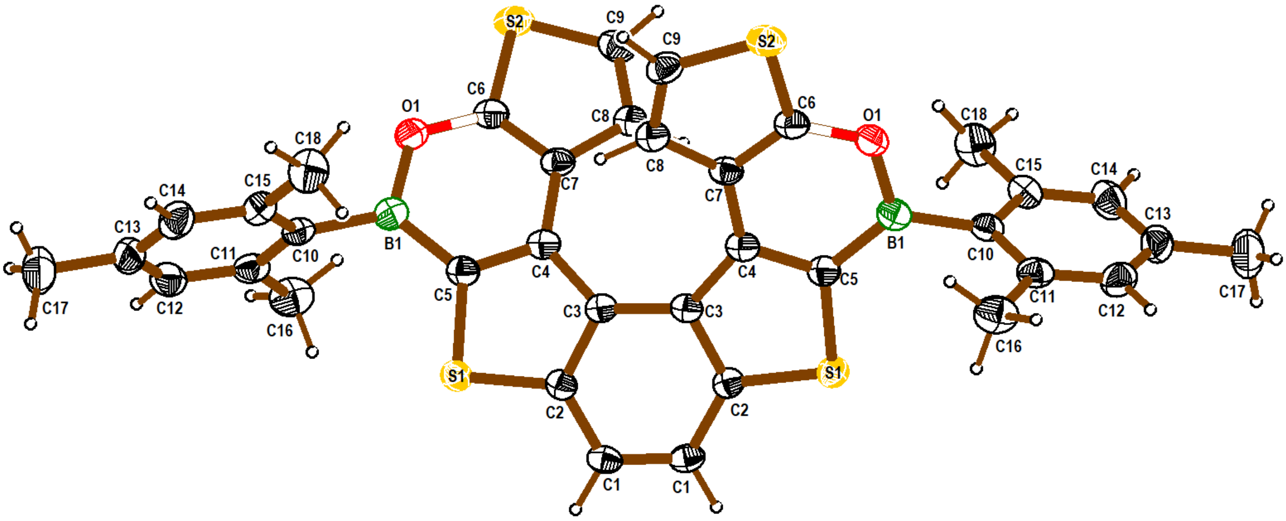

Figure S35. Molecular structure of **2** in the solid state. Displacement ellipsoids are drawn at the 50% probability level. Displacement ellipsoids are drawn at the 50% probability level. Selected bond lengths (A) bond angles (°), and torsion angles (°): B(1)-O(1) = 1.393(3), B(1)-C(5) = 1.525(3), B(1)-C(10) = 1.562(3); O(1)-B(1)-C(5) = 115.4(2), O(1)-B(1)-C(10) = 116.71(19), C(5)-B(1)-C(10) = 127.8(2); C(5)-B(1)-C(10)-C(11) = –83.4(3), O(1)-B(1)-C(10)-C(11) = 98.6(2), O(1)-B(1)-C(10)-C(15) = -79.2(2), C(3)^{i}-C(3)-C(4)-C(7) = 17.3(4), C(4)-C(3)-C(3)-C(4) = 24.91(5), C(3)-C(4)-C(7)-C(8) = 5.3(4), O(1)-B(1)-C(5)-S(1) = -169.36(15). Dihedral angle between the two terminal thiophene rings: 58.36(6).

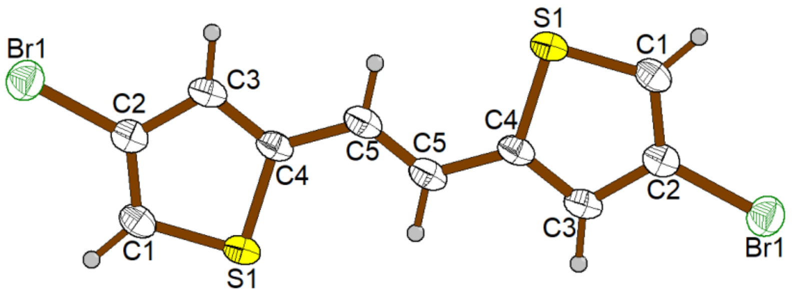

Figure S36. Molecular structure of *trans*-**4** in the solid state. Displacement ellipsoids are drawn at the 50% probability level. Displacement ellipsoids are drawn at the 50% probability level. Selected bond lengths (A), bond angles (°), and torsion angles (°): Br1-C2 = 1.883(2), S1-C1 = 1.713 (2), S1-C4 = 1.734(2), C1-C2 = 1.356(3), C2-C3 = 1.421(3), C3-C4 = 1.369(3), C4-C5 = 1.453(3), C5-C5^{i} = 1.336(5); C1-S1-C4 = 92.16(11), C2-C1-S1 = 110.98(16), C1-C2-C3 = 114.0(2), C1-C2-Br1 = 123.68(17), C3-C2-Br1 = 122.34(16), C4-C3-C2 = 111.89(19), C3-C4-C5 = 125.99(19), C3-C4-S1 = 110.98(17), C5-C4-S1 = 123.02(18), C5^{i}-C5-C4 = 125.9(3); C4-S1-C1-C2 = –0.59(16), S1-C1-C2-C3 = 1.0(2), S1-C1-C2-Br1 = 179.81(11), C1-C2-C3-C4 = –1.1(3), Br1-C2-C3-C4 = –179.85(14), C2-C3-C4-C5 = –179.89(19), C2-C3-C4-S1 = 0.6(2), C1-S1-C4-C3 = 0.00(17), C1-S1-C4-C5 = –179.56(18), C3-C4-C5-C5^{i} = 178.0(3), S1-C4-C5-C5^{i} = –2.6(4).

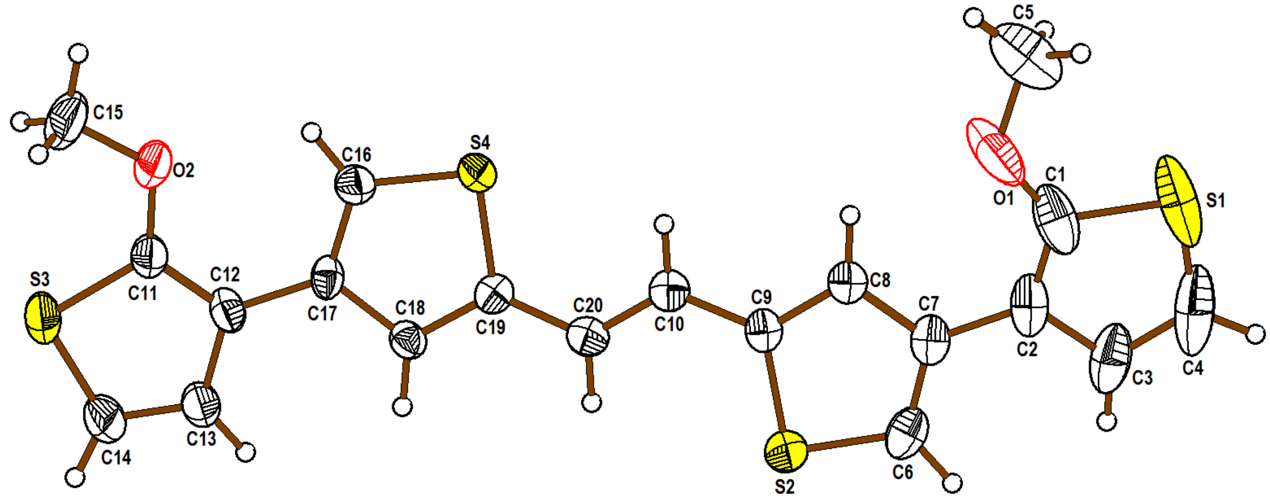

Figure S37. Molecular structure of *trans*-**5** in the solid state. Displacement ellipsoids are drawn at the 50% probability level. Selected bond lengths (A), bond angles (°), and torsion angles (°): O(1)-C(1) = 1.355(13), O(2)-C(15) = 1.411(13), C(2)-C(7) = 1.473(9), C(12)-C(17) = 1.475(8), C(10)-C(20) = 1.348(9); C(4)-S(1)-C(1) = 90.5(5), C(14)-S(3)-C(11) = 90.8(4), C(1)-O(1)-C(5) = 120.2(8), O(1)-C(1)-S(1) = 121.7(7), C(20)-C(10)-C(9) = 127.7(6); C(8)-C(9)-C(10)-C(20) = –174.9(6), S(2)-C(9)-C(10)-C(20) = – 4.8(9), C(3)-C(2)-C(7)-C(8) = –160.0(7), C(9)-C(10)-C(20)-C(19) = –178.9(6).

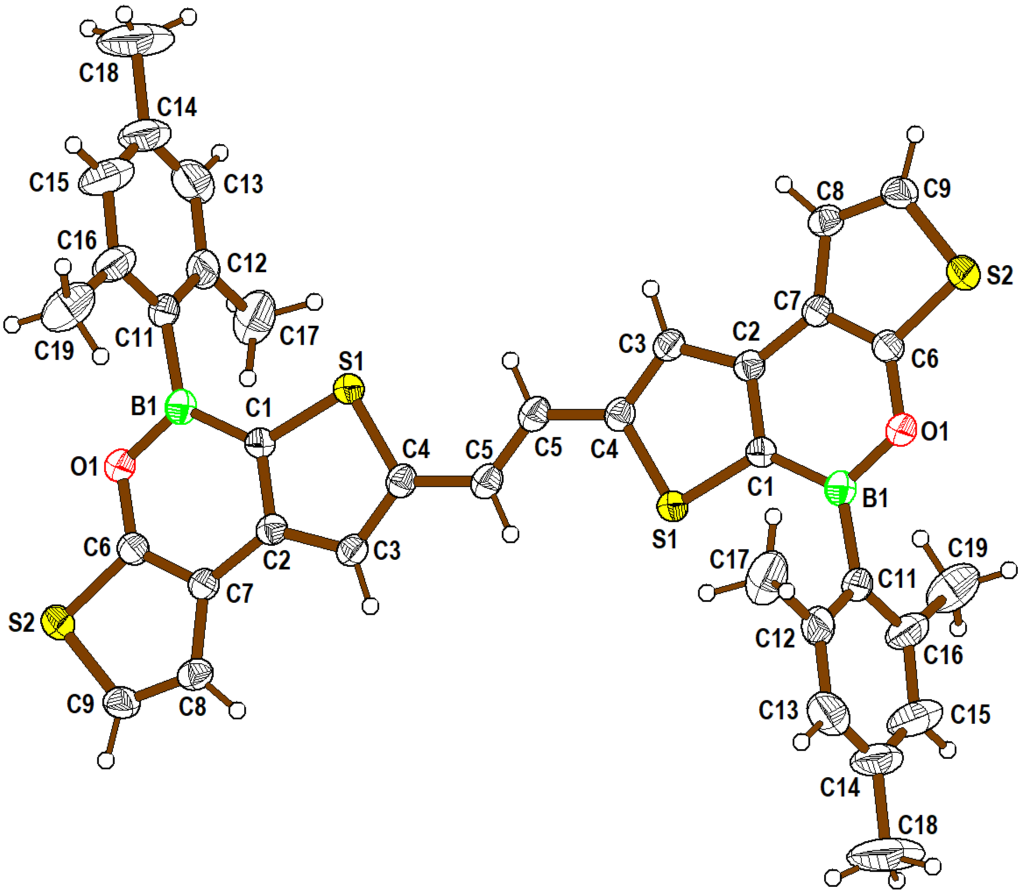

Figure S38. Molecular structure of *trans*-**6** in the solid state. Displacement ellipsoids are drawn at the 50% probability level. Displacement ellipsoids are drawn at the 50% probability level. Selected bond lengths (A), bond angles (°), and torsion angles (°): B1-O1 = 1.400(3), B1-C1 = 1.518(3), B1-C11 = 1.568(3), S1-C1 = 1.727(2), C5-C5^{i} = 1.337(4), S2-C6 = 1.725(2), C4-C5 = 1.447(3); O1-B1-C1 = 115.26(19), O1-B1-C11 = 119.24(18), C1-B1-C11 = 125.5(2), C5^{i}-C5-C4 = 125.7(2); C1-B1-O1-C6 = 0.7(3), C11-B1-O1-C6 = –179.8(2), O1-B1-C1-C2 = 1.5(3), C11-B1-C1-C2 = –178.0(2), O1-B1-C1-S1 = 177.10(16), C3-C4-C5-C5^{i} = 177.9(3), S1-C4-C5-C5^{i} = –2.0(4).

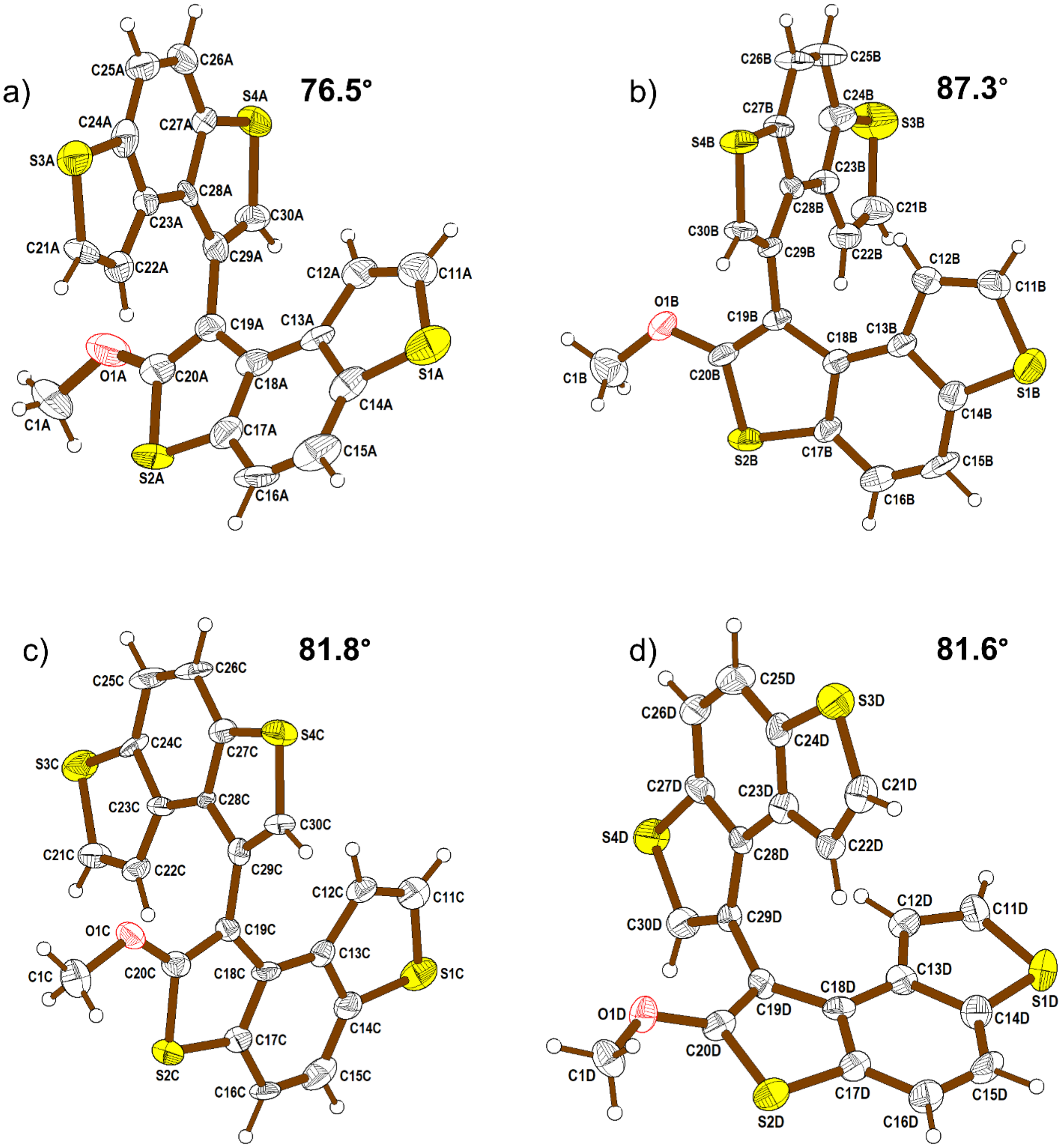

Figure S39. Molecular structure of **7** in the solid state showing four crystallographically unique molecules (a, b, c, and d) with the corresponding internal interplanar angles. Displacement ellipsoids are drawn at the 50% probability level. Displacement ellipsoids are drawn at the 50% probability level. Bond lengths (A), bond angles (°), and torsion angles (°) are given in the CIF file deposited together with the Supporting Information.

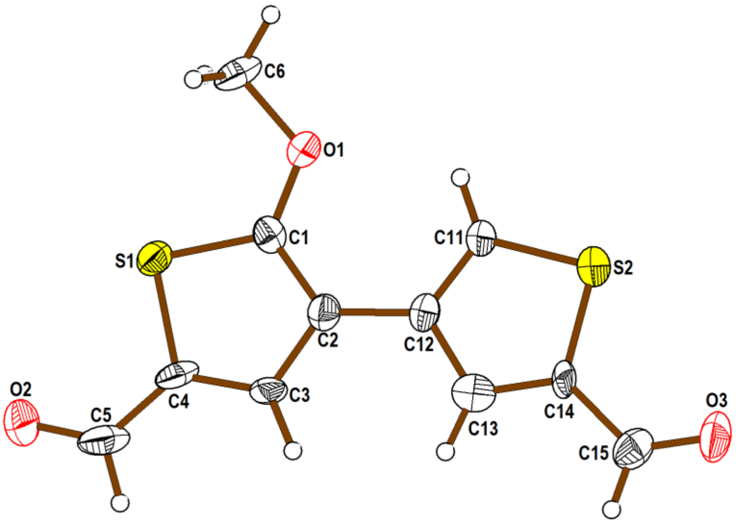

Figure S40. Molecular structure of **8** in the solid state. Displacement ellipsoids are drawn at the 50% probability level. Displacement ellipsoids are drawn at the 50% probability level. Selected bond lengths (A), bond angles (°), and torsion angles (°): O(1)-C(1) = 1.339(9), O(2)-C(5) = 1.223(10), O(3)-C(15) = 1.214(9), C(2)-C(12) = 1.489(10), C(1)-S(1) = 1.724(8), C(11)-S(2) = 1.715(8), C(1)-C(2) = 1.391(11), C(3)-C(4) = 1.360(11), C(13)-C(14) = 1.341(10); C(1)-C(2)-C(12) = 125.3(7), C(2)-C(12)-C(11) = 125.8(7), O(1)-C(1)-C(2) = 123.1(7); C(1)-C(2)-C(12)-C(11) = -12.0(15).

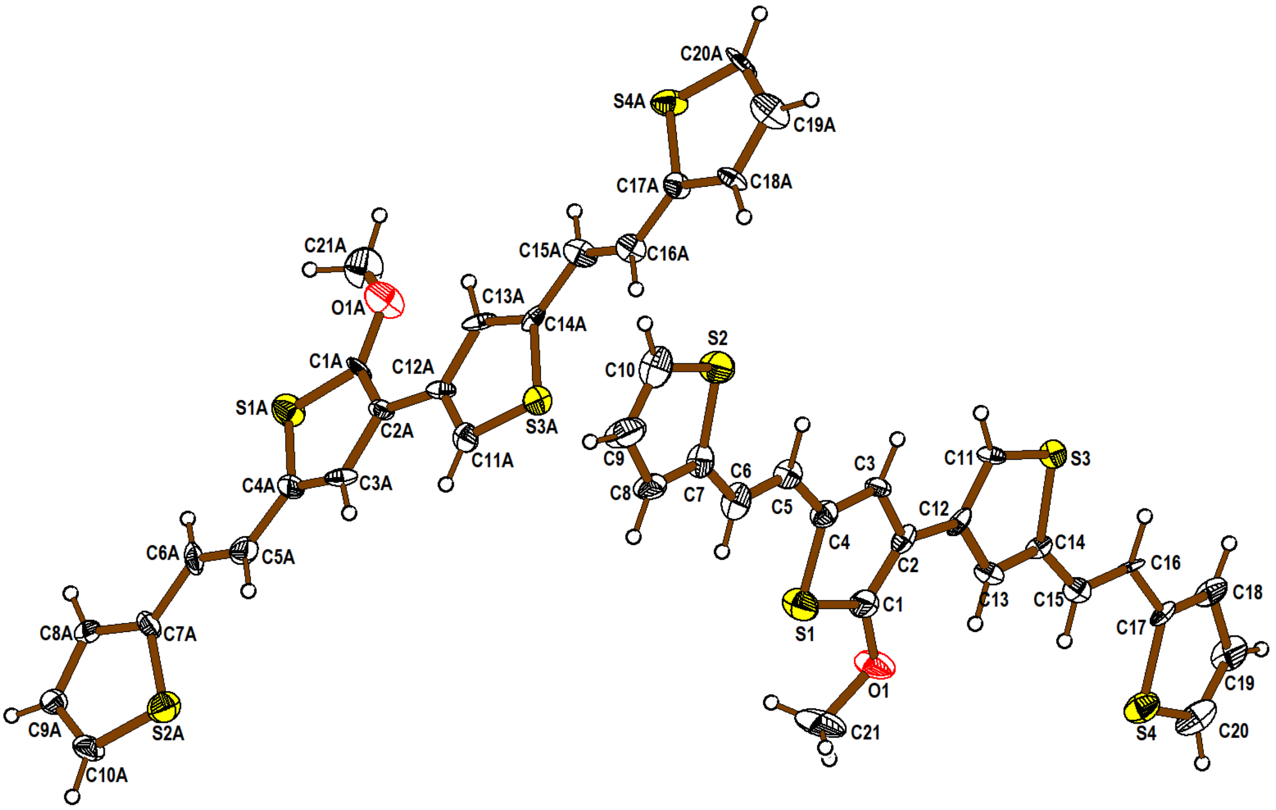

Figure S41. Molecular structure of *E*,*E*-**9** in the solid state. Displacement ellipsoids are drawn at the 50% probability level. Displacement ellipsoids are drawn at the 50% probability level. Selected bond lengths (A), bond angles (°), and torsion angles (°): O(1)-C(1) = 1.374(11), C(11)-S(3) = 1.706(9), C(1)-S(1) = 1.738(10), C(2)-C(12) = 1.467(12), C(5)-C(6) = 1.351(12), C(15)-C(16) = 1.366(11); C(1)-C(2)-C(12) = 127.2(9), C(13)-C(12)-C(2) = 124.9(8), O(1)-C(1)-C(2) = 123.0(9); C(1)-C(2)-C(12)-C(13) = -9.9(15).

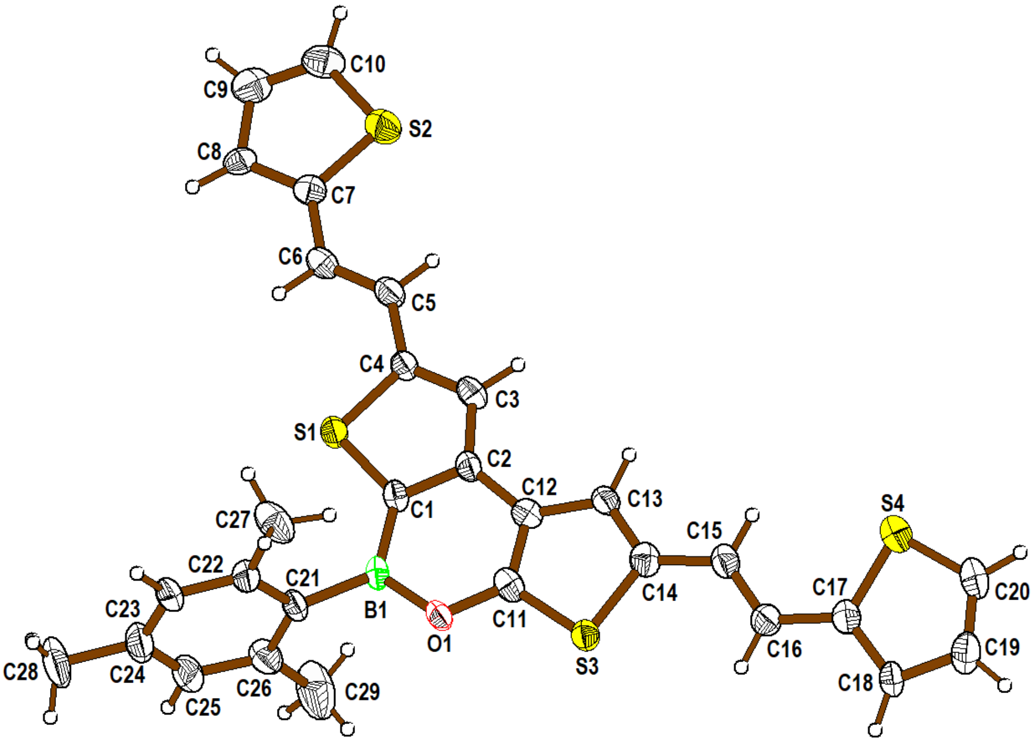

Figure S42. Molecular structure of *E*,*E*-**10** in the solid state. Displacement ellipsoids are drawn at the 50% probability level. Selected bond lengths (A), bond angles (°), and torsion angles (°): O(1)-B(1) = 1.418(13), B(1)-C(1) = 1.516(14), B(1)-C(21) = 1.563(12), C(5)-C(6) = 1.342(14), C(15)-C(16) = 1.334(14); O(1)-B(1)-C(1) = 115.6(8), O(1)-B(1)-C(21) = 120.4(9), C(1)-B(1)-C(21) = 123.9(9), C(6)-C(5)-C(4) = 127.9(9), C(5)-C(6)-C(7) = 126.5(8), C(16)-C(15)-C(14) = 127.4(9), C(15)-C(16)-C(17) = 124.9(9); C(4)-C(5)-C(6)-C(7) = –178.8(9), C(11)-O(1)-B(1)-C(1) = 1.3(12), O(1)-B(1)-C(1)-S(1) = 179.9(7), B(1)-O(1)-C(11)-S(3) = 179.6(7), C(14)-C(15)-C(16)-C(17) = –175.6(9).

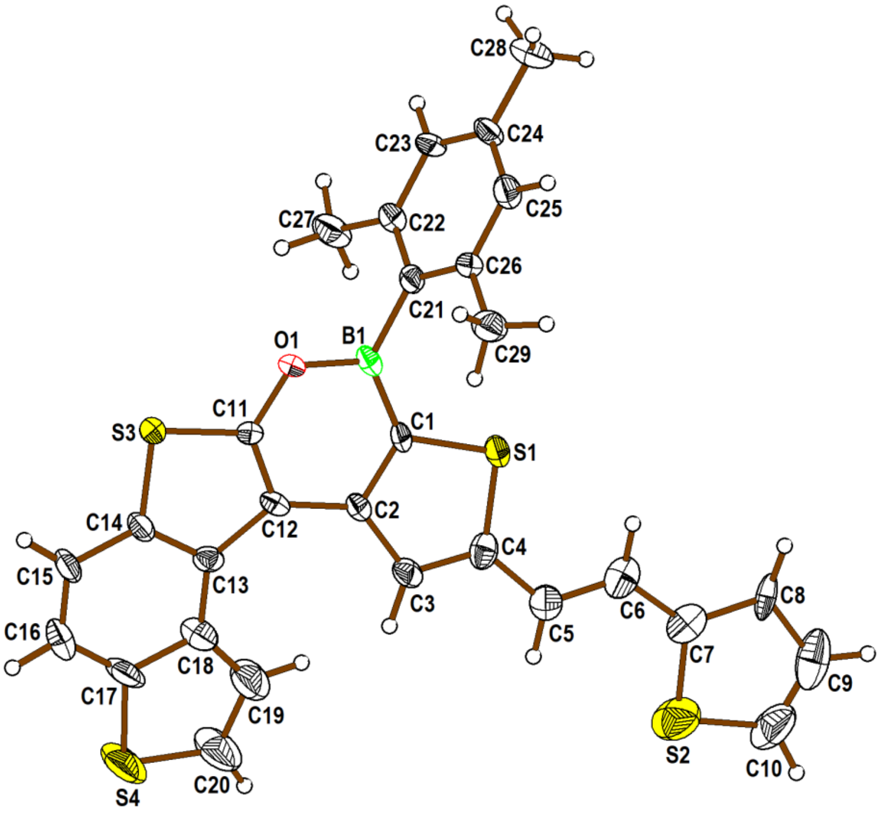

Figure S43. Molecular structure of *E*-**11** in the solid state. Displacement ellipsoids are drawn at the 50% probability level. Displacement ellipsoids are drawn at the 50% probability level. Selected bond lengths (A), bond angles (°), and torsion angles (°): O(1)-B(1) = 1.392(9), O(1)-C(11) = 1.349(7), C(1)-S(1) = 1.725(6), C(1)-S(3) = 1.726(6), C(5)-C(6) = 1.37(1), C(15)-C(16) = 1.35(1), C(2)-C(12) = 1.463(8), C(13)-C(18) = 1.418(8); C(3)-C(2)-C(12) = 131.1(5), C(13)-C(18)-C(19) = 132.4(6), B(1)-O(1)-C(11) = 120.7(5); B(1)-C(21)-C(26)-C(29) = –3.7(9), C(3)-C(2)-C(12)-C(13) = –12.0(1), C(12)-C(13)-C(18)-C(19) = –4.0(1). Dihedral angle between the two terminal thiophene rings of the penta-fused fragment: 20.4(4).

8. Chiroptical and kinetic studies of 2

8.1 UHPLC resolution and racemization kinetics of 2

The (P)-/(M)-enantiomers of **2** were separated by chiral stationary phase ultra-high performance liquid chromatography (CSP-UHPLC) on a (*S*,*S*)-Whelk-O 1 column, using *n*-hexane/ CH_2Cl_2 (95 :5) as eluent (please refer to Figure S44 for chromatogram data).

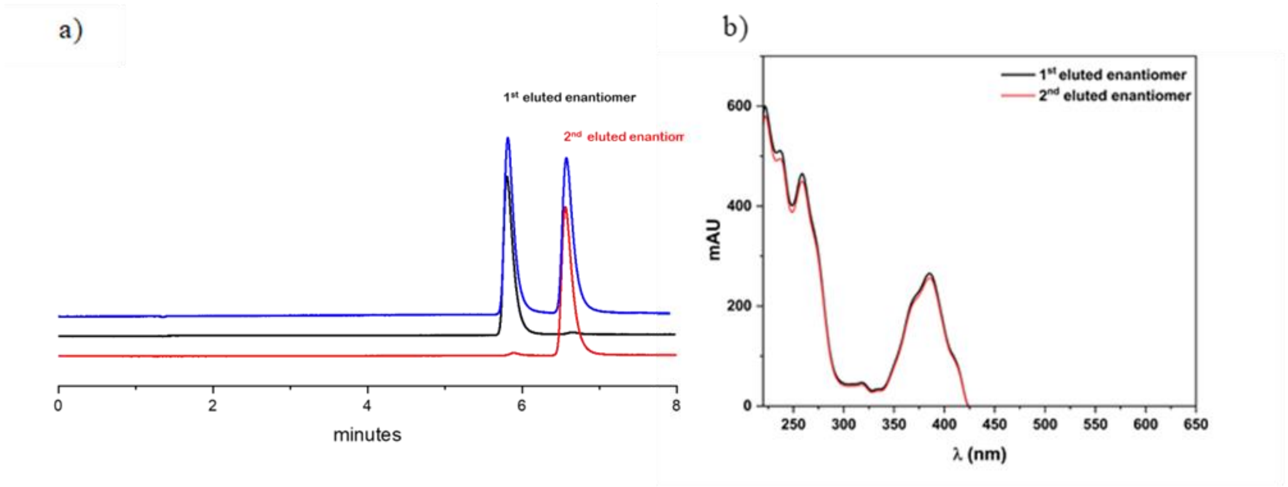

Figure S44. a) UHPLC resolution of **2**: racemic mixture (blue trace), first eluted enantiomer (black trace), second eluted enantiomer (red trace) - stationary phase: (*S*,*S*)-Whelk-O 1, mobile phase: *n*-hexane/CH_2Cl_2 (95:5), flow rate = 1.0 mL/min, 35 °C; UV at 385 nm b) UV spectra of the first (black trace) and second (red trace) eluted enantiomer, *n*-hexane/CH_2Cl_2 (95:5).

Table S13. HPLC resolution parameters for the separation of **2** enantiomers.

Eluted peak	R_t (min) [a]	k (t_0 = 1.4)[b]	Relative Area %	A_s [c]	α [d]	R [e]
1	5.81	3.94	50	1.76	1.14	3.20
2	6.57	4.62	50	1.75		

[a] R_t = retention time. [b] k = retention factor, t_0 = void time; k was calculated according to the equation $k = (R_t - t_0)/t_0$. [c] A_s = asymmetry factor, back-to-front ratio of a bisected peak measured at 10% of height. [d] α = selectivity, calculated from the ratio of k values, $\alpha = k_2/k_1$. [e] R = resolution, calculated according to the EP formula equation.

The enantiomers of **2** are stable at room temperature as revealed by preliminary racemization tests carried out on the UHPLC isolated single enantiomers. Scale-up to semipreparative level of the HPLC separation was easily obtained using a 10 mm internal diameter column. The second eluted enantiomer, has been isolated with high enantiomeric excess (e.e.=97%, R_t = 6.5 min; Figure S45, red trace).

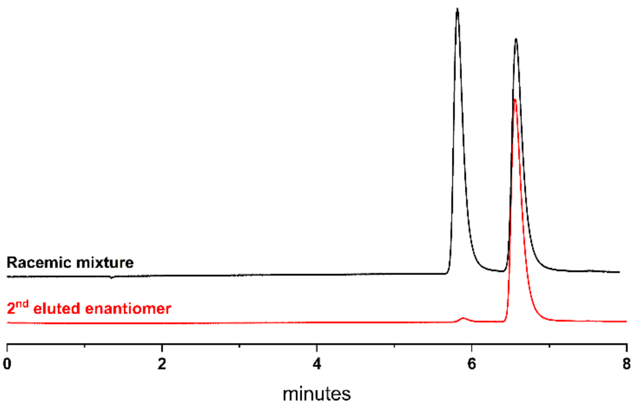

Figure S45. Second eluted enantiomer of **2** after semipreparative HPLC separation.

The collected fractions containing only the second eluted enantiomer were combined and evaporated at room temperature. The solid residue was dissolved in decalin and subjected to thermal racemization at 80 °C. Time monitoring of the changes in the enantiomeric excess of the sample were monitored by CSP-UHPLC.

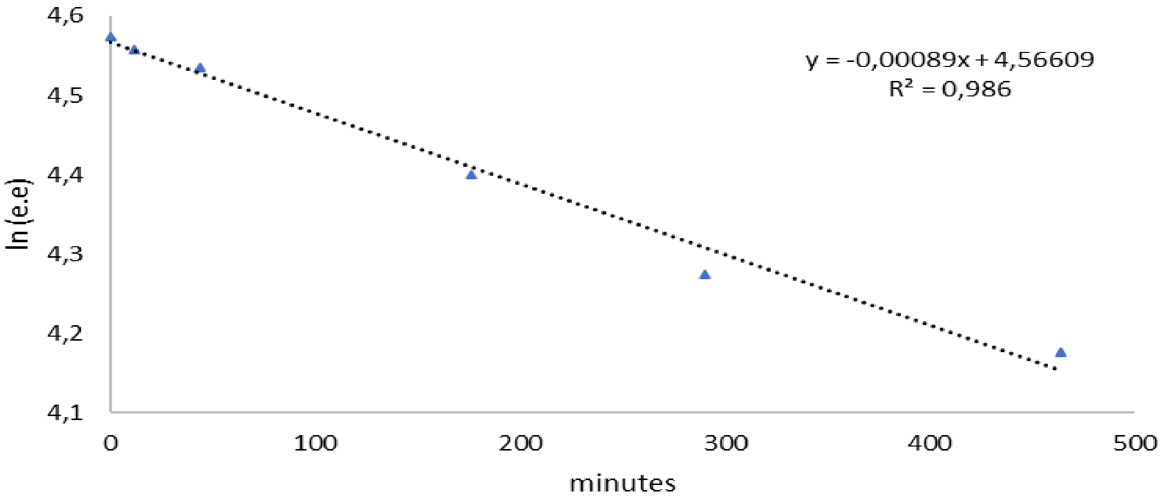

Figure S46. *ln(e.e.)* vs *time* plot used to estimate the racemization constant. The mathematical expression of the linear regression is given in the top right corner.

No additional peaks were observed, showing that 1 undergoes no chemical degradation even at the highest temperatures explored. The *e.e.* data were collected over 464 min and used to determine the racemization constant k_{rac}=1.48×10^{-5} s^{-1}. The associated enantiomerization constant is obtained by the relation k_{enant} = 0.5 × k_{rac}. The associated free energy of activation ΔG_{rac} =28.63± 0.1 kcal mol^{-1} (at 353 K) and ΔG_{enant}=29.37± 0.1 kcal/mol (353 K) were calculated by using the Eyring equation (reported below in linear form) and setting a transmission coefficient equal to 0.5. The free activation of enantiomerization is calculated through the following equation:

$$\Delta G^{\ddagger} = 4.576 * 10^{-3} * T\ [10.319 + log(T/k)]$$

$k = k_{enant}$; $\Delta G^{\ddagger}$ = free energy of enantiomerization; T = absolute temperature in Kelvin (K); k_B = Boltzmann's constant; h = Planck's constant; R = universal gas constant.

Where

$$k = \kappa\left(\frac{k_B T}{h}\right)e^{-\Delta G^{\ddagger}/RT}$$

Assuming the transmission coefficient κ =0.5.

8.2 Optical rotation and CD spectra

Circular dichroism spectra recorded in *n*-hexane/CH_2Cl_2 (95: 5) at 20 °C show a perfect mirror-image relationship between the first and second eluted enantiomer of **2** (Figure S47, black and red trace); the optical rotation values are -264 (*e.e.* = 98%) and +261 (*e.e.* = 97%) respectively (*c* = 0.1 in *n*-hexane/CH_2Cl_2 95:5).

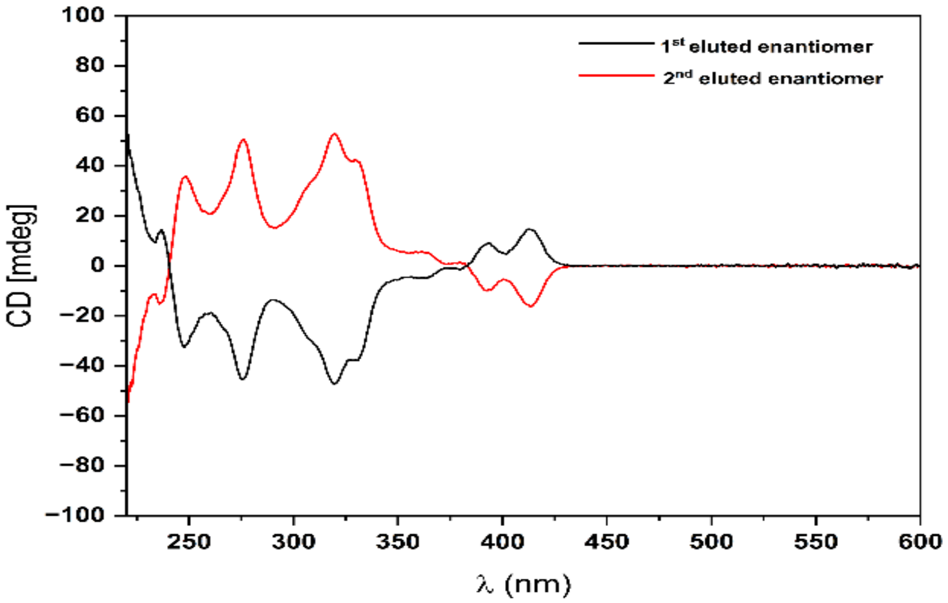

Figure S47. CD spectra of first (black trace) and second (red trace) eluted enantiomers of **2** measured by using a standard quartz cuvette (pathlength 10 mm); the concentration of the measured samples is 0.05 mg/mL.

9. Theoretical studies of 2

9.1 Assignment of 2 absolute configuration and electronic transitions characterization[S17]

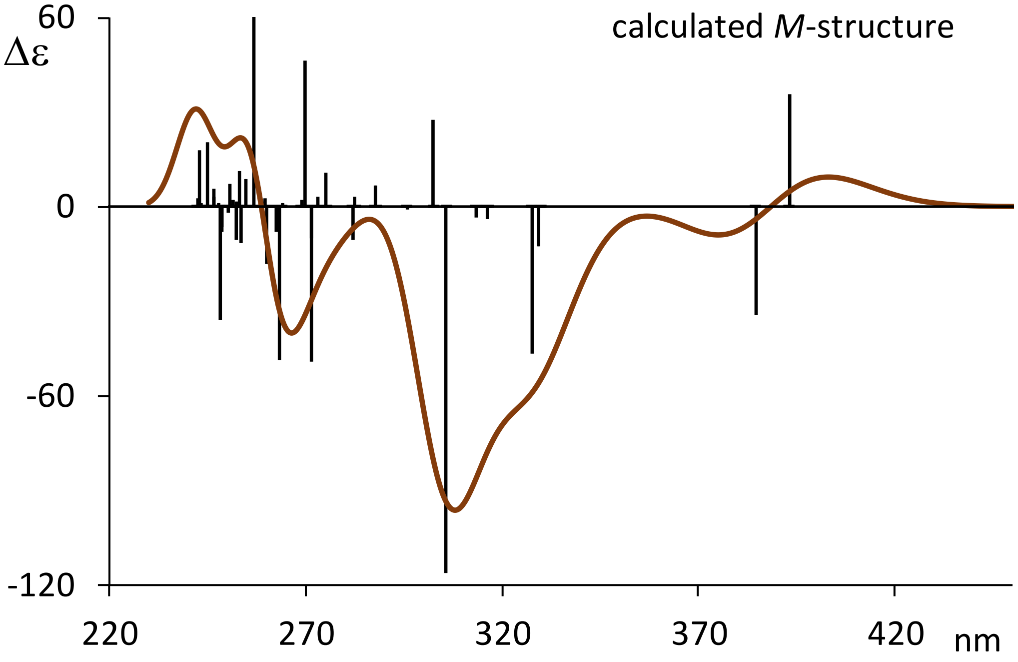

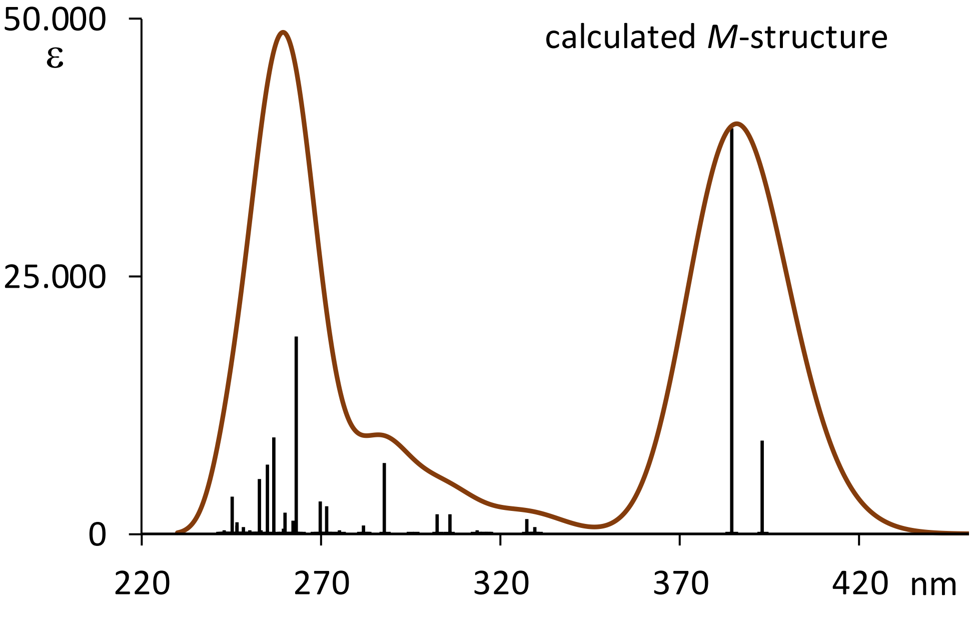

Figure S48. Calculated CD (top) and absorption (bottom) spectra of **2**, optimization and TD-DFT calculation at M06/6-311g G(d,p) level of theory.[S17]

Table S14. Characteristics of the first two transitions calculated for compound **1** (calculated energies, wavelengths, dipole strengths, rotational strengths, electric (mu) and magnetic (m) dipole transition moments in atomic units, angle formed by electric and magnetic dipole transition moments, molecular states involved in transition).

	eV	nm	Dip.	R	|mu|	|m|	E-M	Main transition			
1	3.41	363	187849	-6.3	1.71E+00	1.71E+00	90	167	->	168	0.695
2	3.75	331	99126	-13.4	1.24E+00	4.56E-02	180	167	->	169	0.678

The two first transitions in the two compounds are different in nature. In the case of compound **1**, i) the first transition mainly involves HOMO/LUMO orbitals and it is associated to electric and magnetic dipole transition moments directed within a plane perpendicular to the C2 symmetry axis, ii) the second transition is associated dipole transition moments directed along the symmetry axis.

Table S15. Characteristics of the first two transitions, and of the transition contributing with the highest g_{abs}, calculated for compound **2** (calculated energies, wavelengths, dipole strengths, rotational strengths, electric (mu) and magnetic (m) dipole transition moments in atomic units, angle formed by electric and magnetic dipole transition moments, molecular states involved in transition).

	eV	nm	Dip.	R	|mu|	|m|	E-M	Main transition			
1	3.15	393	60946	35.4	9.71E-01	1.52E-01	0	166	->	168	0.699
2	3.22	384	271248	-34.3	2.05E+00	8.50E-01	95	167	->	168	0.697
9	4.06	306	13266	-116.1	4.53E-01	1.13E+00	168	166	->	169	0.664

On the contrary in case of compound **2**, the first two transitions have quite similar energy values. The first transition correspond to dipole transition moments directed along the C2 symmetry axis. From calculations (M06/ 6-311+g(d,p)) the HOMO and HOMO-1 orbitals are nearly degenerate for this compound (see Table below).

The transition responsible for the highest g_{abs} observed feature (transition number 9) is associated to dipole transition moments transverse to the symmetry axis with an angle of 168° between them, the magnetic dipole transition moments being parallel to the helix axis.

Table S16. Calculated energy (eV) relative to the orbitals involved in the first two transitions, HOMO-LUMO gap and first transition energy. Optimization and TD-DFT calculations at M06/6-311g G(d,p)

Helicene **1**

LUMO+1	-1.36	
LUMO	-1.65	gap
HOMO	-5.88	4.22
HOMO-1	-6.46	

First optical transition: 3.41

Helicene **2**

LUMO+1	-1.28	
LUMO	-2.22	gap
HOMO	-6.16	3.94
HOMO-1	-6.17	

First optical transition: 3.15

a) Helicene **1**

LUMO (168) LUMO+1 (169)

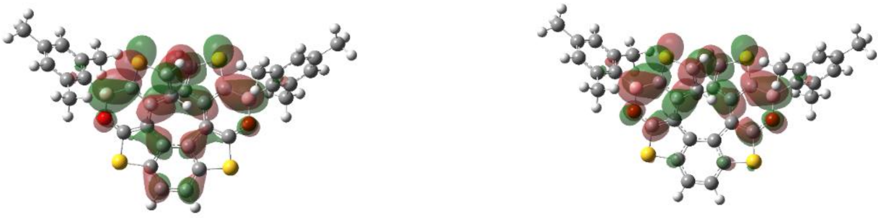

HOMO (167) HOMO-1 (166)

b) Helicene **2** ---

LUMO (168) LUMO+1 (169)

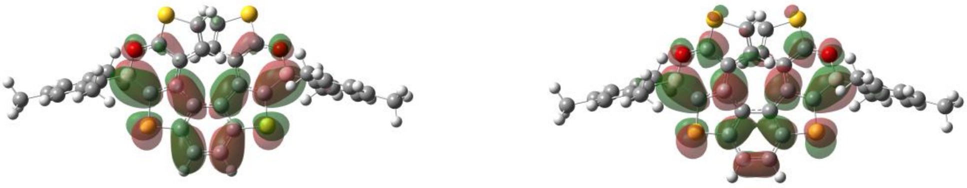

HOMO (167) HOMO-1 (166)

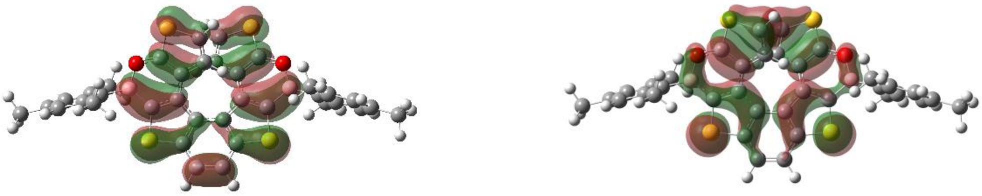

Figure S49. Orbitals involved in the first electronic transitions for helicene **1** (a), **2** (b) and **3** (c) calculated at the M06/6-311g G(d,p) level.

c) Helicene **3** (not synthesized)

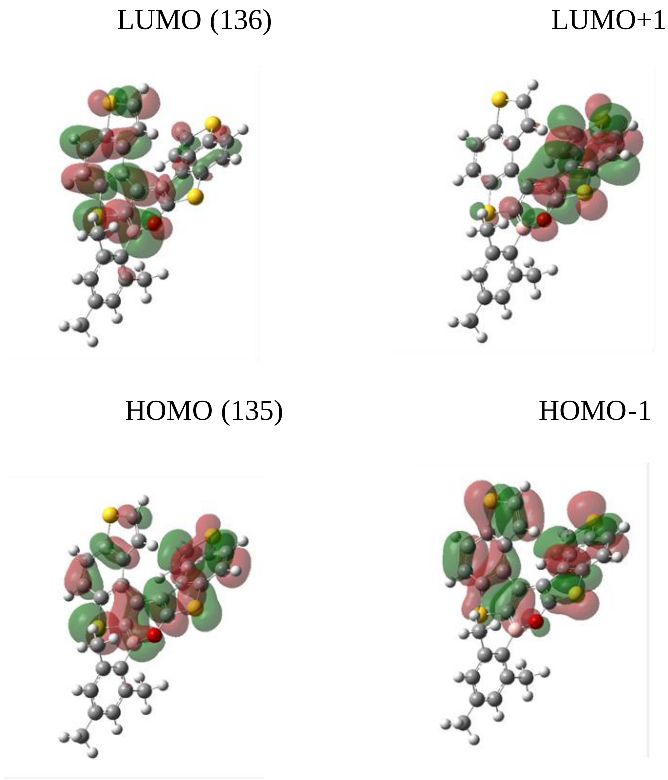

Figure S49. Orbitals involved in the first electronic transitions for helicene **1** (a), **2** (b) and **3** (c) calculated at the M06/6-311g G(d,p) level.

For sake of comparison, we report also the HOMO-1, HOMO, LUMO and LUMO+1 orbitals of the non-symmetric compound **3**. In this case the first calculated transition is a pure HOMO-LUMO (135-136) and it is isolated from the higher energy ones.

9.2 Studies on the enantiomerization barrier of 2

Besides optimizing TS state at the PBE1-PBE/TZVP level with empirical dispersion corrections as reported in the text, we also evaluated enantiomerazation barrier following the procedures previously adopted for compound **1**. We compared model compounds without mesityls with carbo[6]helicene and tetrathia[7]helicene performing a scan along a dihedral angle coordinate defined as indicated considering also diffuse functions at PBE1-PBE 6-311++G(d,p) level,[S18] with empirical dispersion corrections.[S19]

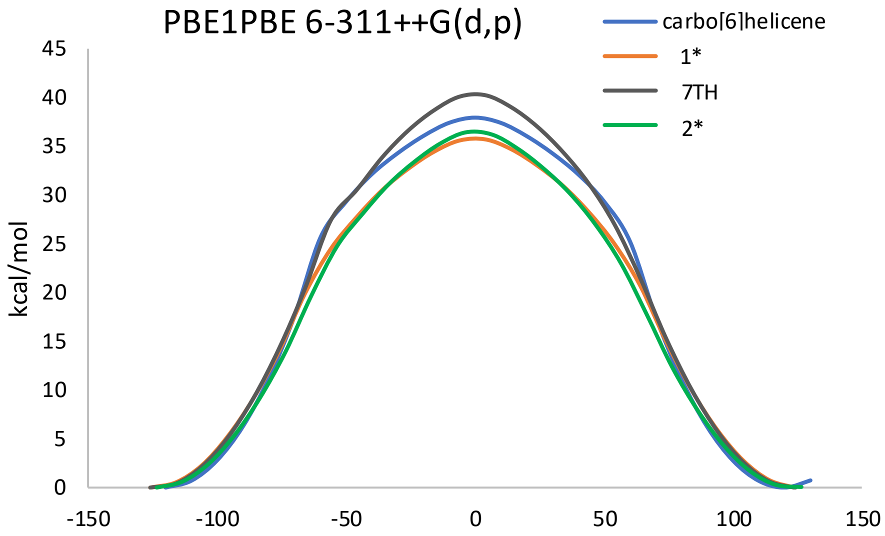

Figure S50. Comparison between the energy scan of **carbo[6]helicene** (blue trace), model compound **1*** (orange trace), **7TH** (grey trace) and model compound compound **2*** (green trace).

A similar analysis conducted on compound **1** and **2** and **carbo[6]helicene** at the semiempirical AM1 level gives the following result which, despite the low level of calculation adopted, seems to better fit experimental results (Figure S51).

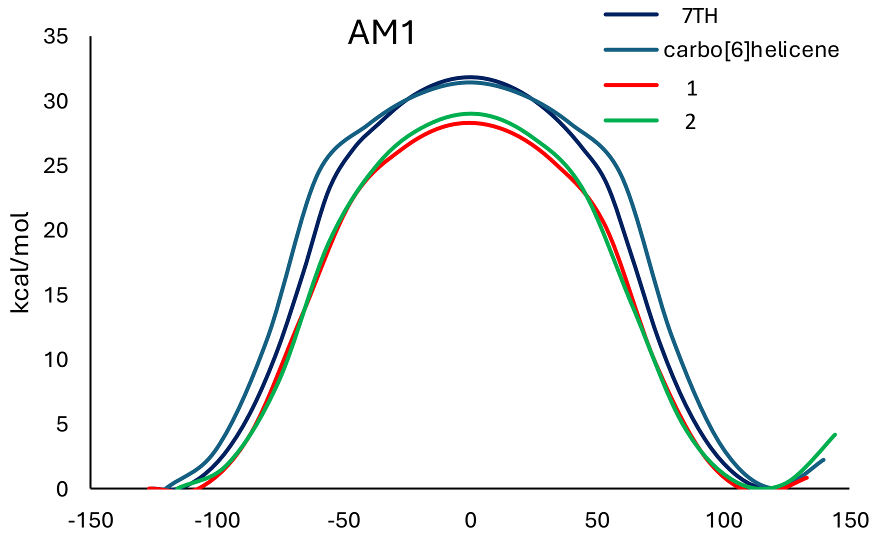

Figure S51. Comparison between the energy scan of **carbo[6]helicene** (blue trace), compound **1** (red trace), compound **2** (green trace) and **7TH**.

A comparison of minimum and transition state calculated structures for the model compounds **1*** and **2*** and tetrathia[7]helicene, with particular attention to the six-membered ring bearing oxygen and boron atoms was performed. Once defined the average six-membered ring plane, distances of the six atoms with respect to the plane are reported: we may infer that, on average, six carbon atom force the ring to be flatter, particularly considering the transition state. Level of calculation: PBE1-PBE/6-311++G(d,p) (Figure S52).

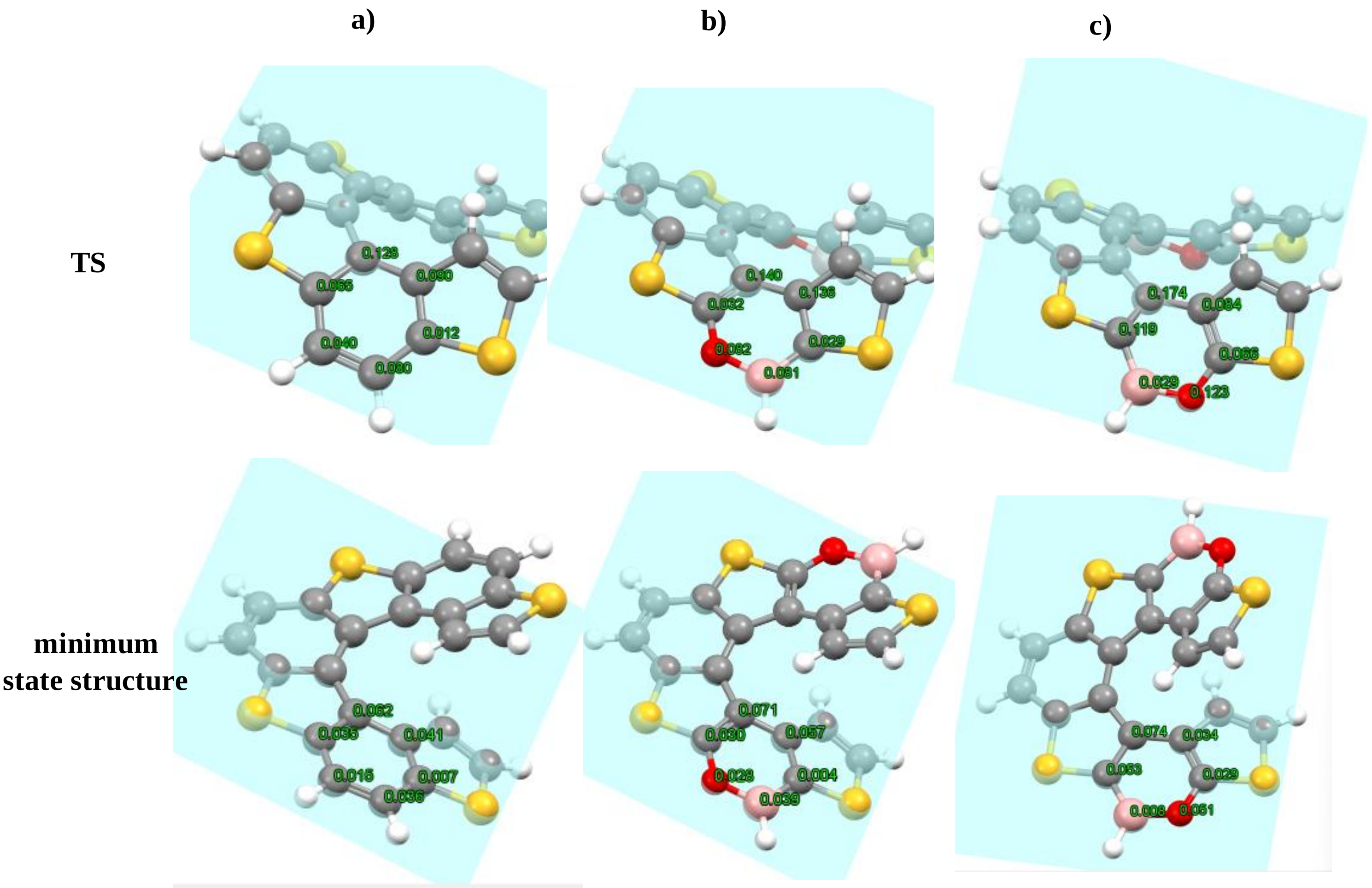

7TH	1*	2*
	Minimum	
0.062	0.071	0.074
0.041	0.057	0.034
0.007	0.004	0.029
0.036	0.039	0.051
0.015	0.028	0.008
0.035	0.030	0.053
	TS	
0.128	0.140	0.174
0.090	0.136	0.084
0.012	0.029	0.066
0.080	0.081	0.123
0.040	0.082	0.029
0.065	0.032	0.119

Figure S52. Distances atom-ring plane (Å) for **7TH** (a) and the six-membered ring containing oxygen and boron atoms of model compound **1*** (b) and **2*** (c) in the calculated transition state structure (top) and the minimum state structure (bottom). The above-mentioned atom-ring plane distances are listed in the right top corner.

The plane defined by the six ring atoms and atom-plane distances have been calculated with Mercury program (https://www.ccdc.cam.ac.uk/solutions/csd-core/components/mercury).

9.3 Optimized coordinates of compound 2 at PBE1-PBE TZVP level, with empirical dispersion corrections.

Minimum

```
                    Standard orientation:
 ---------------------------------------------------------------------
 Center     Atomic      Atomic             Coordinates (Angstroms)
 Number     Number       Type             X           Y           Z
 ---------------------------------------------------------------------
      1         16           0       -2.183776    3.370393    1.806461
      2         16           0       -3.094578   -2.381626   -0.162911
      3         16           0        2.181685    3.374605   -1.801808
      4         16           0        3.096455   -2.379746    0.159048
      5          5           0       -4.141313    0.283911    0.270787
      6          5           0        4.141333    0.287151   -0.270805
      7          8           0       -3.802433    1.571969    0.691269
      8          8           0        3.801514    1.575673   -0.689116
      9          6           0       -2.551721    1.861932    1.039317
     10          6           0       -1.454539    1.035641    0.909464
     11          6           0       -0.298666    1.630700    1.508485
     12          1           0        0.664522    1.147612    1.568245
     13          6           0       -0.534471    2.863601    2.012677
     14          1           0        0.163626    3.525680    2.500928
     15          6           0       -2.974893   -0.679567    0.154287
     16          6           0       -1.658142   -0.268218    0.333248
     17          6           0       -0.709235   -1.314158    0.049922
     18          6           0       -1.364864   -2.552537   -0.086604
     19          6           0       -0.679999   -3.775877   -0.082012
     20          1           0       -1.226290   -4.708561   -0.156035
     21          6           0        0.682796   -3.775520    0.076332
     22          1           0        1.229708   -4.707936    0.149128
     23          6           0       -5.641583   -0.026644   -0.018515
     24          6           0       -6.098032   -0.230403   -1.328676
     25          6           0       -7.435275   -0.539759   -1.548898
     26          1           0       -7.782266   -0.690301   -2.567473
     27          6           0       -8.337360   -0.663585   -0.498859
     28          6           0       -7.870688   -0.468723    0.796123
     29          1           0       -8.559173   -0.570725    1.630548
     30          6           0       -6.543131   -0.147048    1.049527
     31          6           0       -5.159672   -0.107515   -2.496362
     32          1           0       -5.700433   -0.165579   -3.442258
     33          1           0       -4.409517   -0.903745   -2.491074
     34          1           0       -4.621140    0.844140   -2.477410
     35          6           0       -9.781718   -0.971276   -0.757303
     36          1           0      -10.220587   -1.539652    0.065231
     37          1           0       -9.907741   -1.546589   -1.676579
     38          1           0      -10.362541   -0.049549   -0.864717
     39          6           0       -6.077763    0.062890    2.462741
     40          1           0       -5.181652   -0.526428    2.680548
     41          1           0       -6.848728   -0.224589    3.179218
     42          1           0       -5.825071    1.111588    2.642489
     43          6           0        2.550656    1.865244   -1.036931
     44          6           0        1.454064    1.037954   -0.908469
     45          6           0        0.297824    1.633063   -1.506723
     46          1           0       -0.664996    1.149339   -1.567314
     47          6           0        0.532782    2.866904   -2.009011
     48          1           0       -0.165737    3.529216   -2.496340
     49          6           0        2.975583   -0.677336   -0.155866
```

50	6	0	1.658559	-0.266636	-0.334229
51	6	0	0.710368	-1.313612	-0.052332
52	6	0	1.366837	-2.551727	0.082521
53	6	0	5.641613	-0.023279	0.018336
54	6	0	6.544905	-0.135864	-1.048891
55	6	0	7.874119	-0.450590	-0.794770
56	1	0	8.565750	-0.539082	-1.628126
57	6	0	8.339270	-0.651503	0.499665
58	6	0	7.437050	-0.527297	1.549749
59	1	0	7.785782	-0.668919	2.569004
60	6	0	6.098471	-0.224881	1.328880
61	6	0	6.082126	0.083568	-2.461509
62	1	0	6.853039	-0.202529	-3.178598
63	1	0	5.832793	1.133979	-2.635886
64	1	0	5.184516	-0.501837	-2.683547
65	6	0	9.769871	-1.020504	0.754269
66	1	0	9.899674	-2.107463	0.740050
67	1	0	10.104902	-0.664073	1.730362
68	1	0	10.430321	-0.602445	-0.008034
69	6	0	5.160918	-0.095935	2.496547
70	1	0	4.393898	-0.875680	2.480634
71	1	0	4.643022	0.867358	2.487966
72	1	0	5.698657	-0.176704	3.442481

Transition State

Standard orientation:

Center Number	Atomic Number	Atomic Type	Coordinates (Angstroms) X	Y	Z
1	16	0	2.984954	3.772485	-1.387020
2	16	0	2.949876	-1.215405	2.051969
3	16	0	-2.985885	3.772732	-1.385829
4	16	0	-2.949833	-1.215041	2.053321
5	5	0	3.832454	0.131594	-0.322425
6	5	0	-3.833110	0.131900	-0.320838
7	8	0	3.604285	1.197751	-1.187586
8	8	0	-3.605350	1.198052	-1.186078
9	6	0	2.776422	2.163808	-0.781882
10	6	0	1.864493	2.075599	0.250195
11	6	0	1.453720	3.384224	0.642130
12	1	0	0.898149	3.575265	1.541659
13	6	0	1.941472	4.374608	-0.140985
14	1	0	1.761674	5.435388	-0.063377
15	6	0	2.897602	0.042832	0.876886
16	6	0	1.744721	0.815731	0.963713
17	6	0	0.727822	0.210954	1.820178
18	6	0	1.339808	-0.830606	2.563319
19	6	0	0.680938	-1.656029	3.483506
20	1	0	1.243549	-2.357183	4.088327
21	6	0	-0.680329	-1.655919	3.483840
22	1	0	-1.242769	-2.356983	4.088923
23	6	0	4.941729	-0.904318	-0.681794
24	6	0	6.279702	-0.610914	-0.384602
25	6	0	7.267463	-1.546482	-0.666949
26	1	0	8.302104	-1.311792	-0.432122
27	6	0	6.961608	-2.773353	-1.244706
28	6	0	5.631852	-3.048192	-1.543053
29	1	0	5.376363	-3.998312	-2.004087
30	6	0	4.619520	-2.136840	-1.266592

```
    31          6           0        6.643391    0.712860    0.226105
    32          1           0        6.486245    1.530037   -0.484174
    33          1           0        7.689725    0.733923    0.534612
    34          1           0        6.030220    0.928684    1.106787
    35          6           0        8.034490   -3.786000   -1.512072
    36          1           0        7.780252   -4.419035   -2.364530
    37          1           0        8.174885   -4.442063   -0.646960
    38          1           0        8.993181   -3.305267   -1.716773
    39          6           0        3.195465   -2.464847   -1.614560
    40          1           0        3.115758   -3.459775   -2.055147
    41          1           0        2.787953   -1.747167   -2.332494
    42          1           0        2.553523   -2.437306   -0.729041
    43          6           0       -2.777234    2.164070   -0.780707
    44          6           0       -1.864911    2.075827    0.251009
    45          6           0       -1.453870    3.384436    0.642719
    46          1           0       -0.897915    3.575476    1.542011
    47          6           0       -1.941851    4.374825   -0.140245
    48          1           0       -1.761929    5.435592   -0.062761
    49          6           0       -2.897975    0.043241    0.878266
    50          6           0       -1.744954    0.815966    0.964533
    51          6           0       -0.727723    0.211063    1.820517
    52          6           0       -1.339502   -0.830411    2.563945
    53          6           0       -4.941949   -0.904497   -0.680350
    54          6           0       -6.278856   -0.616354   -0.373445
    55          6           0       -7.265033   -1.555567   -0.649247
    56          1           0       -8.297904   -1.327963   -0.400122
    57          6           0       -6.959278   -2.778804   -1.234737
    58          6           0       -5.629564   -3.051813   -1.534966
    59          1           0       -5.372519   -4.004781   -1.989229
    60          6           0       -4.618807   -2.136709   -1.265239
    61          6           0       -6.641902    0.702099    0.249050
    62          1           0       -6.483542    1.525420   -0.453824
    63          1           0       -6.029363    0.909637    1.132182
    64          1           0       -7.688533    0.721315    0.556652
    65          6           0       -8.039037   -3.767156   -1.559256
    66          1           0       -8.876886   -3.683533   -0.864177
    67          1           0       -7.664513   -4.792072   -1.522188
    68          1           0       -8.431326   -3.597825   -2.567176
    69          6           0       -3.194089   -2.464874   -1.610348
    70          1           0       -2.779182   -1.736902   -2.313445
    71          1           0       -3.115946   -3.452483   -2.067378
    72          1           0       -2.557372   -2.455246   -0.720613
 ---------------------------------------------------------------------
```

10. References

[S1] A. F. Burchat, J. M. Chong and N. Nielsen, *J. Am. Chem. Soc*. **1997**, *542*, 281.

[S2] A. Hallberg, S. Gronowitz, *Chemica Scripta*, **1980**, *16*, 38.

[S3] K. Shigemori, M. Watanabe, J. Kong, K. Mitsudo, A. Wakamiya, H. Mandai and S. Suga, *Org. Lett*., **2019**, *21*, 2, 2171.

[S4] R. M. F. Batista, S. P. G. Costa, M. Belsley, C. Lodeiro, M. Manuela, M. Raposo, *Tetrahedron*, **2008**, *64*, 9230.

[S5] PCT Int. Appl., 2010040839 CAS 77133-21-2.

[S6] A. El Jaouhari, Y. Wang, B. Zhang, X. Liu, J. Zhu, *Materials Science & Engineering, C: Materials for Biological Applications*, **2020**, *114*, 111067.

[S7] Y. Zhang, A. B. Hornfeldt, S. Gronowitz, and C. Stalhandske, *Acta Chemica Scandinavica*, **1994**, *48*(10), 843.

[S8] F. Li, Y. Hu, Y. Wang, C. Ma, J. Wang, *J. Med. Chem.* **2017**, *60*, 1580−1590.

[S8a] A.K. Mishra, S.Vaidyanathan, H. Noguchi, F. Doetz, S. Koehler, M. Kastler, **2010**, WO 2010/079064 A2.

[S9] R. M. Kellogg, M. B. Groen and H. Wynberg, *J. Org. Chem.* **1967,** *32* (10), 3093.

[S10] S. Maiorana, A. Papagni, E. Licandro, R. Annunziata, P. Paravidino, D. Perdicchia, C. Giannini, M. Bencini, K. Clays, A. Persoons, *Thetrahedron*, **2003**, *59*, 6481.

[S11] T. Caronna, M. Catellani, S. Luzzati, L. Malpezzi, S. V. Meille, A. Mele, C. Richter and R. Sinisi, *Chem. Mater*., **2001**, *13*, 3906.

[S12] a) G. A. Hunter, H. McNab, *New J. Chem.*, **2010**, *34*, 2558.

b) S. Gronowitz, Thiophene and its Derivatives IV, *Chemistry of Heterocyclic Compounds, 44* – **1991**, Wiley.

[S13] a) D. Krause, Glasses, *Nonmetallic Materials: Part C*, **2018**, *19*, 537.

b) F. B. Mallory, C. W. Mallory, Photocyclization of Stilbenes and Related Molecules, *Organic Reactions, 30* – **1984**, Wiley.

[S14] L. Liu, B. Yang, T. J. Katz, M. K. Poindexter, *J. Org. Chem.*, **1991**, *56*, 3769.

[S15] Stoe & Cie, X-AREA. Diffractometer control program system. Stoe & Cie, Darmstadt, Germany, 2002.

[S16] a) G. M. Sheldrick, *Acta Crystallogr. Sect. A.*, **2015**, 71, 3; b) G. M. Sheldrick, *Acta Crystallogr. Sect. A*, **2008**, *64*, 112.

[S17] Gaussian 16, Revision C.01, M. J. Frisch, G. W. Trucks, H. B. Schlegel, G. E. Scuseria, M. A. Robb, J. R. Cheeseman, G. Scalmani, V. Barone, G. A. Petersson, H. Nakatsuji, X. Li, M. Caricato, A. V. Marenich, J. Bloino, B. G. Janesko, R. Gomperts, B. Mennucci, H. P. Hratchian, J. V. Ortiz, A. F. Izmaylov, J. L. Sonnenberg, D. Williams-Young, F. Ding, F. Lipparini, F. Egidi, J. Goings, B. Peng, A. Petrone, T. Henderson, D. Ranasinghe, V. G. Zakrzewski, J. Gao, N. Rega, G. Zheng, W. Liang, M. Hada, M. Ehara, K. Toyota, R. Fukuda, J. Hasegawa, M. Ishida, T. Nakajima, Y. Honda, O. Kitao, H. Nakai, T. Vreven, K. Throssell, J. A. Montgomery, Jr., J. E. Peralta, F. Ogliaro, M. J. Bearpark, J. J. Heyd, E. N. Brothers, K. N. Kudin, V. N. Staroverov, T. A. Keith, R. Kobayashi, J. Normand, K. Raghavachari, A. P. Rendell, J. C. Burant, S. S. Iyengar, J. Tomasi, M. Cossi, J. M. Millam, M. Klene, C. Adamo, R. Cammi, J. W. Ochterski, R. L. Martin, K. Morokuma, O. Farkas, J. B. Foresman, and D. J. Fox, Gaussian, Inc., Wallingford CT, 2019.

[S18] J. Barroso, J. L. Cabellos, S. Pan, F. Murillo, X. Zarate, M. A. Fernandez-Herrera, G. Merino, *Chem. Commun.*, **2018**, *54*, 188.

[S19] S. Grimme, J. Antony, S. Ehrlich and H. Krieg, *J. Chem. Phys*., **2010**, *132*, 1.